VILNIUS UNIVERSITY

Justina **KAZOKAITĖ**

Investigation of human carbonic anhydrase VI and IX inhibitor efficacy and toxicity

Doctoral dissertation

Physical sciences, biochemistry (04 P)

Vilnius, 2018

This doctoral thesis work was performed from October 2014 to September 2018 at the Life Sciences Center, Vilnius University, Lithuania.

Supervisor:

Prof. Daumantas MATULIS (Vilnius University, Physical Sciences, biochemistry – 04 P)

Acknowledgments

Contents

List of publications and personal contribution

Publications included in this thesis

1. **Kazokaitė J**, Niemans N, Dudutienė V, Becker H, Leitans J, Zubrienė A, Baranauskienė L, Gondi G, Zeidler R, Matulienė J, Tars K, Yaromina A, Lambin P, Dubois LJ, Matulis D. Novel fluorinated carbonic anhydrase IX inhibitors reduce hypoxia-induced acidification and clonogenic survival of cancer cells. *Oncotarget.* 9 (**2018**) 26800-16.

   I have performed experiments in cancer cells, except mass spectrometry, analyzed the data, wrote the first version of manuscript, and reviewed its drafts.

2. **Kazokaitė J**, Aspatwar A, Parkkila S, Matulis D. An update on anticancer drug development and delivery targeting carbonic anhydrase IX. *PeerJ.* 5 (**2017**) e4068.

   I have performed literature analysis of methods applied for the screening of CA IX-selective inhibitors and contributed to the description of novel CA IX-targeting strategies.

3. **Kazokaitė J**, Aspatwar A, Kairys V, Parkkila S, Matulis D. Fluorinated benzenesulfonamide anticancer inhibitors of carbonic anhydrase IX exhibit lower toxic effects on zebrafish embryonic development than ethoxzolamide. *Drug Chem Toxicol.* 40(3) (**2017**) 309-19.

   I have determined lethal concentrations of lead inhibitors that caused 50% zebrafish mortality, evaluated compound-induced phenotypic abnormalities, contributed to histochemical analysis, wrote the first version of manuscript, and reviewed its drafts.

4. **Kazokaitė J**, Ames S, Becker HM, Deitmer JW, Matulis D. Selective inhibition of human carbonic anhydrase IX in *Xenopus* oocytes and MDA-MB-231 breast cancer cells. *J Enzyme Inhib Med Chem.* 31(sup4) (**2016**) 38-44.

I have performed pH measurements in *Xenopus* oocytes and analyzed the affinity of lead compounds toward heterologously expressed CA isoforms. I wrote the first version of manuscript and reviewed its drafts.

5. **Kazokaitė J**, Milinavičiūtė G, Smirnovienė J, Matulienė J, Matulis D. Intrinsic binding of 4-substituted-2,3,5,6-tetrafluorobenezenesulfonamides to native and recombinant human carbonic anhydrase VI. *FEBS J.* 282(5) (**2015**) 972-83.

I have purified recombinant and native CA VI, performed and analyzed biophysical experiments of fluorescent thermal shift assay and isothermal titration calorimetry, wrote the first version of manuscript, and reviewed its drafts.

6. Dudutienė V, Matulienė J, Smirnov A, Timm DD, Zubrienė A, Baranauskienė L, Morkūnaitė V, Smirnovienė J, Michailovienė V, Juozapaitienė V, Mickevičiūtė A, **Kazokaitė J**, Bakšytė S, Kasiliauskaitė A, Jachno J, Revuckienė J, Kišonaitė M, Pilipuitytė V, Ivanauskaitė E, Milinavičiūtė G, Smirnovas V, Petrikaitė V, Kairys V, Petrauskas V, Norvaišas P, Lingė D, Gibieža P, Čapkauskaitė E, Zakšauskas A, Kazlauskas E, Manakova E, Gražulis S, Ladbury JE, Matulis D. Discovery and characterization of novel selective inhibitors of carbonic anhydrase IX. *J Med Chem.* 57(22) (**2014**) 9435-46.

I have measured and analyzed the binding of synthesized lead compounds to recombinant CA VI by fluorescent thermal shift assay.

Publications not included in this thesis

1. Dudutienė V, Zubrienė A, Smirnov A, Timm DD, Smirnovienė J, **Kazokaitė J**, Michailovienė V, Zakšauskas A, Manakova E, Gražulis S, Matulis D. Functionalization of fluorinated benzenesulfonamides and their inhibitory properties toward carbonic anhydrases. *ChemMedChem.* 10(4) (**2015**) 662-87.

I have performed and analyzed measurements of synthesized compound binding to recombinant CA VI by fluorescent thermal shift assay.

2. Rutkauskas K, Zubrienė A, Tumosienė I, Kantminienė K, Kažemėkaitė M, Smirnov A, **Kazokaitė J**, Morkūnaitė V, Čapkauskaitė E, Manakova E, Gražulis S, Beresnevičius ZJ, Matulis D. 4-amino-substituted benzenesulfonamides as inhibitors of human carbonic anhydrases. *Molecules.* 19(11) (**2014**) 17356-80.

I have performed and analyzed measurements of synthesized compound binding to recombinant CA VI by fluorescent thermal shift assay.

3. Čapkauskaitė E, Zubrienė A, Smirnov A, Torresan J, Kišonaitė M, **Kazokaitė J**, Gylytė J, Michailovienė V, Jogaitė V, Manakova E, Gražulis S, Tumkevičius S, Matulis D. Benzenesulfonamides with pyrimidine moiety as inhibitors of human carbonic anhydrases I, II, VI, VII, XII, and XIII. *Bioorg Med Chem.* 21(22) (**2013**) 6937-47.

I have performed and analyzed measurements of synthesized compound binding to recombinant CA VI by fluorescent thermal shift assay.

List of conferences

Oral presentation

1. **Kazokaitė J**, Niemans R, Dudutienė V, Becker H, Leitans J, Zubrienė A, Baranauskienė L, Gondi G, Zeidler R, Matulienė J, Tars K, Yaromina A, Lambin P, Dubois LJ, Matulis D. Novel benzenesulfonamides as selective carbonic anhydrase IX inhibitors exhibit functional effects to reduce hypoxia-induced acidification and clonogenicity in cancer cell lines. 18th FEBS Young Scientists' Forum. Prague, Czech Republic; July 4–7, 2018.

Poster presentations

1. **Kazokaitė J**, Niemans R, Dudutienė V, Becker H, Leitans J, Zubrienė A, Baranauskienė L, Gondi G, Zeidler R, Matulienė J, Tars K, Yaromina A, Lambin P, Dubois LJ, Matulis D. Novel benzenesulfonamides as selective carbonic anhydrase IX inhibitors exhibit functional effects to reduce hypoxia-induced acidification and clonogenicity in cancer cell lines. 43rd FEBS Congress. Prague, Czech Republic; July 7–12, 2018.

2. **Kazokaitė J**, Niemans R, Dudutienė V, Becker H, Leitans J, Zubrienė A, Baranauskienė L, Gondi G, Zeidler R, Matulienė J, Tars K, Yaromina A, Lambin P, Dubois LJ, Matulis D. Novel benzenesulfonamides as selective carbonic anhydrase IX inhibitors exhibit functional effects to reduce hypoxia-induced acidification and clonogenicity in cancer cell lines. 11th International Conference on Carbonic Anhydrases. Bucharest, Romania; June 27–30, 2018.

3. **Kazokaitė J**, Niemans R, Yaromina A, Aspatwar A, Parkkila S, Deitmer JW, Becker H, Lambin P, Matulienė J, Zubrienė A, Dudutienė V, Dubois LJ, Matulis D. Carbonic anhydrase IX-selective inhibitors diminish acidification in cancer cell cultures and *Xenopus* oocytes and exhibit low toxicity in zebrafish. European Radiation Research Society Meeting. Essen, Germany; September 17–21, 2017.

4. **Kazokaitė J**, Niemans R, Yaromina A, Aspatwar A, Parkkila S, Deitmer

JW, Becker H, Lambin P, Matulienė J, Zubrienė A, Dudutienė V, Dubois LJ, Matulis D. Carbonic anhydrase IX-selective inhibitors diminish acidification in cancer cell cultures and *Xenopus* oocytes and exhibit low toxicity in zebrafish. 42nd FEBS Congress. Jerusalem, Israel; September 10–14, 2017.

5. **Kazokaitė J**, Aspatwar A, Kairys V, Parkkila S, Deitmer JW, Matulis D. Novel benzenesulfonamides exhibit low toxicity on zebrafish development and selectively inhibit human carbonic anhydrase IX with nanomolar affinity. Grow Science Day. Maastricht, The Netherlands; November 23, 2016.

6. **Kazokaitė J**, Aspatwar A, Kairys V, Parkkila S, Deitmer JW, Matulis D. Novel benzenesulfonamides exhibit low toxicity on zebrafish development and selectively inhibit human carbonic anhydrase IX with nanomolar affinity. 12th International Congress of Cell Biology. Prague, Czech Republic; July 21–25, 2016.

7. **Kazokaitė J**, Aspatwar A, Kairys V, Parkkila S, Matulis D. Fluorinated benzenesulfonamide anticancer inhibitors of carbonic anhydrase IX exhibit lower toxic effects on zebrafish embryonic development than ethoxzolamide. 11th COINS, Vilnius, Lithuania; February 29–March 3, 2016.

8. **Kazokaitė J**, Aspatwar A, Kairys V, Parkkila S, Matulis D. Fluorinated benzenesulfonamide anticancer inhibitors of carbonic anhydrase IX exhibit lower toxic effects on zebrafish embryonic development than ethoxzolamide. VitaScientia, Vilnius, Lithuania; January 4, 2016.

9. **Kazokaitė J**, Milinavičiūtė G, Smirnov A, Matulis D. Investigation of Inhibitor Binding Affinity to the Native and Recombinant Carbonic Anhydrase VI. 10th International Conference on Carbonic Anhydrase, Maastricht, The Netherlands; April 20–22, 2015.

10. **Kazokaitė J**, Milinavičiūtė G, Gylytė J, Dudutienė V, Matulienė J, Matulis D. Differences in Stability Profiles and Thermodynamics of Inhibitor Binding to Target Protein Purified from *E. coli*, Mammalian Cells and Human Saliva. European Biotechnology Congress. Lecce; Italy; May 15–18, 2014.

Abbreviations

AE	anion exchanger
ANS	8-anilino-1-naphthalenesulfonic acid ammonium salt
AZM	acetazolamide
BHI	brain heart infusion medium
BSA	benzenesulfonamide
CA	carbonic anhydrase
CARP	CA-related protein
CBP	CREB-binding protein
DMEM	Dulbecco's modified Eagle medium
DMSO	dimethylsulfoxide
dpf	days post-fertilization
EC_{50}	concentration causing half-maximal viability response
ECD	ectodomain
EMA	European Medicines Agency
EP	electrode potential
EZA	ethoxzolamide
FDA	Food and Drug Administration (a federal agency of the United States Department of Health and Human Services)
FIH-1	factor inhibiting HIF-1
FTSA	fluorescent thermal shift assay
Hepes	2-[4-(2-hydroxyethyl)piperazin-1-yl]ethanesulfonic acid
HIF	hypoxia-inducible factor
hpf	hours post-fertilization
IC_{50}	half-maximal inhibitory concentration
ITC	isothermal titration calorimetry
K_b	binding constant
k_{cat}	catalytic constant
K_d	dissociation constant
K_M	Michaelis constant
KO	knockout
LC_{50}	half-maximal lethal concentration
LE	logarithmic ^{18}O enrichment

mAb	monoclonal antibody
MCT	monocarboxylate transporter
Mes	2-morpholin-4-ylethanesulfonic acid
MS	mass spectrometry
NBC	Na^+/HCO_3^- co-transporter
NHE	Na^+/H^+ exchanger
T_m	protein melting temperature
PG	proteoglycan-like domain
PIMO	pimonidazole
Pipes	1,4-piperazinediethanesulfonic acid
PHD	prolyl hydroxylase domain-containing protein
pH_e	extracellular pH
pH_i	intracellular pH
PPI	proton pump inhibitor
SDS-PAGE	sodium dodecyl sulfate-polyacrylamide gel electrophoresis
siRNA	small interfering RNA
shRNA	short hairpin RNA
TME	tumor microenvironment
Tris	2-amino-2-(hydroxymethyl)propane-1,3-diol
V-ATPase	vacuolar-type H^+-adenosine triphosphatase

Introduction

Nowadays enzymes comprise over one-third of distinct drug targets found within the portfolios of large pharmaceutical companies [1], thereby emphasizing the relevance of target-based drug approach. This strategy is focused on the discovery of drugs, which significantly affect certain key proteins involved in disease condition. Numerous techniques of diverse scientific fields are applied to derive insight into possibilities to modulate pathology-linked targets or their expression levels with the goal of translating *in vitro* data to a clinical disease setting.

Since the discovery over 80 years ago [2], carbonic anhydrases (CAs) have been found as widespread enzymes in nature and have been involved in diverse research areas from basic enzymology to clinical medicine. There are twelve catalytically active human CA isoforms. They significantly contribute to the cellular pH homeostasis via catalysis of the reversible CO_2 hydration to HCO_3^- with the release of a proton. This reaction is substantial for many physiological processes and therefore the abnormal levels or activities of CAs have been implicated in many diseases, including glaucoma, epilepsy, obesity, and cancer. The design of compounds exhibiting both great affinity and high CA isoform-selectivity has been a major focus of attention over decades for the specific disease treatment without causing side effects due to off-target CA modulation. However, it is a complicated task because of the high structural homology between human CA isoforms.

The *in vitro* evaluation of compound effect on mammalian proteins, including human CAs, can be performed by diverse assays, which employ the isolated recombinant protein. These studies significantly contribute to the identification of lead compounds with adequate efficacy against the biological target, leading to further preclinical and clinical development. Therefore, it is fundamentally important to ensure that the recombinant protein would properly represent its corresponding endogenous native target. Only if this condition is fulfilled, the therapeutic benefit for patients can be obtained during later clinical investigation. Interestingly, CA VI can be purified from bacteria *Escherichia coli* and human saliva, allowing the comparison of inhibitor binding to both recombinant CA VI and endogenous native CA VI produced from human saliva (indicated as native CA VI in this thesis).

Among a broad spectrum of CA-linked pathologies, CA IX has been associ-

ated with the cancer progression because of the increased expression levels under hypoxic conditions in cell line dependent manner. The most successful strategies of modulating CA IX catalytic activity to date include the application of sulfonamide-based compounds. Even though a vast collection of CA IX inhibitors has been reported, only a handful of sulfonamide derivatives have progressed to clinical trials with unfavorable or unavailable results so far. Thus, the design of different, more efficient CA IX-targeting compounds and the clinical benefit of CA IX inhibitors to patients remain important issues to be investigated.

The most common method to evaluate interactions between CAs and inhibitors is the stopped-flow CO_2 hydration assay. However, this technique has several limitations, such as the largely unknown concentration of CO_2 and the inability to determine inhibition constant below several nM [3]. Therefore, biophysical methods, including the fluorescent thermal shift assay and isothermal titration calorimetry, have become promising alternatives to measure observed binding parameters and calculate intrinsic affinity of compound according to them. Only intrinsic profiles subtract the linked protonation events occurring upon the binding reaction of CA and inhibitor and thereby provide important information about the molecular recognition for the design of compounds with desired affinity properties.

The combination of data obtained from enzymatic inhibition or biophysical binding methods with results from biological assays significantly strengthens the conclusions of compound structure-activity relationships and thus is important for the drug discovery and development. In recent years, zebrafish (*Danio rerio*) and *Xenopus laevis* as convenient and cost-effective alternative vertebrate models have greatly contributed to the compound characterization, thereby filling the gap between traditional enzymatic or binding methods and preclinical mammalian assays. According to the ability to target cancer cells without inducing toxicity in healthy tissues, drug candidates are usually proposed for the clinical investigation. Therefore, the most common practice in biomedical research is based on human cancer cells as a model system to determine anti-tumor properties. Overall, invoking of listed biophysical, biochemical, and biological approaches is essential for sufficient compound characterization during the initial development stage, which may reveal more effective and less toxic therapeutic options with prospective clinical applications.

The goal of the study

To study recombinant CA VI as a model of native human CA VI for the inhibitor intrinsic binding reactions and to explore CA IX lead inhibitors in biological systems as an initial step of their development towards anti-cancer drugs.

Objectives

- To determine the observed binding affinities of a series of sulfonamides to native and recombinant CA VI.

- To identify the most effective inhibitor from a series of sulfonamides against recombinant CA VI by distinguishing the observed and intrinsic thermodynamic binding parameters.

- To determine the protonation pK_a values of the zinc-bound hydroxide/water molecule of recombinant and native CA VI and the protonation enthalpy of zinc-bound hydroxide/water molecule of recombinant CA VI.

- To study the toxic effects of lead CA IX inhibitors in zebrafish embryos/larvae.

- To assess the effect of lead CA IX inhibitors on pH regulation in oocytes of *Xenopus laevis* with heterologously expressed CA isoforms.

- To determine anti-proliferative and functional activities of lead CA IX inhibitors against a panel of human cancer cell lines.

Scientific novelty

In this study, the observed and intrinsic binding parameters of a series of novel inhibitors to CA VI were determined for the first time. The observed affinities of the inhibitors were essentially identical towards the native CA VI that was obtained from human saliva and recombinant CA VI purified from *Escherichia coli*. This result demonstrated the suitability of recombinant CA VI as a model of native CA VI. Moreover, only the observed binding parameters between CAs and their inhibitors are usually provided in the literature. In this work, the observed and intrinsic binding parameters were evaluated, emphasizing that the observed values may be misleading for the understanding of the chemical structural basis for the binding affinity.

Recently, many efforts have been dedicated to discover anti-cancer compounds towards CA IX, an important characteristic of many hypoxic tumors. This thesis described a novel approach of combining various *in vitro* data obtained by biophysical, biochemical, and cellular assays to explore the newly designed CA IX inhibitors VD11-4-2, VD12-09, and VR16-09. The compounds are fluorinated benzenesulfonamides differing from previously reported inhibitors by bulky hydrophobic groups at *ortho* and *meta* positions. These groups ensure high selectivity and picomolar affinity towards CA IX as confirmed by the enzymatic inhibition and binding assays and crystallographic analysis.

In this study, the biological model systems, zebrafish embryos/larvae, *Xenopus laevis* oocytes, and human cancer cells were used together with the enzymatic and

biophysical methods to characterize compound efficacy. Studies using *Xenopus* oocytes for the first time revealed high selectivity and 15 nM inhibitory potency of compound VD11-4-2 against hetereologous CA IX in a biological model system. Experiments employing human cancer cells were the first which showed CA IX-dependent functional activities of three tested inhibitors to reduce the hypoxia-induced acidosis. Furthermore, the investigation of CA IX-targeting compounds in the three-dimensional (3D) cell model with clonogenic cell survival as endpoint was introduced as a promising strategy to determine hypoxia-dependent impact of compounds on cell proliferation. This approach may be applied in the research of other CA IX inhibitors to determine hypoxia-dependent anti-proliferative activities. Thus, this thesis provides a novel concept to characterize compound efficacies, which is beneficial for further development.

Defending statements

- Recombinant CA VI protein is a suitable model of native CA VI for measuring affinities of binding sulfonamide inhibitors, and only the intrinsic parameters should be used to correlate the binding energetics with the compound chemical structures for rational drug design.

- Prior to clinical development, it is relevant to combine the enzymatic inhibition and biophysical binding approaches with biological assays of diverse model systems, such as zebrafish, *Xenopus laevis* oocytes, and human cancer cells, to gain a deeper insight into the action mode of the compound and confirm its efficacy.

- High efficacy of novel CA IX inhibitors as demonstrated by inhibition and binding to recombinant CA IX and confirmed in zebrafish embryos/larvae, *Xenopus laevis* oocytes, and human cancer cells, shows that they are suitable for further development directed toward CA IX-specific anti-cancer therapy.

Literature overview

1 Tumor microenvironment and hypoxia

Cancer is the second leading cause of death in developing countries [4]. Recently, substantial progress has been made in cancer prevention and treatment. Advances in this field have been significantly promoted by the studies of molecular mechanisms in cancer, as discussed in this thesis.

During cancer development, the heterogeneous and dynamic network of interacting malignant, vascular, stromal, and immune cells is formed, that is surrounded by extracellular matrix and diverse physiological gradients, such as oxygen, nutrients, and growth factors. Therefore, numerous elements of the tumor microenvironment (TME) can closely interact and affect cancer cells. Recent studies have confirmed that targeting various TME components possesses a great promise to develop an effective strategy of cancer treatment [5–8].

Hypoxia is a prominent TME attribute featuring a low partial pressure of oxygen as a consequence of the low tumor perfusion and increased demand for oxygen and nutrients in rapidly proliferating cancer cells. There are various statuses of hypoxic conditions depending on the vascularization: moderate or severe, acute or chronic, intermittent or persistent [9]. Hypoxia induces transcriptomic and proteomic alterations, which are critical for the adaptation and survival of cancer cells. Therefore, hypoxia has been linked with a poor prognosis in patients with many types of malignancies, such as bladder, brain, breast, colon, esophagus, head and neck, liver, lung, pancreas, skin, stomach, or uterus cancer, and lymphocytic or myeloid leukemia [10, 11].

Transcriptional responses to the depletion of O_2 are mediated through hypoxia-inducible factors (HIFs). HIFs function as heterodimers composed of an oxygen-labile HIF-1α, HIF-2α, or HIF-3α subunit and a constitutively expressed HIF-1β subunit [12, 13]. The relevant correlation between the over-expression of HIF-1/2α and the aggressive tumor phenotype has been observed [14–16], whereas the mode of HIF-3α action remains to be elucidated because of its dual role of suppressing the HIF-1/2α-mediated gene expression [17, 18] and inducing the transcription of hypoxia-related [19] or unrelated genes [20].

HIF-1, consisting of HIF-1α and HIF-1β subunits, is mostly absent in cancer cells grown in normoxia (Figure 1). The stability of HIF-1 is regulated by prolyl hydroxylase domain-containing protein (PHD), also known as α-ketoglutarate–dependent dioxygenases. Three mammalian isoforms of PHDs (PHD1-3) have been identified with the diverse subcellular localization and tissue-specific expression pattern [21,22]. Hydroxylated on 402 and 564 proline residues, HIF-1α interacts with the ubiquitin E3 ligase domain of von Hippel-Lindau tumor suppressor protein (pVHL), leading to the proteasomal degradation of HIF-1α [23–25]. Moreover, the factor inhibiting HIF-1 (FIH-1) hydroxylates asparagine residue 803 of HIF-1α subunit in O_2-dependent manner, thereby blocking the ability to bind with coactivators CREB-binding protein (CBP) and p300 [26,27].
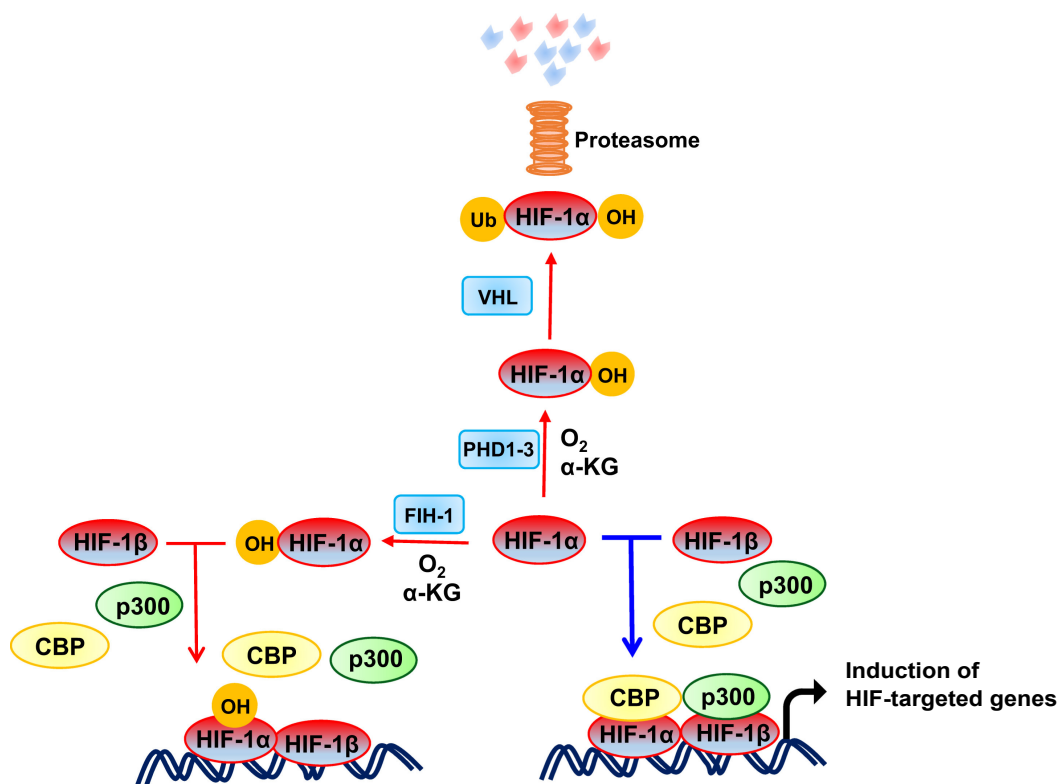
Figure 1: Regulation of HIF-1. Under normoxic conditions, PHD1-3 dioxygenases use O_2 and α-ketoglutarate (α-KG) to hydroxylate HIF-1α, that subsequently is bound by VHL, ubiquitylated, and degraded by the proteasome. In addition, FIH-1 hydroxylates HIF-1α and thereby its interaction with coactivators CBP and p300 is blocked. Therefore, the active transcription complex is not formed. Under hypoxic conditions, hydroxylation reactions are inhibited, stable HIF-1α binds with HIF-1β, recruits coactivators CBP and p300, and induce the transcription of HIF-targeted genes. Red and blue arrows indicate processes occurring under aerobic and hypoxic conditions, respectively (modified with permission from [28]).

Under hypoxia, both previously mentioned pathways of HIF-1α hydroxylation are inhibited. Therefore, the stable HIF-1α dimerizes with HIF-1β. The formed complex enters the nucleus, recruits coactivators CBP and p300, and binds to

hypoxia responsive elements in promoters of numerous genes, whose transcription is crucial for the adaptive response to hypoxia.

2   Adaptive responses by hypoxic tumor cells

Chromatin immunoprecipitation and gene-expression profiling studies have identified more than 1000 cell-specific genes, which are up-regulated in response to hypoxia [11, 29, 30]. Alterations in metabolic pathways of cancer cells belong to a broad variety of HIF-activated adaptive processes, which are important to promote cell survival and drive tumor progression. Upon hypoxic conditions, metabolic reprogramming is provoked by the increased glycolysis and attenuated oxidative phosphorylation. HIF-1 induces the expression of glycolytic enzymes, glucose transporters, and enzymes involved in glycogen synthesis, allowing an efficient storage of glucose as glycogen [31–33]. Such metabolic shift provides less effective, though sustained generation of energy and substrates for the biosynthesis of macromolecules [34, 35], thereby promoting the survival of rapidly proliferating cancer cells. Therefore, glycolytic metabolism is maintained even under well-oxygenated conditions, known as the Warburg effect [36, 37]. Alternatively, some cancer cells rely more on glutaminolysis than glycolysis to generate energy and provide biosynthetic precursors [38, 39].

Owing to oncogenic transformation and regulation of gene expression by HIFs, the vast production and accumulation of lactate, H^+, and CO_2 can compromise cell survival. The structure and activity of enzymes can be drastically affected by changed cellular pH. It may significantly influence cell signaling and metabolism. Thus, a hypoxic and acidic TME might become cytotoxic [40]. Generally, intracellular pH (pH_i, $\sim$7.2) is slightly lower than extracellular pH (pH_e, $\sim$7.4) in normally differentiated cells, whereas cancer cells possess a higher pH_i ($>$7.4) than pH_e ($\sim$6.5–7.1) [41–44]. Such pH gradient reversal is essential for tumor growth [44].

Cellular pH homeostasis under hypoxic conditions is mediated through several membrane-located proteins, which contribute to two major pH-regulating mechanisms: H^+ extrusion and pH_i buffering (Figure 2). The efflux of H^+ is carried out by Na^+/H^+ exchangers (NHEs), vacuolar-type H^+-adenosine triphosphatases (V-ATPases), and monocarboxylate transporters (MCTs). The crucial impact of NHE isoform 1 (NHE1) on tumor development has been shown by significantly decreased rates of tumor growth in xenografts using NHE1-deficient cells [45]. Recent studies have also highlighted the significant role of V-ATPases in malignant tumors. The knockdown of particular V-ATPase isoforms using specific small interfering RNAs (siRNAs) reduced both invasion of cancer cells *in vitro* and metastasis *in vivo* [46–48]. Moreover, the blockade of H^+-coupled lactate

export has emerged as a promising anti-cancer strategy [49, 50]. Recent studies have showed that the knockdown of several MCT isoforms, particularly MCT1 or MCT4, by specific siRNAs significantly impaired tumor growth *in vivo* [51, 52].
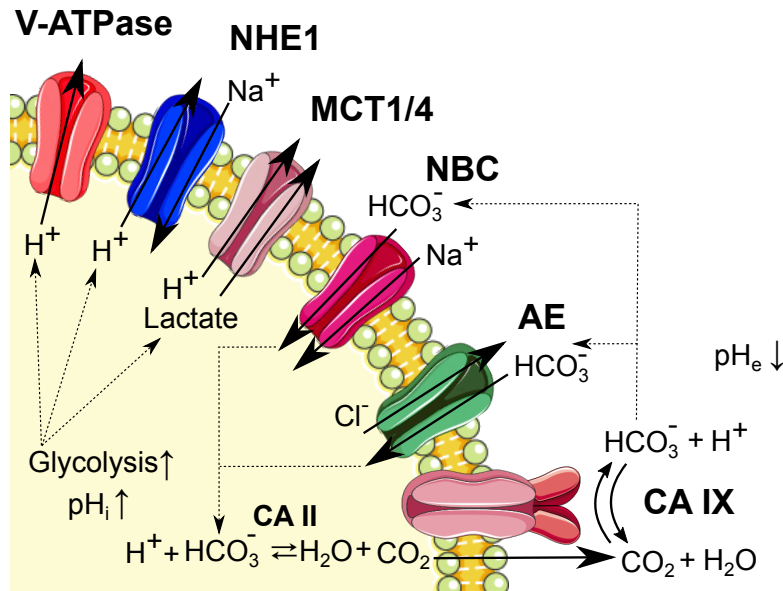
Figure 2: A schematic model of membrane-bound pH-regulatory proteins in the hypoxic cancer cell (drawn not to scale). Major components of this system, that maintains alkaline pH_i ($pH_i\uparrow$) and acidic pH_e ($pH_e\downarrow$), are vacuolar-type H^+-adenosine triphosphatase (V-ATPase), Na^+/H^+ exchanger (NHE) 1, monocarboxylate transporter (MCT) 1/4, Na^+/HCO_3^- co-transporter (NBC), anion exchanger (AE), and carbonic anhydrase (CA) IX. Intracellular CA isoforms, such as CA II, are also involved in the regulation of cellular acid-base balance.

The reversible hydration of pericellular CO_2 to HCO_3^- and H^+ is catalyzed by the extracellular catalytic domain of carbonic anhydrase (CA) IX, which creates CO_2 concentration gradient directed extracellularly and thereby enables passive diffusion of CO_2 across the membrane. CA IX-generated H^+ ions exacerbate the extracellular acidification, whereas HCO_3^- is transported into the cell via Na^+/HCO_3^- co-transporters (NBCs) and anion exchangers (AEs) to alkalize pH_i by binding H^+ ions. This neutralization of H^+ by HCO_3^-, catalyzed by intracellular CAs, such as CA II, allows the generation of CO_2, that diffuses across the membrane and is reconverted to HCO_3^- and H^+ by CA isoforms with extracellularly directed catalytic domain, such as CA IX. Many sodium- and chloride-driven transporters have been reported to interact with CA isoforms and form a metabolon, providing the efficient HCO_3^- flux across the cell membrane [53, 54]. Gene silencing studies have shown that the knockdown of various NBC members via short hairpin RNAs (shRNAs) increased cell mortality *in vitro* and reduced growth of tumor xenografts [55, 56]. Furthermore, the knockdown of AE isoform 2 (AE2) by specific shRNA inhibited the proliferation of cancer cells both *in vitro*

and *in vivo* by inducing G1-phase arrest [57]. To summarize, studies listed in this section indicate the significant importance of specified key pH-regulators to tumorigenesis. The relevance of CA IX to pH control mechanisms in cancer will be discussed in the next section.

3 Human carbonic anhydrases as targets for therapeutic applications

The main function of CAs (EC 4.2.1.1) is the catalysis of the fundamental reversible conversion of CO_2 to H^+ and HCO_3^- ($CO_2 + H_2O \rightleftharpoons HCO_3^- + H^+$), allowing the regulation of both intracellular and extracellular concentrations of these metabolically important ions. The CAs are ubiquitous metalloenzymes categorized into several evolutionarily distinct classes based upon their structural fold and predominant organisms of expression [58–64]. To date, there are fifteen α-CA isoforms in humans, which display diverse sub-cellular localization, tissue-specific expression, and kinetic properties, as summarized in Table 1.

Since the discovery over 80 years ago [2], human α-CAs have gained the most scientific attention due to relevant functions in physiology and pathology. Therefore, this thesis is on human α-CAs, focusing on isoforms CA VI and CA IX, which are highly involved in a broad range of vital processes.

3.1 Carbonic anhydrase VI

The CA enzymatic activity in saliva was observed for the first time in 1946 [68]. This activity in human saliva was later demonstrated to be induced by the novel protein, named as gustin [69]. Independently from the previous study, the enzyme exhibiting CA catalytic function was detected in sheep parotid gland and saliva [70]. This protein was also isolated from saliva of different mammals, such as rats [71] and humans [72], and thereafter identified as CA VI [73].

Among α-CA family, CA VI is the only secreted isozyme produced by salivary parotid, submandibular [74], and lingual von Ebner's glands [75]. The expression of CA VI has also been found in serum [76], milk [77], tears [78], respiratory airways [79], and alimentary canal [80]. Interestingly, Parkkila and colleagues have shown the tight circadian periodicity of the salivary CA VI secretion: low levels were measured during sleep, whereas these levels increased rapidly after awakening and breakfast [81]. In contrast, the intracellular form of CA VI has been reported as an adaptive response to cellular stress to promote viability [82, 83].

The recently solved crystal structure of CA VI has revealed its dimeric arrangement with the active sites of monomers facing each other and directed towards the center of the dimer (Figure 3) [84]. The catalytic zinc ion is located in the active

Table 1: Distribution and catalytic efficiency of human α-CAs [65–67]. k_{cat} - catalytic constant, K_M - Michaelis constant.

Isoform	Sub-cellular compartment	Tissue/organ localization	k_{cat}/K_M ($M^{-1}s^{-1}$)
CA I	Cytosol	Erythrocytes, gastrointestinal tract, eye	5.0×10^7
CA II	Cytosol	Erythrocytes, gastrointestinal tract, eye, osteoclasts, kidney, brain, testis	1.5×10^8
CA III	Cytosol	Adipocytes, skeletal muscle, liver	3.0×10^5
CA IV	Membrane-bound	Kidney, lung, pancreas, brain, colon, heart	5.1×10^7
CA VA	Mitochondria	Liver	2.9×10^7
CA VB	Mitochondria	Heart and skeletal muscles, pancreas, kidney, gastrointestinal tract, spinal cord	9.8×10^7
CA VI	Secreted	Salivary and mammary glands	4.9×10^7
CA VII	Cytosol	Colon, liver, skeletal muscle, brain	8.3×10^7
CA VIII	Cytosol	Central nervous system	Acatalytic
CA IX	Transmembrane	Tumors, gastrointestinal tract	1.5×10^8
CA X	Cytosol	Central nervous system	Acatalytic
CA XI	Cytosol	Central nervous system	Acatalytic
CA XII	Transmembrane	Tumors, kidney, lung, prostate, ovary, uterine endometrium, breast	3.5×10^7
CA XIII	Cytosol	Thymus, kidney, submandibular glands, small intestine, reproductive organs	1.1×10^7
CA XIV	Transmembrane	Brain, kidney, colon, small intestine, urinary bladder, liver, heart, spinal cord	3.9×10^7

site of each monomer. The dimer complex is stabilized via 11 hydrogen bonds and an intramolecular disulfide linkage between 42 and 224 cysteine residues, suggesting the explanation for retained enzymatic activity in the harsh environment of gastric lumen [85, 86].

Several groups have reported investigations of modulating the catalytic activity of CA VI *in vitro* by both activators, such as certain amino acids and amines [88], and inhibitors, including sulfonamides with incorporated sugar moieties [89]. However, there is still a high demand for effective and selective CA VI inhibitors. They would be important to understand the exact physiological role of CA VI, that still remains uncertain. Several studies have presented the association of CA VI

Figure 3: The dimeric assembly of human CA VI (PDB ID: 3FE4). Surface of two CA VI monomers are shown in different colors (purple and rose). The zinc ion in each active site is indicated by an arrow and shown as a red sphere. Graphic representation was made with Pymol [87].

with the regulation of taste perception, especially its bitter modality, [90–92] and the protection of excess acidity-caused dental caries [93, 94] and injuries of the esophageal or gastric epithelium [85]. High amounts of CA VI have been detected in the colostrum milk, which is delivered to the infantile alimentary tract during the early postnatal period, thus, suggesting CA VI to be an essential factor for the maturation [77]. Links of CA VI with certain cancers, such as that of salivary glands, have been speculated by gene comparison studies, which have shown the close relation of CA VI with CA IX, a marker of tumors [95].

Proposed hypotheses can already be investigated *in vivo* by using recently generated CA VI-deficient mice, which are viable, fertile, and have normal life spans [96]. Neither morphological abnormalities of the salivary, lacrimal, mammary glands, nor the transcriptional up-regulation of other active CAs are found in this knockout (KO) mouse model. Notably, CA VI deficiency induces the increase of lymphoid follicles in intestinal Peyer's patches [96] and alterations of antigen transfer to the lymphoid tissue as compared with wild-type (WT) mice [97], indicating the immunological function of CA VI.

3.2 Carbonic anhydrase IX

CA IX belongs to the family of α-CAs as the zinc-containing glycoprotein, that contributes to maintening the cellular pH balance. This CA isoform was discovered in 1992 as a tumor-associated antigen, originally called MN, in human cervical carcinoma cell line of HeLa using monoclonal antibody (mAb) M75 [98]. The

MN identification was followed by the analysis of its cDNA [99] and gene [100] sequences. Results of these studies revealed the highly conserved CA catalytic domain, thus, allowing the classification of MN as the ninth member of CA family. Therefore, MN was renamed to CA IX. Another research group found a renal cell cancer-linked antigen, termed G250 [101], that was later demonstrated to be identical to CA IX [102].

Mature CA IX consists of an N-terminal proteoglycan-like domain (PG), a conserved CA catalytic domain, a hydrophobic membrane-spaning helix, and a short intracytoplasmic tail at the C-terminus [100]. The PG domain is homologous to the keratan sulfate binding domain of a large proteoglycan, known as aggrecan [100]. Being absent from other human CA isozyme, the PG region represents a distinctive feature of CA IX. It is recognized by mAb M75, that binds to the repetitive epitope in this area and therefore enables selective detection of CA IX among other CAs [103]. The cytoplasmic tail of CA IX contains three phosphorylation sites and is important for the regulation of the enzymatic activity and signaling [104, 105]. Due to the alternative splicing, the expression of shorter CA IX has been described [106, 107].

The monomeric form of CA IX is visualized as a 54/58 kDa double band by immunoblotting in reducing conditions, whereas the trimeric CA IX have been previously observed under non-reducing conditions [98]. The subsequently resolved crystal structure of the recombinant CA IX suggested the homodimeric state of CA IX [108]. In this complex, two catalytic domains of CA IX are associated and stabilized via the intermolecular disulfide bond.
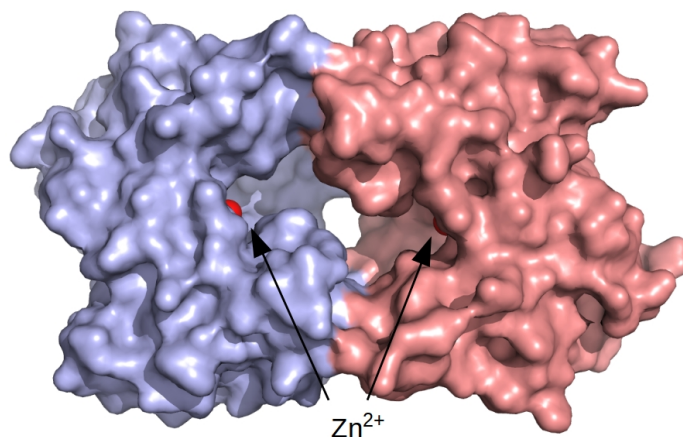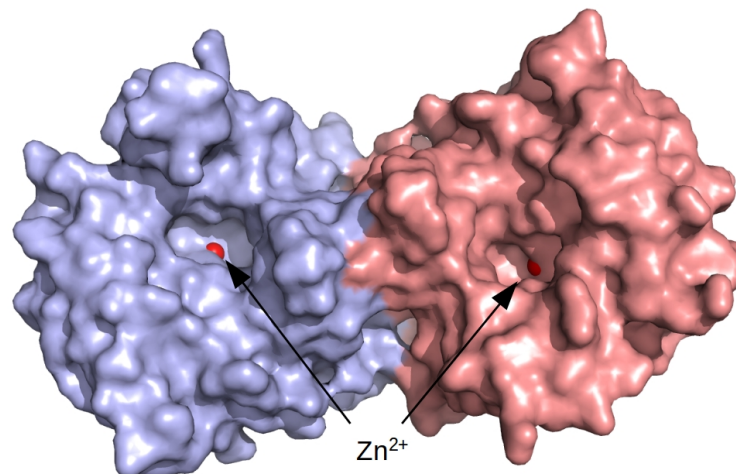

Figure 4: The dimeric catalytic domain of human CA IX (PDB ID: 3IAI). Surface of two CA IX monomers are shown in different colors (purple and rose). The zinc ion in each active site is indicated by an arrow and shown as a red sphere. Graphic representation was made with Pymol [87].

The expression pattern proposes CA IX to be a potential cancer-specific target. In normal tissues, the transmembrane CA IX is only found in the epithelia of gastrointestinal tract [109]. However, CA IX is over-expressed in a wide spectrum of solid tumors including malignancies of the brain, kidney, colon, head and neck, lung, breast, esophagus, ovary, and liver [110–112]. The transcription of *CA9* gene is strongly induced in a HIF-dependent manner [113] and can be regulated by other pathways [114–117]. Alternatively, CA IX also exists as a shed ectodomain (ECD), circulating in the body fluids of cancer patients [118]. ECD is composed of CA catalytic and PG domains and is formed as a stimuli of signal transduction after the cleavage by metalloproteinases, namely, TACE/ADAM17 [119]. Hence, the detection of ECD has been proposed to possess prognostic applications, but its clinical significance is inconclusive so far [120–123].

The functional contribution of CA IX is mainly directly linked with its catalytic activity. Through the conversion of CO_2 to HCO_3^- and H^+, CA IX significantly facilitates both the acidification of pH_e and the alkalization of pH_i, which are critical for cancer progression. The elevated levels of extracellular H^+ lead to the tumor aggressiveness-promoting acidosis [124], while the generated HCO_3^- ions are imported into the cell to maintain a moderately alkaline pH_i and thereby assure cell survival [125, 126]. Conversely, CA IX has been recently reported to undergo nuclear translocation and interact with proteins involved in nucleo-cytoplasmic transport, implying the still unknown functionality of the intracellular CA IX that might be different from the catalytic CA IX role at the cell surface [127].

In vitro and *in vivo* studies have indicated that the depletion of CA IX expression or its enzymatic activity results in the increase of cancer cell death and the attenuation of primary tumor growth. The negative effect on viability has been shown in human cancer cells after the exposure to CA IX selective inhibitors, which reduced the extracellular acidification [128–130] or caused intracellular acidification [131] under hypoxic conditions. The decreased cell growth and clonogenic survival have also been described as a consequence of depleted CA IX via RNA interference [132]. The over-expression of CA IX has been associated with the increased growth rate in spheroids [126]. In mouse models, the reduced growth rates of tumor xenografts have been observed when CA IX was knocked down by shRNAs [126, 133, 134] or knocked out using CRISPR-Cas9 system [135]. Moreover, CA IX has been associated with several stem cell markers [136] and the inhibition of CA IX has been reported to reduce the expansion of cancer stem cells and thereby diminish tumor growth and metastasis [137]. Interestingly, the partial compensatory mechanism of CA IX knockdown by the up-regulation of CA XII has been demonstrated [126, 133, 135], emphasizing the cross-talk between CAs to maintain pH homeostasis.

During migration, the essential pH gradients are created inside and outside

the cell by several pH regulators, including CA IX. The pH$_i$ is more alkaline in the front than at the end of migrating cells, while pH$_e$ is acidic on the outer side of the membrane [138]. Recent studies have indicated the localization of CA IX in lamellipodia, where it promotes migration via the catalytic activity, enhances the bicarbonate uptake by interacting with specific transporters [54], and directly regulates collagen degradation mediated by the matrix metalloproteinase isoform 14 [139]. CA IX also modulates the cell-cell adhesion by competing with E-cadherin for binding with β-catenin, causing the detachment of E-cadherin from the cytoskeleton and thus supporting cell motility [140]. Furthermore, CA IX has been found to be involved in PI3K/Akt [104], FAK/PI3K/mTOR [141], and Rho/ROCK [142] signaling pathways, which can influence migration rates. The elimination of CA IX using selective inhibitors or gene silencing methods has been shown to reduce the invasive phenotype of cancer cells *in vitro* and *in vivo* [134, 139, 143, 144].

3.3   Roles of other carbonic anhydrase isoforms

Next to pH regulation, there is a wide spectrum of physiological processes depending on the function of other human CAs, excluding previously discussed CA VI and CA IX. CA isozymes are involved in bone resorption, calcification, respiration, signal transduction, electrolyte secretion, biosynthetic reactions (e.g., gluconeogenesis, lipogenesis, and ureagenesis), and many others [66, 145]. Therefore, abnormal CA levels or their activities are commonly related with various human diseases.

The cytosolic CA I is expressed in diverse tissues, including red blood cells and eye. The significantly lower expression of CA I in patients than in control group has emerged as a marker for hemolytic anemia, when erythrocytes are prematurely destroyed [146]. Moreover, the correlation between high levels of the extracellular CA I and prognosis of the vision-impairing disorders, namely, macular edema or retinopathy, has been described, as a consequence of the increased retinal vascular permeability [147]. Two studies have shown that CA I plays a significant role in patients with ankylosing spondylitis, a condition of abnormal bone formation in the spine and joints [148, 149]. This chronic inflammatory disease has been characterized by over-expression of CA I, that enhances CO_2 hydration rate leading to the improper calcification. Due to increased production, CA I has been proposed to be a potential biomarker for prostate cancer [150]. On the other hand, significantly lower levels of CA I have been detected in colon epithelium as compared with normal tissues, serving the indicative marker for prediction of colorectal cancer [151].

Among the family of human CAs, the cytosolic CA II has the highest distribu-

tion in tissues and organs. CA II has been linked with numerous pathologies, such as glaucoma [152, 153], edema [154, 155], epilepsy [156, 157], atherosclerosis [158], and osteoporosis [159]. CA II has been also involved in acute mountain sickness caused by the lack of oxygen at high altitude with symptoms of headache, nausea, anorexia, and gastrointestinal distress [160, 161]. The over-expression of CA II has been detected in certain forms of cancers [162, 163], whereas the CA II deficiency has been reported as the recessive syndrome with increased bone density, renal tubular acidosis, cerebral calcification, and growth retardation [164].

The cytosolic CA III is a member of human CAs, that exhibits the lowest catalytic activity to catalyze CO_2 hydration (Table 1). The expression of CA III is limited to highly metabolically active tissues, involving skeletal muscles, adipose tissues, and liver. CA III possesses two surface cysteine residues, which can be glutathionylated, thereby providing the protection from oxidative stress [165], as confirmed in cells of myeloid leukemia [166]. Due to increased levels as compared with control tissue, CA III has been introduced as a biomarker for several neuromuscular disorders [167], whereas significantly reduced amounts of CA III have been indicated upon the progression of liver carcinoma [168] and hepatitis infection [169]. Furthermore, adipogenesis has been significantly enhanced in CA III-deficient mice, revealing an important role of CA III in modulating obesity [170].

CA IV is attached to the membrane via a glycosylphosphatidyl-inositol anchor and located on the extracellular surface of cells. CA IV is a structurally unique isoform due to two intramolecular disulfide bonds, which make CA IV to be remarkably stable due to the resistance to high concentrations of sodium dodecyl sulfate, thereby allowing CA IV to be purified without contamination by other CAs [171, 172]. Mutant forms of CA IV have been associated with retinitis pigmentosa - the disease of retinal degeneration induced by the accumulation of a misfolded CA IV that can lead to blindness [173, 174]. The expression of these CA IV mutants has been demonstrated to cause progressive renal injuries, as shown in transgenic mice [175]. Interestingly, the functions of CA IV in suppressing colon cancer development [176], accelerating the wound healing [177], and sensing the taste of carbonated beverages [178] have been recently identified.

Both CA VA and CA VB isozymes are present in the mitochondrial matrix of distinct tissues. CA VA is primarily produced in the liver [179], whereas CA VB is found in the heart and skeletal muscles, kidney, pancreas, gastrointestinal tract, and spinal cord [180]. Since the mitochondrial membrane is impermeable to HCO_3^- [181] and no transporters for the uptake of HCO_3^- are found in the inner mitochondrial membrane [66], *de novo* synthesis of HCO_3^- catalyzed by CA VA and CA VB within the mitochondria is crucial to provide the substrate for enzymes, which participate in lipogenesis [182], ureagenesis [183], and gluconeoge-

nesis [184]. The mitochondrial CAs have been linked with obesity [185], insulin resistance [186], and oxidative stress in the brain [187, 188].

The cytosolic CA VII is distributed in colon, liver, skeletal muscle, and brain [189]. Like CA III, CA VII contains several reactive cysteines, which can be glutathionylated, suggesting its function in mechanisms of cell defense against oxidative damage [190]. CA VII has been demonstrated to drive the neuronal excitation by generating HCO_3^- ions, which mediate the current via channels coupled to $GABA_A$ receptors [191, 192]. Therefore, CA VII has been shown to play a role in neurological disorders, such as epileptic seizures [193] and neuropathic pain, known for a shooting or burning sensation resulting in the nerve damage [194].

CA XII is a transmembrane protein, which exists as a dimer with active sites oriented on the extracellular space [195]. The transcription of gene encoding for CA XII can be regulated by hypoxia [110] and estrogen receptors [196, 197]. In contrast to CA IX, CA XII is present in many healthy tissues [198–201]. CA XII has been also identified as a tumor marker [198]. The increased expression of CA XII has been described as a prognostic marker of a lower grade disease leading to a better prognosis only in breast cancer [202], whereas the over-expression of CA XII in other multiple tumors has been related with poor prognosis [110, 163, 200]. The alternatively spliced form of CA XII has been detected in brain tumors and is associated with a poor patient survival [203]. The knockdown of CA XII has exhibited promising antitumor results [204, 205]. The implication of CA XII has been also found in patients with glaucoma [206] and chronic back pain [207]. Furthermore, mutant forms of CA XII have been linked with cystic fibrosis-like syndrome [208] and salt wasting disease [209, 210], which both are characterized by a high concentration of chloride in sweat.

The cytosolic CA XIII is a monomeric protein [211] localized in thymus, kidney, submandibular gland, small intestine, and is notably abundant in reproductive organs of both sexes, emphasizing the physiological function in fertility [212]. It is speculated that CA XIII controls the optimal HCO_3^- concentration and pH homeostasis for sperm motility and thereby contributes to reproductive processes [212]. Moreover, the down-regulated levels of CA XIII have been observed in colorectal cancer [213].

The monomeric CA XIV belongs to the group of transmembrane CA isoforms and contains the extracellular active site [214]. CA XIV is present in brain, kidneys, colon, small intestine, urinary bladder, liver, heart, and spinal cord [215–217]. CA XIV has been demonstrated to be essential for the normal retinal light response [218] and the intracellular [219] and extracellular pH regulation in the central nervous system [220]. In hypertensive rats, the elevated amounts of CA XIV has been found in the hypertrophic myocardium [221].

Three cytosolic isozymes CA VIII, CA X, and CA XI are named as CA-related

proteins (CARPs). They lack one or more of histidine residues that coordinate the catalytic zinc ion in the active site and therefore are inactive to catalyze the reversible CO_2 hydration [222, 223]. CARPs are predominantly expressed in central nervous system [224, 225]. Mutant CA VIII forms have been associated with ataxia, mental retardation, and quadrupedal gait in humans [226] or the lifelong gait disorder in mice [227]. The knockdown of CA VIII in zebrafish has been shown to cause defects in motor coordination, as it is common to the ataxic human phenotype [228]. The increased levels of CA VIII and CA XI have been indicated in certain tumors [229–231]. CA X has been proposed to be involved in neurological disorders [232, 233].

To summarize, CA dysregulation has been linked with many pathological states in human body. Therefore, there is a need to develop the CA isoform-selective compounds exhibiting sufficient affinity and selectivity properties. They would be suitable for the translation into the clinic because they would be therapeutically beneficial and avoid causing undesired side effects due to off-target CA inhibition.

3.4 Strategies for modulating activities of carbonic anhydrases

The design of CA-specific compounds is a challenging task because of the high structural homology among human CAs, especially within their active sites [67]. The crystal structures of human recombinant CA isoforms, except for mitochondrial CA VA and CA VB, have been determined [84, 108, 195, 211, 214, 234–238], indicating diverse oligomeric states: CA isozymes are monomers, except for CA VI, CA IX, and CA XII which are dimers. Monomers of each active human CA were overlayed in Figure 5A. The analysis of these complexes has revealed that the catalytic domain of each human CA typically consists of a central antiparallel β-sheet surrounded by 7 α-helices. The active site is positioned in a cone-shaped cavity where catalytic zinc resides at the bottom and is tetrahedrally coordinated by three conserved histidine residues and a water molecule/hydroxide ion. The active site also contains hydrophobic and hydrophilic sides (Figure 5B), which are responsible for orienting CO_2 for nucleophilic attack by the zinc-bound hydroxide and creating a hydrogen-bond network for the proton shuttle from the zinc-bound water molecule to the solvent [239, 240]. The core of active site is highly conserved among human CAs. However, residues of its periphery (10 Å–15 Å from the zinc) are variable in terms of the polarity and hydropathicity [67, 241]. This part of the active site, defined as the selective pocket (Figure 5B), has been exploited to design the chemical compounds targeting the specific CA isoform, that is related to the certain disease.

The modulation of the increased human CA levels or catalytic activities by

chemical compounds has been extensively studied [145, 242]. Five different mechanisms of CA inhibition have been identified so far [243]. In this thesis, the research interest is devoted to the derivatives of primary sulfonamides. They are classical CA inhibitors, which directly interact with the catalytic zinc and displace the zinc-bound water/hydroxide ion [145, 244].
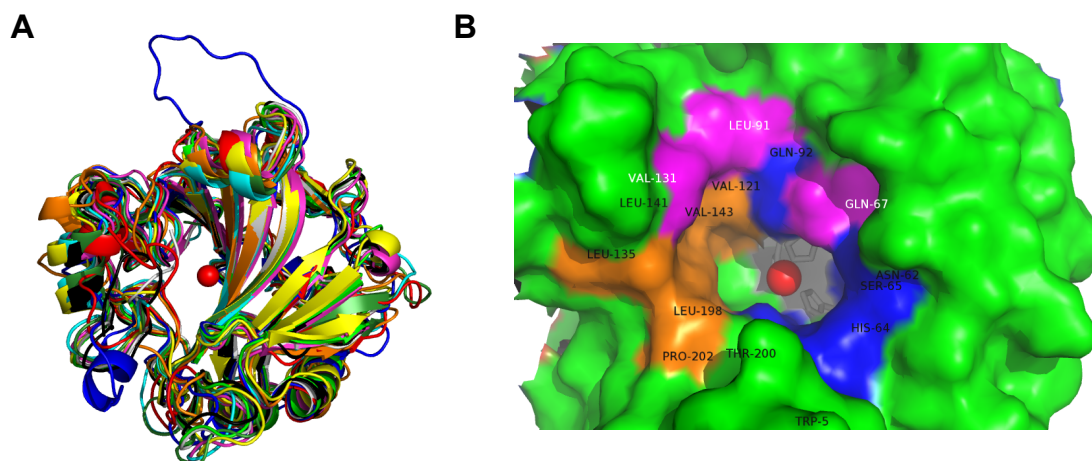
Figure 5: (A) Overlay of catalytically active human CA monomers, which are currently available. PDB IDs: 1HCB for CA I (yellow), 3KS3 for CA II (green), 1Z93 for CA III (magenta), 1ZNC for CA IV (blue), 3FE4 for CA VI (orange), 3ML5 for CA VII (grey), 3IAI for CA IX (red), 1JCZ for CA XII (dark green), 3D0N for CA XIII (black), and 4LU3 for CA XIV (cyan). (B) Surface representation of human CA IX monomer (PDB ID: 3IAI). Hydrophobic and hydrophilic regions of active site are indicated with black labels and colored in orange and blue, respectively. Residues of selective pocket are shown in pink with white labels [67]. The catalytic zinc is shown as a red sphere, which is coordinated by three histidine residues specified in grey. Graphic representations were made with Pymol [87].

Several classes of non-classical CA inhibitors have been developed [245]. The CA inhibitors anchoring to the zinc-bound water molecule/hydroxide ion have been reported, including phenols [246], polyamines [247], carboxylates [248], sulfocoumarins [249], and 2-thioxocoumarins [250]. For the carboxylic acid derivative, the binding outside the active site has been described [251]. Moreover, the alternative inhibition mode has been observed for coumarins and their isosteres, which occlude the entrance to the cavity of CA active site by binding near or within the selective pocket [252, 253]. Lastly, several compounds with the unknown CA-binding manner have been found, such as secondary/tertiary sulfonamides [254], imatinib/nilotinib [255], and fullerenes [256].

The low level or insufficient catalytic activity of human CAs is also linked with pathological states, as described in 3.3 subsection. Therefore, many studies have explored CA activators, generally amines, amino acids, and oligopeptides, as promising agents with pharmacological applications [145, 257, 258]. The first crystal structure of the CA-activator adduct was published in 1997 [259]. It con-

firmed that CA activators bind at the entrance of the CA active site and assist the proton shuttling between the zinc-bound water molecule and the environment, thereby enhancing the catalytically activity via the generation of the zinc-linked hydroxide for nucleophilic attack of CO_2.

Diverse strategies to deliver CA activators or inhibitors have been described with the aim to target the disease-related CA isoform for the therapy and diagnostic imaging. Thus, numerous probes have been reported, including fluorescent labels [128, 260], radiolabels [261], absorbers of near-infrared light [262], and nanomaterials [263]. Although the vast library of CA-targeting compounds has been designed, only several chemical derivatives have progressed to clinical trials (discussed in subsection 4.2).

3.5 Zebrafish and *Xenopus* oocytes in carbonic anhydrase research

In the preclinical studies of drug development, screens using animal models are essential to uncover new compounds and characterize their important properties, such as efficacy, distribution, and toxicity. Commonly, large-scale toxicology studies before entering a clinical safety trial are focused on a rodent (rats) and a non-rodent (beagle dogs) species. However, such experiments are expensive and time-consuming. Therefore, several alternative animal models, including zebrafish and *Xenopus laevis* (*X. laevis*), have been introduced in biomedical research.

Zebrafish

The zebrafish has emerged as a valuable tool in drug discovery [264, 265]. For toxicological studies, the zebrafish model has been applied for more than 60 years [266, 267]. Recently, the National Institutes of Health has assessed zebrafish as the third most relevant experimental organism after rats and mice, while FDA has accepted the assessments of toxicity in zebrafish for investigative approvals of novel drugs [268]. Several compounds, which have been primarily discovered from zebrafish chemical screens, are being investigated in clinical trials [269–272].

The zebrafish model greatly contributes to the phenotype-based drug screening. There are several significant advantages of using the phenotype-driven approach. First, phenotypic screens are able to identify the therapeutic compounds even though the target is not validated yet. Second, phenotype-driven approaches determine compounds, which benefit from activity at diverse targets simultaneously. Third, phenotypic screens allow the detection of more promising compounds than target-based approaches due to apprising its both curative and harmful properties at the same time. Consequently, the minimum optimization of pharmacological properties is required for the translation of compounds to other mammalian

models [264, 272].

In the high-throughput screening, zebrafish exhibits numerous advantages, such as transparency of embryo and larva, external fertilization, easy manipulations, regenerative capacity, high fecundity, and relatively rapid development. Zebrafish also offers cheaper experimental cost and lower amount of compound consumption [268]. Despite the lack of a few mammalian organs, zebrafish shares a highly conserved but not absolutely identical physiology and anatomy with mammals [264]. The genome of zebrafish has been sequenced, showing the set of over 26 000 protein-coding genes [273]. Approximately 70 % of human genes have been defined to possess at least one zebrafish orthologue [274]. Therefore, zebrafish has become a convenient and relevant vertebrate model for human drug discovery.

The zebrafish screens of inhibitors, which target human CAs, is a relatively novel scientific topic with a few reported studies. In 2009, the exposure of zebrafish to the membrane-impermeable human CA inhibitor F3500 was described for the first time [275]. Phenotypical abnormalities of zebrafish induced by the treatment with acetazolamide (AZM), a non-selective CA inhibitor, were thereafter published [276]. It was followed by the investigation of zebrafish developmental toxicity caused by common CA inhibitors, which are applied in clinics [277]. Subsequently, the roles of zebrafish CA isozymes, including acatalytic CAs [228, 278], CA II [279–281], and CA VI [282], were explored during zebrafish development by using gene silencing methods. These studies provided phenotypic characteristics of zebrafish with the inactivated CA isoform and/or suggested the relevant information about the structure and biological functions of the CAs in mammals and non-mammalian organisms.

Xenopus oocytes

Originated in South Africa, the clawed frog of *X. laevis* has been widely used as an animal model in the molecular and physiological research. Until the 1960s, *X. laevis* was applied for a rapid diagnosis of early pregnancy and thereby became as a regular laboratory animal [283]. Nowadays, *Xenopus* oocytes are often employed as a model system because they possess many advantages, such as easy manipulations due to the big cell size (1.1 mm–1.3 mm), a convenient laboratory maintenance, and a large number of offsprings [284].

Importantly, *Xenopus* oocytes enable the study of diverse eukaryotic proteins due to the efficient transcription and translation of the exogenous nucleic acid into protein. The production of functionally active exogenous protein in oocytes is carried out by nuclear injections of cDNA or mostly by cytoplasmic injections of *in vitro* synthesized cRNA [285]. However, the developmental stage of oocyte has been shown to influence the activity of the heterologously expressed proteins. To overcome this drawback, oocytes at the developmental stages IV to VI are used

for the experiments when they have been demonstrated to possess the highest translational capacity [286]. Furthermore, native *Xenopus* oocytes contain a variety of endogenous ion channels and membrane transporters [287]. However, their activities are relatively low as compared with heterologous proteins [288]. Thus, results of electrophysiological measurements obtained in *Xenopus* oocytes are not affected by the activity of endogenous proteins, thereby making these cells to be a versatile tool in a wide spectrum of biological and biochemical applications.

Native *Xenopus* oocytes feature undetectably low level of CA activity [289]. Therefore, the injections of cRNA coding for a certain human CA isozyme into these cells allow the expression of the target CA and investigation of CA inhibition in the live biological system. The affinity and selectivity of compounds against target CA isoform heterologously expressed in oocytes can be monitored with microelectrodes by measuring the pH in the cytosol and at the outer membrane surface and additionally determined by mass spectrometry (MS) [284]. Recently, significant inhibitory properties of $10\,\mu M$–$30\,\mu M$ ethoxzolamide (EZA), a membrane-permeable and non-selective CA inhibitor, against CA II [290], CA IV [291], and CA IX [292] have been described in oocytes. Moreover, oocytes have been used to reveal the non-catalytic function of CA II [293], CA IV [294], and CA IX [295] linked with the ability to enhance activities of diverse MCTs isoforms and thereby increase lactate flux. This function remained not affected by EZA which is known as CA inhibitor. Based on the listed observations, *Xenopus* oocytes are promising models to study roles of CAs and characterize the affinity and selectivity of human CA inhibitors in the living eukaryotic cell with fully matured target CA isozyme.

4 Compound discovery and development toward anti-cancer drugs

Over the years, tremendous resources have been invested to discover, develop, produce, and trade numerous compounds as efficient medicines. In the pharmaceutical industry, the bringing a new molecule to the market is a long, complicated, high risk, and expensive task. It can take 10–15 years with the cost per drug launch recently estimated to exceed $2.6 billion [296]. The discovery of a drug-candidate is flexible and depends on the creativity, whereas the drug development is planned and highly structured with regulations introduced by the US Food and Drug Administration (FDA) and the European Medicines Agency (EMA) [297].

4.1 Stages of drug development

The process of drug discovery and development includes many stages, such as the lead compound identification, its optimization, preclinical testing, clinical trials,

and FDA approval (Figure 6). At the beginning of a project, new drugs can be discovered by the phenotype- or target-based approach [298,299]. Phenotypic screenings permit the identification of compounds against targets, which are unknown so far. This approach was predominant in 1970s-1990s [297]. Owing to advances in molecular biology, the application of the target-based drug discovery has increased during the last three decades [299]. It analyzes interactions between the compound and the molecular target linked with disease. Comparison of both approaches for drugs approved by FDA from 1999 to 2008 has demonstrated that phenotypic screenings were more predictive for the discovery of first-in-class drugs [264,300]. They differ from existing medicines by modulating the unprecedented target or biological pathway [301]. However, the target-based approach was more successful for following, nearly five times higher amount of drugs, which were discovered during the previously mentioned period. Therefore, the target-driven drug discovery has been actively pursued with over 1300 companies in the United States focusing on molecular targets, of which over half are for cancer treatment [302].
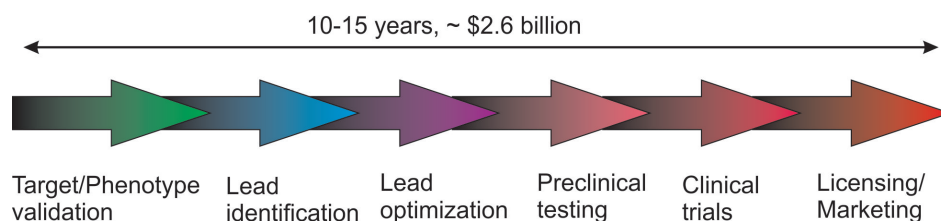
Figure 6: A general scheme for drug discovery and development showing the important stages of drug progress to the market [296].

Nowadays, numerous methods of high-throughput screening are employed to identify and optimize hits toward the biological target *in vitro*. The interest in large-scale techniques for the thermodynamic profiling of biomolecular interactions has recently increased [303]. These approaches significantly contribute to the analysis of structure-activity relationship that provides valuable information in medicinal chemistry for the rational drug design to generate the lead compound [304].

During preclinical development, sufficient quantities of the drug candidate are produced to evaluate its quality, efficacy, and safety before testing in humans. Screenings in cell cultures and animal models are involved in this stage. Anti-cancer compounds are usually investigated *in vitro* by using viability and clonogenic survival assays, which are followed by *in vivo* studies in xenograft mouse models [302]. For instance, the National Cancer Institute in United States has a rule to test new compounds for cytostatic or cytotoxic activity against eight cancer cell lines, which represent the most common human malignancies, and then start studies in xenograft mice depending on *in vitro* results [302].

If preclinical testing is successful, clinical development of a drug candidate

begins. There are at least three major distinct phases of clinical research. In phase I clinical trials, safety is determined in non-curative patients using a specific dose escalation concept. Subsequently, phase II studies are conducted in patients to assess efficacy of the compound and confirm the dosage. Phase III studies are carried out to proof that drug candidate combined with the standard treatment is more therapeutically beneficial than the standard treatment alone. If no benefit of the combined therapy is obtained, the standard of care remains to be applied in clinical practice. In phase III studies, a larger population, typically up to a few hundred patients, is involved. Upon completion of the phase III studies, a New Drug Application form is filed by the pharmaceutical company and submitted to FDA for the grant of marketing authorization [297]. If the life cycle of a candidate compound does not fail at any stage listed in this subsection, it becomes available as a drug on the market.

4.2 Clinical trials targeting pH regulators in cancer cells

The pH-modulating mechanisms have been shown to be essential for tumor progression and therapeutic resistance. Therefore, pH regulators have emerged as promising targets for cancer therapy. In the last decade, several chemical molecules and antibodies interfering with MCT1, V-ATPase, or CA IX in tumor cells have been developed and are at various stages of clinical development. The relevant clinical trials are listed in Table 2.

Significant efforts are dedicated to impair the lactate transport across the plasma membrane by targeting MCT members in cancer cells. Currently, there is a phase I clinical trial for MCT1 inhibitor AZD3965. It has demonstrated great anti-cancer effects *in vitro* and *in vivo* and increased sensitivity to radiation in preclinical studies [305, 306].

The V-ATPases have also become attractive therapeutic targets due to the role in the active transport of H^+ out of the cell by using ATP. Proton pump inhibitors (PPIs) are often applied to inhibit V-ATPases. These compounds are acid-activated prodrugs [307] which are clinically used for many years to treat acid-related disorders [308]. Recently, PPIs have been reported to significantly suppress tumor growth in xenograft mouse models [309, 310] and overcome acid-related chemoresistance [311]. These findings have resulted in multiple clinical investigations of diverse PPIs, such as esomeprazole, pantoprazole, and omeprazole, assessing their efficacies, either alone or in combination with standard chemotherapy, to treat patients with different types of malignancies.

In recent years, CA IX has appeared as a vital regulator of tumor development, as described in subsection 3.2. Therefore, a vast collection of derivatives against CA IX have been designed [145, 312]. Two approaches have been applied

Table 2: Drug candidates which undergo clinical trials targeting MCT1, V-ATPase, or CA IX for the treatment of patients with different types of tumors.

Target	Compound	Type of cancer	Phase	Identifier
MCT1	AZD3965	Solid tumors, prostate cancer, gastric cancer, diffuse large B cell lymphoma	Phase I	NCT01791595
V-ATPase	Esomeprazole	Esophageal cancer	Phase III	NCT00357682
		Breast cancer	Phase I	NCT00849329
	Pantoprazole	Prostate cancer	Phase II	NCT01748500
		Solid tumors	Phase I	NCT01163903
	Omeprazole	Colorectal cancer	Phase II	NCT02518373
		Breast cancer	Phase II	NCT01069081
CA IX	SLC-0111	Solid tumors	Phase I	NCT02215850
	cG250	Clear cell renal cell carcinoma	Phase III	NCT00087022
	^{124}I-cG250	Clear cell renal cell carcinoma	Phase III	NCT00606632
	3ee9-MMAE	Solid tumors	Phase I	NCT01028755

to target CA IX: chemical molecules and monoclonal antibodies (mAb). Several agents belonging to each group have entered clinical trials. SLC-0111 is the ureido-substituted benzenesulfonamide derivative that has finished the phase I clinical trial and is scheduled for the phase II trial [312]. Furthermore, girentuximab (cG250) is the most clinically studied mAb for targeting CA IX in clear cell renal cell carcinoma. Even though results of cG250 in phase I and II trials have been favorable [313, 314], its development as a therapeutic has failed in phase III trials owing to the lack of efficacy to improve the disease-free survival [315]. For tumor radioimmunodetection, cG250 has been labeled with various radionuclides, including ^{124}I, ^{111}In, ^{89}Zr, ^{131}I, ^{90}Y, and ^{177}Lu, and such macromolecular radiotracers are in the preclinical/clinical development [261]. Among them, cG250 radiolabeled with ^{124}I has been recently validated in a phase III study as the imaging biomarker for clear cell renal cell carcinoma [316]. Moreover, the conjugate of CA IX-targeting mAb 3ee9 and monomethyl auristatin E, an anti-mitotic agent, has been recently reported to exhibit anti-tumor efficacy in several xenograft models [317] and have progressed to the phase I clinical trial.

The alternative strategy based on the simultaneous targeting of several proteins involved in H$^+$ flux has been proposed. Recently, the combination of lansoprazole with CA IX inhibitors, such as the sulfamate S4 or the ureido-sulfamate derivative FC9-399A, has been shown to be more effective than single treatments in inducing

cytotoxicity of human melanoma cells [318]. However, the synergistic effects of NHE1 and CA IX combined knockout have not been observed *in vivo*, potentially due to the increase in CA XII expression, as compensatory pH-regulating protein [135]. Moreover, the combined inhibition of MCTs with NHE1 or CA IX have not improved the impact on cancer cell death *in vitro*, as compared with single inhibition [49].

In conclusion, tumor acidosis is important to maintain a malignant phenotype and provide both challenges and opportunities for drug discovery. The key drivers of pH-regulation have become clinically relevant anti-cancer targets. However, there is still a demand for efforts toward better understanding of the molecular basis for pH-dependent cell behavior to improve cancer management and patient outcomes.

Methods

5 Protein production

5.1 Production of the native carbonic anhydrase VI

The native CA VI was purified from a half-liter of human saliva collected from 10 volunteers. The participants were males and females aged 20-44. The experiments were undertaken with the understanding and written consent of each subject. The study methodologies conformed to the standards set by the Declaration of Helsinki. The study methodology was approved by the ethics committee of the Institute of Biotechnology (Protocol number 2014/06/25, No. 63). Approximately 5 mg of native CA VI was obtained. Affinity chromatography was repeated twice in order to get high purity protein. The native CA VI was purified according to previously described procedure [74].

5.2 Production of the recombinant carbonic anhydrase VI

The cDNA encoding human CA VI from 21 to 290 amino acids was amplified by polymerase chain reaction (PCR) from CA VI gene (RZPD Deutsches Ressourcenzentrum für Genomforschung) using forward primer with NdeI recognition site (5′ CCAGCATATGTCTGACTGGACCTAC 3′) and reverse primer with XhoI recognition site (5′ CTTATGCTCGAGTTACTGGAATTCAGAGCC 3′). The PCR product was cloned into the bacterial expression vector pET-15b (Novagen) via NdeI and XhoI restriction sites fusing a 6×His-tag to the N-terminus of the protein. The resultant recombinant CA VI lacked the N-terminal signal peptide and 18 amino acids of C-terminus. Expression of recombinant CA VI was carried out in *Escherichia coli* (*E. coli*) Rosetta^{TM} 2 (DE3) strain (Novagen). A colony of transformed cells was transferred to brain heart infusion (BHI) medium, containing $100 \, \mu g \, mL^{-1}$ ampicillin and $34 \, \mu g \, mL^{-1}$ chloramphenicol and was grown at $37 \, °C$ and $220 \, rpm$ for $16 \, h$. Then the saturated culture was diluted (1:50) in fresh BHI medium, containing $100 \, \mu g \, mL^{-1}$ ampicillin, $34 \, \mu g \, mL^{-1}$ chloramphenicol, and $0.03 \, mM \, ZnSO_4$ and was grown to $OD_{600} \sim 0.8$. The expression of recombinant CA VI was induced with $1 \, mM$ isopropyl-β-D-thiogalactoside containing

0.3 mM ZnSO$_4$. The culture was grown for 20 h at 20 °C and 250 rpm. The cells were harvested by centrifugation at 4000 g for 20 min at 4 °C. The pellet was suspended in lysis buffer (25 mM MES pH 5.6, 0.5 % Triton X-100, 0.1 M Na$_2$SO$_4$, and 1 mM PMSF) containing the protease inhibitor cocktail (Roche Applied Science). The cells were incubated at 4 °C for 60 min and then disrupted by sonication. The supernatant, containing soluble proteins, was obtained after centrifugation at 20 000 g for 25 min. The recombinant CA VI was purified by immobilized metal ion affinity chromatography using Ni^{2+}-sepharose (GE Healthcare Bio-Sciences AB), followed by cation exchange chromatography on sulphopropyl-modified sepharose (GE Healthcare Bio-Sciences AB), and thereafter dialysed against the storage buffer (25 mM MES, 50 mM Na$_2$SO$_4$, pH 5.8) and stored at -80 °C. The purity of CA VI was analyzed by sodium dodecyl sulfate-polyacrylamide gel electrophoresis (SDS-PAGE). Protein concentration was determined by UV-VIS spectrophotometry and confirmed by the standard Bradford method. Molecular weight of the protein was confirmed by MS.

Recombinant CA VI from mammalian FreeStyle 293-F cells (Invitrogen, Life Technologies) was purified by Jurgita Matulienė at the Department of Biothermodynamics and Drug Design (Institute of Biotechnology, Vilnius university) as described in [319].

6 Inhibitors

The commercial CA-targeting ligands AZM and EZA were purchased (Sigma-Aldrich) and used without further purification. The benzenesulfonamide (BSA) was kindly provided by Prof. Peteris Trapencieris (Latvian Institute of Organic Synthesis, Riga). Other CA inhibitors investigated in this study were synthesized by Virginija Dudutienė at the Department of Biothermodynamics and Drug Design (Institute of Biotechnology, Vilnius university). Structures and purity of these compounds were confirmed by NMR, IR spectroscopy, and MS [320].

7 Thermodynamics of protein-inhibitor interactions

7.1 Fluorescent thermal shift assay

Fluorescent thermal shift assay (FTSA), also termed differential scanning fluorimetry or Thermofluor®, is widely applied in academic field and by pharmaceutical companies, such as Johnson & Johnson (New Brunswick, United States) [321–323]. It is a high-throughput method allowing the precise screen of biomolecules

with minimized consumption in order to find the compound exhibiting the most promising therapeutic properties. Importantly, there are low limitations for binding affinity determined by this method, thus both strong (picomolar) and weak (millimolar) compounds can be identified during the same experiment [3]. FTSA has been used to thermodynamically characterize protein-protein [324], protein-ligand [325] interactions as well as thermal protein stability depending on diverse solvents or excipients [326]. Moreover, this technique has recently been optimized for cellular applications enabling the detection of proteins targeted by tested compounds within a cell [327].

FTSA measures the thermal stability of a protein by following the fluorescence of solvatochromic probes, such as 8-anilino-1-naphthalenesulfonic acid ammonium salt (ANS) or SYPRO Orange, while the temperature is steadily increased. These dyes are quenched by water and highly fluorescent when bound to the protein surface clefts, enabling the probe hiding from water. Such conditions are observed upon protein unfolding induced by heat [321,328]. In a typical FTSA experiment, the protein melting temperature (T_m) is determined. The T_m is such a temperature at which half of the protein is unfolded and another half is native. Diverse ligands can increase or reduce T_m by protein stabilization or destabilization, respectively. The binding affinity is calculated from the T_m shift as a function of ligand concentration [321,323,325].

FTSA measurements were performed using a Corbett Rotor-Gene 6000 (Qiagen Rotor-Gene Q) instrument using the blue channel (excitation at 365 ± 20 nm, detection at 460 ± 15 nm). Samples contained 10 µL of 5 µM–10 µM protein, 10 µL of 0 µM–200 µM inhibitor in 50 mM phosphate buffer at pH 7.0 with 100 mM NaCl, 50 µM solvatochromic dye ANS (Sigma-Aldrich), and DMSO with a final concentration of 2 %. Samples were heated from 25 °C to 99 °C with the heating rate of 1 °C min^{-1}. The pH dependence of the binding constant (K_b) was measured in buffer containing 50 mM sodium phosphate, 50 mM sodium acetate, and 25 mM sodium borate at pH 5.5–9.5. For measurements of protein thermal stability, the T_m representing a midpoint of the protein unfolding transition was determined by FTSA at various buffer, pH, and excipient conditions. Samples contained 100 mM buffer at pH 3.5–10.5, 5 µM protein, and 50 µM ANS. Data were fitted and analyzed as previously described [321,325,329]. All experiments were repeated at least twice.

7.2 Isothermal titration calorimetry

According to some researchers, isothermal titration calorimetry (ITC) is the gold standard method for the measurement of binding energetics [330]. It allows the direct determination of stoichiometry and thermodynamic parameters, such as

affinity, enthalpy, entropy, and heat-capacity, for a binary system during a single titration experiment. However, this method is time-consuming, demands relatively large quantities of proteins, and has limitations for assessing the binding affinity [3].

For studies of compound binding to target protein, ITC experiments are typically performed in the calorimeter with solution of target protein in the cell and ligand in the syringe. The ligand from syringe is injected at constant temperature into the cell preloaded with protein solution until all binding sites of the protein become occupied by the ligand. The absorbed or released heat caused by biomolecular interactions is directly measured. Beneficially, ITC does not require biomolecules to be labeled, modified, or immobilized [331].

ITC measurements were performed using a VP-ITC instrument (Microcal Inc.) with $250\,\mu L$ of $40\,\mu M$–$60\,\mu M$ ligand solution in the syringe and $2\,mL$ of $4\,\mu M$–$6\,\mu M$ protein solution in the cell (active volume $1.4315\,mL$). A typical experiment consisted of 25 injections ($10\,\mu L$ each) added at $200\,s$–$240\,s$ intervals. In order to determine the pH dependence of the observed binding enthalpy, experiments were performed at $25\,°C$ and $37\,°C$ in $50\,mM$ phosphate or $50\,mM$ Tris buffer containing $100\,mM$ NaCl at pH 5.5–9.5 with a final DMSO concentration of $1\,\%$, equal in the syringe and the cell. Data were integrated, fitted, and analyzed as previously described [332]. All experiments were repeated at least twice.

7.3   Observed and intrinsic thermodynamic parameters

The experiment of measuring the interaction between CA isoform and inhibitor by any enzymatic or biophysical method always provides the *observed* binding parameters. However, they do not represent the true binding affinity because both the CA and inhibitor exist in different protonation states in the solution as compared with ones in the complex. Thus, the protonation-deprotonation reactions are necessary to initiate the binding of inhibitor to CA. To obtain the *intrinsic* parameters, energetic contribution of protonation reactions should be subtracted. Only intrinsic values do not depend on pH or buffer and therefore are significant for the rational drug design.

Several reactions occur during the interaction between CA VI and the inhibitor: protonation of zinc-bound hydroxide ion in the active site of CA VI, deprotonation of inhibitor sulfonamide group, bond formation between CA VI and inhibitor, and compensating protonation–deprotonation reactions of the buffer. They significantly influence the changes in thermodynamics upon the binding reaction.

Intrinsic binding constant (K_{b_intr}) is directly related to the observed binding constant (K_{b_obs}) and inversely related to the fractions of deprotonated inhibitor and protonated zinc-bound hydroxide anion of CA VI.

$$K_{b\_intr} = \frac{K_{b\_obs}}{f_{\mathrm{CAZnH_2O}} f_{\mathrm{RSO_2NH^-}}} \tag{1}$$

The fractions of deprotonated sulfonamide inhibitor and CA VI with the protonated hydroxide ion (water molecule) bound to zinc in the active site can be calculated if both the pK_a of sulfonamide amino group (p$K_{a,SA}$) and the pK_a of water molecule in the active site of CA VI (p$K_{a,CA}$) are known:

$$f_{\mathrm{RSO_2NH^-}} = \frac{10^{\mathrm{pH}-\mathrm{p}K_{a,SA}}}{1 + 10^{\mathrm{pH}-\mathrm{p}K_{a,SA}}} \tag{2}$$

$$f_{\mathrm{CAZnH_2O}} = \frac{10^{\mathrm{p}K_{a,CA}-\mathrm{pH}}}{1 + 10^{\mathrm{p}K_{a,CA}-\mathrm{pH}}} \tag{3}$$

Observed or intrinsic binding affinity is often reported by dissociation constant (K_d), which can be evaluated according to equation 4. The smaller value of K_d, the greater binding affinity of compound to target.

$$K_d = \frac{1}{K_b} \tag{4}$$

Observed or intrinsic K_b and K_d values are associated with the change in observed or intrinsic Gibbs energy for the binding reaction, $\Delta_b G$:

$$\Delta_b G = -RT \ln K_b = -RT \ln \frac{1}{K_d} = \Delta_b H - T\Delta_b S \tag{5}$$

The observed enthalpy ($\Delta_b H_{obs}$) determined by ITC is the sum of enthalpies induced by the binding reaction and all protonation events, such as protonation enthalpies of buffer ($\Delta_p H_{buf}$), sulfonamide inhibitor ($\Delta_p H_{SA}$), and hydroxide bound to zinc in the active site of CA VI ($\Delta_p H_{CA}$):

$$\Delta_b H_{intr} = \Delta_b H_{obs} - n_{SA}\Delta_p H_{SA} - n_{CA}\Delta_p H_{CA} + n_{buf}\Delta_p H_{buf} \tag{6}$$

where $n_{SA} = f_{\mathrm{RSO_2NH^-}} - 1$ is the number of protons released from the inhibitor to buffer, $n_{\mathrm{CA}} = 1 - f_{\mathrm{CAZnH_2O}}$ is the number of protons bound to zinc-bound hydroxide of CA VI, and $n_{buf} = n_{CA} + n_{SA}$ is the sum of uptaken or released protons by buffer. The enthalpy of protonation of Tris and sodium phosphate buffers is equal to -47.4 kJ mol^{-1} and -5.1 kJ mol^{-1}, respectively, at 25 °C (or -46.6 kJ mol^{-1} and -2.9 kJ mol^{-1}, respectively, at 37 °C) [333].

The evaluation of K_{b_intr} or $\Delta_b H_{intr}$ by the equation 1 or 6, respectively, is suitable for all recombinant CA isoforms, which are catalytically active. The intrinsic binding parameters allow correlations with ligand chemical structures and provide valuable information about the nature of protein ligand recognition phenomena.

8 Methods applied in experiments with diverse biological systems

8.1 Zebrafish embryos/larvae

Maintenance and exposure to the inhibitors

Zebrafish of the AB strain were maintained at $28.5\,°C$ [334]. Embryos were collected from the breeder tanks with a sieve, rinsed with the embryonic medium ($5.0\,mM$ NaCl, $0.17\,mM$ KCl, $0.33\,mM$ $CaCl_2$, $0.33\,mM$ $MgSO_4$, and $0.1\,\%$ w/v methylene blue, Sigma-Aldrich), and placed in a petri dish containing the medium.

Normal embryos were randomly selected at $0\,h$–$2\,h$ post-fertilization (hpf) and transferred into 6-well, flat bottom plates containing the embryonic medium. Different dilutions of inhibitors were added to each well. Zebrafish embryos were exposed to $1\,µM$–$1000\,µM$ concentration of VD11-4-2, VD12-09, and EZA inhibitors. In the control group, we included similar number of WT embryos (untreated) and embryos exposed to $0.1\,\%$–$1.0\,\%$ of DMSO. In total, 5 sets of experiments were carried out for each inhibitor. The embryos/larvae were examined every morning for any debris and dead embryos and the wells were cleaned. The mortality of embryos/larvae was noted every $24\,h$. The phenotypic appearance of the inhibitor treated and control embryos/larvae were analyzed using light microscopy. The images were taken using a Lumar V1.12 fluorescence stereomicroscope attached to a camera with a $1.5\times$ lens (Carl Zeiss MicroImaging GmbH). The images were analyzed with AxioVision software versions 4.7 and 4.8. We used 5 days post-fertilization (dpf) larvae for morphological examination using histochemical staining.

Ethical statement

All experiments using zebrafish embryos/larvae were performed according to the Provincial Government of eastern Finland Province Social and Health Department Tampere Regional Service Unit protocol LSLH-2007–7254/Ym-23. The care was taken to ameliorate suffering by euthanizing the zebrafish larvae by prolonged immersion in the embryonic medium containing the overdose of tricaine.

Determination of inhibitor lethal concentrations

Dependences of zebrafish embryos/larvae mortality on the dosage of inhibitor VD11-4-2, VD12-09, and EZA were evaluated at $120\,hpf$. Dose-dependent lethality curves were generated using Origin 7.0 (OriginLab). According to the survival rate, half-maximal lethal concentrations (LC_{50}) for each inhibitor were determined using sigmoidal dose-response Hill model with Hill coefficient of 4–8.

Histochemical analysis

To study the morphology of zebrafish larvae exposed to different concentration of inhibitors, histochemical analysis was performed on 5 dpf experimental and control zebrafish larvae. The 5 dpf zebrafish larvae were washed with phosphate buffered saline (PBS) and fixed in 4 % paraformaldehyde in PBS for 3 h at room temperature and the fixed larvae were transferred to 70 % ethanol and stored at 4 °C before being embedded in paraffin.

The further work was performed by Ashok Aspatwar (University of Tampere, Finland). The paraffin-embedded samples were sectioned into 5 µM slices for the histochemical staining. The fixed sections containing samples were deparaffinized in xylene, rehydrated in an alcohol series and histologically stained with Mayer's hematoxylin and eosin Y (both from Sigma-Aldrich). After dehydration, the slides were mounted with EntellanNeu (Merck), examined, and photographed using a Nikon Microphot microscope (Nikon Microphot-FXA). All these procedures were carried out at room temperature.

8.2   *Xenopus* oocytes

Constructs, oocytes, and injections of cRNA

X. laevis females were purchased from Xenopus Express, Vernassal, France. Segments of ovarian lobules were surgically removed under sterile conditions from frogs anesthetized with $1 \, \mathrm{g} \, \mathrm{L}^{-1}$ of 3-amino-benzoic acid ethylester (MS-222, Sigma-Aldrich), and rendered hypothermic. After disection frogs were kept solitary in a basin for one week to recover. The wound was checked regularly for infections. The procedure was approved by the Landesuntersuchungsamt Rheinland-Pfalz, Koblenz (23 177–07/A07–2-003 §6). Afterwards the oocytes were dispersed by collagenase (Collagenase A, Roche) treatment and stored overnight in oocyte saline (82.5 mM NaCl, 2.5 mM KCl, 1 mM $CaCl_2$, 1 mM $MgCl_2$, 1 mM Na_2HPO_4, and 5 mM Hepes, pH 7.8) at 18 °C to recover. A detailed description of the frog dissection and processing of oocytes is given in [284]. Oocytes of the stages V and VI were injected with 1 ng–6 ng of cRNA coding either for human CA II, CA IV, CA IX, or CA XII, cloned into the *Xenopus* oocyte expression vector pGemHe-Juel. Measurements were carried out 3–5 days after target cRNA microinjections. For pH measurements, the oocyte saline was titrated to pH 7.4. In bicarbonate-containing saline, 25 mM NaCl was replaced by an equivalent amount of $NaHCO_3$ and the solution was aerated using 5 % CO_2.

Intracellular and extracellular pH measurements

Single-barreled microelectrodes were used to measure intracellular $[H^+]$ ($[H^+]_i$) while double-barreled microelectrodes - for extracellular $[H^+]$ at outer membrane surface ($[H^+]_s$). Their manufacture and application have been described previously [284, 335, 336].

Briefly, microelectrodes were prepared from borosilicate glass capillaries which were pulled to a needle using the electrode puller (Type PE-2, Narishige Scientific Instruments Lab) and thereafter silanized by backfilling with a drop of 5 % tri-N-butylchlorosilane (Selektophore, Fluka, Sigma-Aldrich) in 99.9 % pure carbon tetrachloride (Fluka, Sigma-Aldrich). For the pH-sensitive microelectrode, the tip of silanized electrode was backfilled with a drop of H^+-selective cocktail (Hydrogen ionophore I-cocktail A, Fluka, Sigma-Aldrich) and filled up with 0.1 M sodium citrate (pH 6.0). For the reference electrode, the tip of silanized electrode was backfilled with 3 M KCl. The chlorinated silver wire was placed in each electrode and fixed with dental wax. Double-barreled microelectrodes were made by directly attaching both the reference and pH-sensitive microelectrodes by using the electrode puller.

Before every experiment, the pH-sensitive microelectrode was calibrated using Hepes-buffered solution at two different pH values (pH 7.4 and pH 6.8). Oocytes were clamped to a holding potential of -40 mV. For $[H^+]_i$ measurements, the pH-sensitive electrode was located near the inner surface of the oocyte plasma membrane and the reference electrode was positioned independently. For $[H^+]_s$ measurements, a double-barrelled microelectrode was gently pushed against the outer cell membrane without penetrating the cell, ensured by the absence of negative (membrane) potential recorded by the reference electrode. Experiments were performed at room temperature.

For data analysis, changes of electrode potential (EP) were plotted against the corresponding pH and fitted by linear regression to obtain slope and intercept. These parameters were applied to calculate pH and nanomolar $[H^+]$ values:

$$pH = intercept + slope \times EP \qquad (7)$$

$$[H^+] = 10^{-pH} \times 10^9 \qquad (8)$$

The absolute change of $[H^+]_s$ ($\Delta[H^+]_s$) and the rate of change in $[H^+]_i$ ($\Delta[H^+]_i/\Delta t$) during application or removal of substrate (5 % CO_2/25 mM HCO_3^-) were determined after the exposure of *Xenopus* oocytes expressing certain CA isoform to inhibitors or DMSO. The $\Delta[H^+]_i/\Delta t$ was calculated according to the slope of a linear fit for the steepest part of the recorded trace representing $[H^+]_i$. Half-maximal inhibitory concentrations (IC_{50}) for the compound VD11-4-2 were de-

termined using the sigmoidal dose-response Hill model with Hill coefficient of 0.5.

Mass spectrometry measurements using *Xenopus* oocytes

The MS method is based on following the ^{18}O depletion of doubly labeled $^{13}C^{18}O_2$ through several hydration and dehydration steps of CO_2 and HCO_3^- [290, 337]. Briefly, isotopic CO_2 species were distinguished according to a mass to charge ratio (m/z) by this method. The reaction sequence of ^{18}O loss from $^{13}C^{18}O^{18}O$ (m/z = 49) over the intermediate product $^{13}C^{18}O^{16}O$ (m/z = 47) and the end product $^{13}C^{16}O^{16}O$ (m/z = 45) was monitored with a quadrupole mass spectrometer (OmniStar GSD 320; Pfeiffer Vacuum). The relative ^{18}O change, termed logarithmic ^{18}O enrichment (LE), was calculated from the measured 45, 47, and 49 m/z abundance as a function of time according to equation 9, where the numbers in parentheses represent the amplitudes of corresponding mass peaks.

$$LE = \log \frac{[49] \times 100}{[45] + [47] + [49]} \tag{9}$$

For the calculation of CA activity, the rate of ^{18}O depletion was obtained from the linear slope of the log enrichment over the time, using OriginPro 8.6. The rate was compared with the corresponding rate of the non-catalyzed reaction. Enzyme activity in units (U) was calculated from these two values as defined previously [338]. From this definition, 1 U corresponds to 100 % stimulation of the non-catalyzed ^{18}O depletion of doubly labeled $^{13}C^{18}O_2$.

The effect of 1 nM and 10 nM VD11-4-2 on CA IX activity was determined in lysate of 20 native or CA IX-expressing oocytes at 25 °C. The non-catalyzed reaction was determined for 5 min in the absence of inhibitor before the oocyte lysate was added to the measuring cuvette. After the catalyzed reaction was determined for 5 min, the increasing doses of inhibitor VD11-4-2 were added to the same cuvette every 5 min and the catalyzed degradation was determined.

Statistics

Results are presented as mean ± standard error of the mean (SEM). Student's *t*-test or, if possible, a paired *t*-test was used for the determination of significance in differences. The *p*-value less than 0.05 was assumed to be significant (*$p < 0.05$, **$p < 0.01$, ***$p < 0.001$).

8.3 Cancer cells

Cell culture

Human cervical (HeLa), lung (H460, A549), breast (MDA-MB-231), and pancreatic (AsPC-1) cancer cells were cultured in Dulbecco's Modified Eagle's Medium (DMEM, Lonza) supplemented with $10\,\%$ fetal bovine serum (FBS, Lonza). Cells were exposed to hypoxic conditions in the hypoxic chamber (MACS VA500 microaerophilic workstation, Don Whitley Scientific) with $0.2\,\%$ O_2, $5\,\%$ CO_2, and residual N_2. Simultaneously, normoxic cells were grown in the humidified incubator with $21\,\%$ O_2, $5\,\%$ CO_2 at $37\,°C$.

Generating HeLa CA IX knockout cells

HeLa CA IX KO clones were established according to the previous study [339]. HeLa cells were routinely cultured in DMEM (Lonza) supplemented with $10\,\%$ FBS and transfected with a vector containing a CA IX-CRISPR guide RNA (5′ CACCGGGGAATCCTCCTGCATCCG 3′) using linear polyethylenimine (Polysciences Inc.). 24 h after transfection, selection with puromycin was started and maintained for 48 h, after which monoclones were picked and routinely cultured. After exposure to hypoxia ($0.2\,\%$, 24 h), an initial screening for CA IX expression was performed by Western blotting (Figure 27), followed by genetic confirmation of CA IX KO in clones that showed no CA IX expression. This was done by single allele sequencing using the TOPO® TA Cloning® Kit (Invitrogen) according to the manufacturer's protocol. KO-causing mutations in the *CA9* gene were confirmed in two alleles per clone.

Experiments were performed by Gabor Gondi (Helmholtz Center for Environmental Health, Germany) and Raymon Niemans (Maastricht University Medical Centre, The Netherlands). I contributed to the clone cultivation and screening for CA IX expression by Western blot during my internship at Maastricht University Medical Centre.

Mass spectrometry measurements using human cancer cells

The total catalytic activity of extracellular CA isoforms in hypoxic MDA-MB-231 and HeLa cancer cells was determined by monitoring the ^{18}O depletion of doubly labeled $^{13}C^{18}O_2$ at $24\,°C$, as described in the previous subsection using *Xenopus* oocytes. Experiments were performed by Holger Becker (University of Veterinary Medicine Hannover, Germany). MDA-MB-231 cells were cultured in Gibco Leibovitz-L15 medium (Life Technologies), supplemented with $10\,\%$ fetal calf serum, $5\,mM$ glucose, and $1\,\%$ penicillin/streptomycin, pH 7.4. HeLa cells were cultured in RPMI-1640 Medium (Sigma Aldrich), supplemented with $10\,\%$

fetal calf serum and 1 % penicillin / streptomycin. Both cell lines were cultured under hypoxia (1 % O_2) for 3 days prior to measurements. Cells were trypsinized, washed and resuspended in Hepes-buffered saline (143 mM NaCl, 5 mM KCl, 2 mM $CaCl_2$, 1 mM $MgSO_4$, 1 mM Na_2HPO_4, 10 mM Hepes, pH 7.2). For determination of IC_{50} values, 2 cell culture plates (58 cm^2), grown to 80 % confluence, were used for every single measurement. To ensure an equal amount of cells within one set of measurements, cells from several plates were pooled and then aliquoted according to the number of tested inhibitor concentrations. For the determination of IC_{50}, the cell suspensions were incubated in the corresponding concentration of inhibitor for up to 3 h. For every measurement, the non-catalyzed reaction was determined for 6 min in the presence of inhibitor before cell suspension was added to the measuring cuvette and the catalyzed reaction was determined for 8 min. CA activity in the presence of inhibitor was normalized to the CA activity in the absence of inhibitor. IC_{50} values were determined by Hill1 fit using OriginPro 8.6 (OriginLab). To investigate specificity of the inhibitors in HeLa WT and HeLa CA IX KO cells, the non-catalyzed reaction was determined for 6 min in the absence of inhibitor before a suspension of 5×10^6 cells was added to the measuring cuvette. After the catalyzed reaction was determined for 6 min, the inhibitor was added to the cuvette and the reaction was determined for another 6 min.

Extracellular acidification (pH) assay

HeLa, H460, MDA-MB-231, and AsPC-1 cells were cultured in DMEM supplemented with 10 % FBS, whereas A549 cells were grown in home-made analogous medium differing only by a lower amount of sodium bicarbonate (final concentration 10 mM). Cell densities for each cell line were optimized to get ∼100 % confluence at the end of experiment under normoxic and hypoxic (0.2 % O_2) conditions upon vehicle (0.05 % DMSO) treatment. Such conditions were necessary to obtain the highest possible level of CA IX-dependent extracellular acidification. Cells were plated in dishes of 6 cm diameter and allowed to attach overnight in normoxia. The plating density is indicated in Table 3. The next day cells were exposed to 5 µM–50 µM doses of each inhibitor or DMSO for 72 h in parallel under normoxic or hypoxic conditions and pH of the culture medium was measured at the end of each experiment as previously reported [128]. Results are shown as a difference between the pH of medium in the control plate (without seeded cells) and the pH of medium in the targeted plate (cells exposed to the compound or vehicle).

Table 3: The plating density of HeLa, H460, A549, MDA-MB-231, and AsPC-1 cells for pH assay. Cells were exposed to the compounds under normoxia (21 % O_2) or hypoxia (0.2 % O_2) for 72 h.

O_2	21 %	0.2 %
HeLa	5.0×10^4 cells/mL	7.5×10^4 cells/mL
H460	5.0×10^4 cells/mL	1.0×10^5 cells/mL
A549	3.1×10^4 cells/mL	6.2×10^4 cells/mL
MDA-MB-231	1.2×10^5 cells/mL	2.2×10^5 cells/mL
AsPC-1	2.0×10^5 cells/mL	3.7×10^5 cells/mL

Cell viability assay

Cytotoxicity of inhibitors was determined by the alamarBlue® cell viability assay (Life Technologies). Cell densities for HeLa, H460, MDA-MB-231, A549, and AsPC-1 were optimized to get ~80 % confluence at the end of experiment under normoxic and hypoxic (0.2 % O_2) conditions upon vehicle (0.25 % DMSO) treatment. Briefly, cells were seeded in 96-well plates and allowed to attach overnight in normoxia. The plating density is indicated in Table 4. On the next day, cells were exposed to normoxia or hypoxia and medium was replaced with pre-incubated normoxic or hypoxic medium with final concentrations of 10 µM–150 µM of inhibitor or DMSO. After 72 h, cells were incubated with 10 % alamarBlue® for 2 h under normoxia at 37 °C. The fluorescence signal was measured using the multi-mode microplate reader (FLUOstar® Omega, BMG Labtech) at 580 nm (excitation at 540 nm). Response to treatments was quantified by evaluating EC_{50} values (the concentration of inhibitor that leads to half-maximum viability response determined by Hill fit).

Table 4: The plating density of HeLa, H460, A549, MDA-MB-231, and AsPC-1 cells for cell viability assay. Cells were exposed to the compounds under normoxia (21 % O_2) or hypoxia (0.2 % O_2) for 72 h, while AsPC-1 cells - for 48 h.

O_2	21 %	0.2 %
HeLa	1.0×10^4 cells/mL	1.5×10^4 cells/mL
H460	7.5×10^3 cells/mL	7.5×10^3 cells/mL
A549	1.5×10^4 cells/mL	3.5×10^4 cells/mL
MDA-MB-231	1.5×10^4 cells/mL	2.5×10^4 cells/mL
AsPC-1	1.5×10^5 cells/mL	1.5×10^5 cells/mL

Clonogenic cell survival assays

Clonogenic survival of HeLa cell monolayers was evaluated using cell densities applied in the extracellular acidification assay to determine the effect of inhibitors on the clonogenic cell survival while having the same acidification conditions. Cells were exposed to 10 µM–50 µM VR16-09, VD11-4-2, VD12-09, or 0.05 % DMSO

for 72 h upon normoxic or hypoxic conditions (0.2 % O_2). Such doses of inhibitors significantly reduced hypoxia-induced acidification. Then cells were trypsinized, reseeded in triplicate with known cell densities and allowed to form colonies for 14 days. To test inhibitors in 3D cell models, non-hypoxic and hypoxic H460 spheroids were exposed to 5 µM–15 µM doses of VR16-09 or 0.25 % DMSO for 24 h on day 4 or day 11, respectively. Single cell suspensions were prepared and cells were plated in triplicate with known cell densities and allowed to form colonies for 14 days. Colonies were quantified after staining and fixation with 0.4 % methylene blue in 70 % ethanol. Surviving fraction was normalized to vehicle (DMSO).

Spheroid growth

To prepare plates for the growth of attachment-free H460 spheroids, autoclaved 1.5 % w/v agarose (Sigma-Aldrich) was dispensed in the inner 60 wells of 96-well plates (50 µM/well) and left for polymerization at room temperature for 30 min. H460 cells were plated in modified 96-well plates to the surface of agarose menisci with a density of 2.5×10^3 cells/mL. The DMEM was refreshed every 2 days. After 7 or 11 days in culture, spheroids were incubated with $20 \, \mu g \, mL^{-1}$ pimonidazole (PIMO, Hypoxyprobe-1, HP-1000, BioConnect) for 2 h at 37 °C, collected and cryoconserved for immunofluorescence analysis. In parallel 4 or 11 days after cell seeding, spheroids of homogeneous volume were treated with 5 µM–15 µM VR16-09 or 0.25 % DMSO for 24 h and collected for clonogenic survival assay.

Western blot

Protein isolates were prepared by incubating scraped cells in RIPA buffer on ice for 30 min, followed by centrifugation to remove cell debris. Protein concentrations were determined using Bradford protein quantification reagent (BioRad). Western blot was performed using primary antibodies, including mouse anti-CA IX (M75, 1:40, kindly provided by Prof. Silvia Pastorekova, Institute of Virology, Slovak Academy of Science, Slovak Republic), mouse anti-CA XII (clone 15A4, 1:100, kindly provided by Prof. Aurelija Žvirblienė, Institute of Biotechnology, Vilnius University, Lithuania), rabbit anti-MCT1 (1:100), rabbit anti-MCT4 (1:400, kindly provided by Holger M. Becker, University of Veterinary Medicine Hannover, Hannover, Germany), rabbit anti-lamin A (1:10 000, Sigma-Aldrich), and mouse anti-actin (1:2 000 000, MP Biomedicals). Primary antibodies were incubated overnight at 4 °C, whereas horseradish peroxidase-linked secondary antibodies (1:2000, Cell Signaling) were incubated for 1 h at room temperature. Amersham ECL Western Blotting Detection Reagent (GE Healthcare Life Sciences) was applied for the detection of CA XII, MCT1, MCT4, and lamin A, while SuperSignal™ West Pico PLUS Chemiluminescent Substrate (Life Technologies)

was used for the visualization of CA IX and actin.

Immunofluorescence analysis

H460 spheroids of day 7 and day 11 were cryoconserved. Frozen sections (7 µm) of spheroids were fixed in acetone (4 °C, 10 min), air-dried and rehydrated in PBS. Non-specific binding was blocked by incubation with 0.5 % goat serum in PBS for 30 min at room temperature. Sections were stained (37 °C, 1 h) using primary rabbit anti-PIMO (1:250) or mouse anti-CA IX (1:100, M75), followed by incubation (37 °C, 1 h) with secondary goat anti-rabbit Alexa Fluor® 488 or goat anti-mouse Alexa Fluor® 594, respectively (both 1:500, from Invitrogen). Nuclei were stained with DAPI (2-(4-Amidinophenyl)-1H-indole-6-carboxamidine, final concentration 5 µg mL^{-1}, Life Technologies) for 2 min at room temperature. Staining without primary antibody was used as negative control. Sections were viewed at 10 × magnification by Nikon Eclipse E800 microscope (Nikon Instruments Inc.).

Statistics

Statistical analysis was performed using GraphPad Prism (version 6.01). A non-parametric Mann-Whitney U test for small groups was applied to evaluate the statistical significance of differences between two independent groups of variables and the p-value less than 0.05 was assumed to be significant (*$p<0.05$, **$p<0.01$, ***$p<0.001$, ****$p<0.0001$).

Results

9 Inhibitor binding to the native and recombinant carbonic anhydrase VI

This part of my thesis project was undertaken to elucidate differences in inhibitor binding affinity to the native CA VI from human saliva and two forms of recombinant CA VI from *E. coli* and mammalian FreeStyle 293-F cells to determine whether the recombinant CA VI is an appropriate *in vitro* model of the native CA VI for inhibitor binding reactions.

Thermodynamics of inhibitor binding to CA VI

Two types of variables can be distinguished when binding reactions are performed: the *observed* parameters obtained from experimental setup and the *intrinsic* values calculated according to the corresponding observed data. Observed binding affinity is disadvantageous due to the dependency on buffer or pH and thus has limited utility for the rational drug design. However, observed values are useful to compare binding affinities of a series of compounds towards one target using the same experimental conditions.

In this study, observed binding affinities represented by K_{d_obs} values of twenty five fluorinated (1–3w) and three nonfluorinated (6a–6c) benzenesulfonamides as inhibitors of native and recombinant CA VI were investigated. Structures of tested compounds are shown in Figure 7. AZM, BSA, and EZA were used as controls. The measured K_{d_obs} values are indicated in Figure 8 in the order of increasing K_{d_intr} (discussed below) and are listed in Table 5. The K_{d_obs} values ranged from 130 nM to 25 000 nM (for inhibitors 3p and 3b, respectively). The most potent inhibitors 3e, 3j, and 3p of the recombinant CA VI (from *E. coli*) and native CA VI bound with K_{d_obs} in the range of 130 nM to 180 nM. Compound 3b exhibited the weakest binding affinity to CA VI from both human saliva and bacteria (K_{d_obs} were 15 000 nM–25 000 nM).

To determine the inhibitor binding affinity towards CA VI from three sources, eight compounds were selected and their interactions with three forms of CA VI were evaluated by FTSA. The differences in K_{d_obs} were essentially identical for the
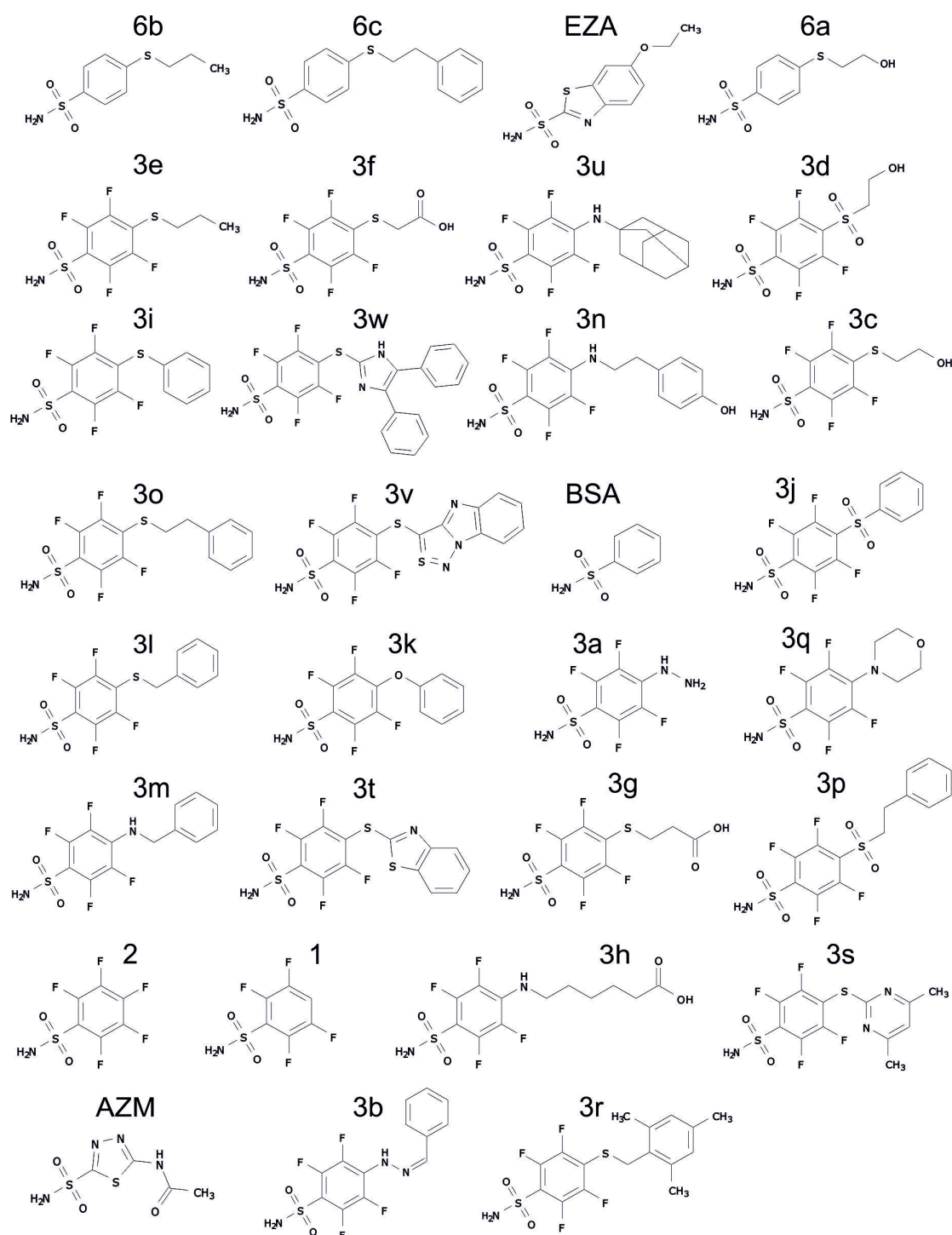
Figure 7: Structures of inhibitors 1, 2, 3a–w, 6a–6c, AZM, BSA, and EZA. Compounds are ranked in the order of decreasing intrinsic affinity towards CA VI.

most compounds and did not exceed 2-fold, the error margin of the experiment. The tested compounds exhibited moderate observed affinities towards CA VI in the submicromolar to double-digit nanomolar range.

The comparison between binding affinities of corresponding fluorinated and nonfluorinated compounds (3c vs 6a, 3e vs 6b, and 3o vs 6c) showed that the flu-
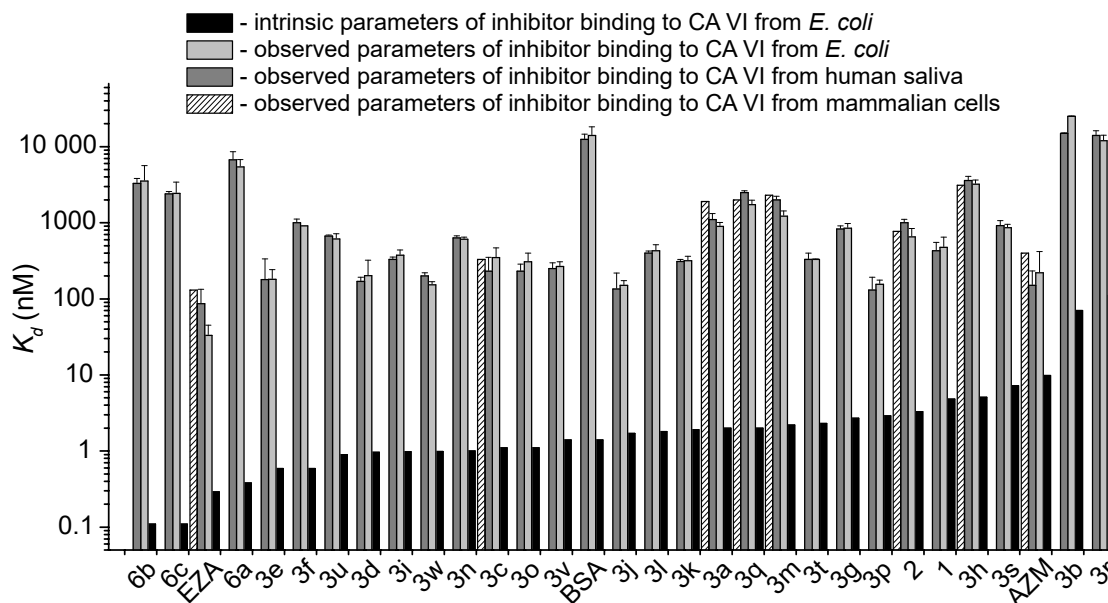
Figure 8: Comparison of experimentally measured K_{d_obs} with the calculated intrinsic K_{d_intr}. The K_{d_obs} values of inhibitor for binding to the native CA VI (from human saliva) and the recombinant CA VI (from *E. coli* and mammalian FreeStyle 293-F cells) were determined by FTSA (extrapolated to 37 °C, performed at pH 7.0). Data are presented as average ± standard deviation (SD) of three independent experiments. The K_{d_intr} of binding to the recombinant CA VI from bacteria were calculated according to equation 1 from the average value of K_{d_obs}.

orination significantly increased the observed binding affinity and diminished the pK_a of sulfonamide amino group. For example, $K_{d\_obs}$ for 6a and 3c binding to native CA VI increased 29-fold upon fluorination (from 6700 nM to 230 nM), whereas K_{d_obs} for 6b and 3e increased the affinity 18-fold (from 3300 nM to 180 nM). Fluorines decreased the pK_a of sulfonamide group significantly, the pK_a values of sulfonamide amino group of 6a and 3c were 9.96 and 8.14, respectively, while pK_as of 6b and 3e were 10.20 and 8.15, respectively (Table 5).

Figure 9A represents the binding of EZA to CA VI isolated from three sources as a function of pH and indicates the significant effect of pH on $\Delta_b G_{obs}$ for the binding reaction, which was evaluated according to K_{d_obs} by equation 5. The strongest interaction was observed near neutral pH and became weaker both in acidic and alkaline pH. Diminished affinity in acidic solution was found because only the deprotonated form of the sulfonamide inhibitor can bind CA. At lower pH, the concentration of the deprotonated sulfonamide was diminished by 10-fold with every pH unit and thus the K_{d_obs} increased 10-fold with every pH unit. Similarly, in alkaline solution, the inhibitor affinity decreased because only the CA protein with the zinc-bound protonated hydroxide in the active site can bind the inhibitor and upon increasing pH this fraction of CA decreased.

Table 5: The K_d values for the interaction between inhibitor and diverse forms of CA VI prepared by three procedures: two recombinant CA VI were obtained from *E. coli* bacteria and mammalian FreeStyle 293-F cells, while the native CA VI was purified from human saliva. The pK_a values of applied sulfonamide amino group (p$K_{a,SA}$) are indicated [340]. The observed values (K_{d_obs}) for all three CA VI forms were determined experimentally by FTSA (extrapolated to 37 °C, performed at pH 7.0), while the intrinsic affinities (K_{d_intr}) of sulfonamide binding to the recombinant CA VI from bacteria *E. coli* were calculated. The binding of several compounds was confirmed by ITC (values are given in the brackets). ND - not determined.

| Compound	p$K_{a,SA}$	K_{d_obs} (nM)			K_{d_intr} (nM)
		Recombinant CA VI from *E. coli*	Recombinant CA VI from mammalian cells	Native CA VI from human saliva	Recombinant CA VI from *E. coli*
1	8.21	480	ND	430	4.8
2	8.12	650	770	1000	3.3
3a	8.84	890	1900	1100	2.0
3b	8.82	25 000	ND	15 000	70
3c	8.14	350	330	230	1.1
3d	7.28	200	ND	170	0.96
3e	8.15	180 (200)	ND	180	0.59
3f	8.14	910	ND	1000	5.9
3g	7.97	850	ND	830	2.7
3h	8.49	3200	3100	3600	5.1
3i	7.80	380	ND	330	0.98
3j	7.07	150	ND	140	1.7
3k	7.86	320	ND	310	1.9
3l	8.53	430	ND	400	1.8
3m	8.47	1200	2300	2000	2.2
3n	8.61	610	ND	630	1.0
3o	8.05	310	ND	230	1.1
3p	7.22	160	ND	130	2.9
3q	8.61	1700	2000	2500	2.0
3r	8.12	12 000	ND	14 000	110
3s	8.02	860	ND	920	7.2
3t	7.83	330	ND	330	2.3
3u	8.58	610	ND	670	0.90
3v	7.69	270	ND	250	1.4
3w	7.69	150	ND	200	0.99
6a	9.96	5400	ND	6700	0.38
6b	10.20	3500	ND	3300	0.11
6c	10.12	2400	ND	2400	0.11
BSA	10.04	14 000	ND	13 000	1.4
AZM	7.03	220	400	150	9.8
EZA	7.82	33 (53)	130	110 (130)	0.29
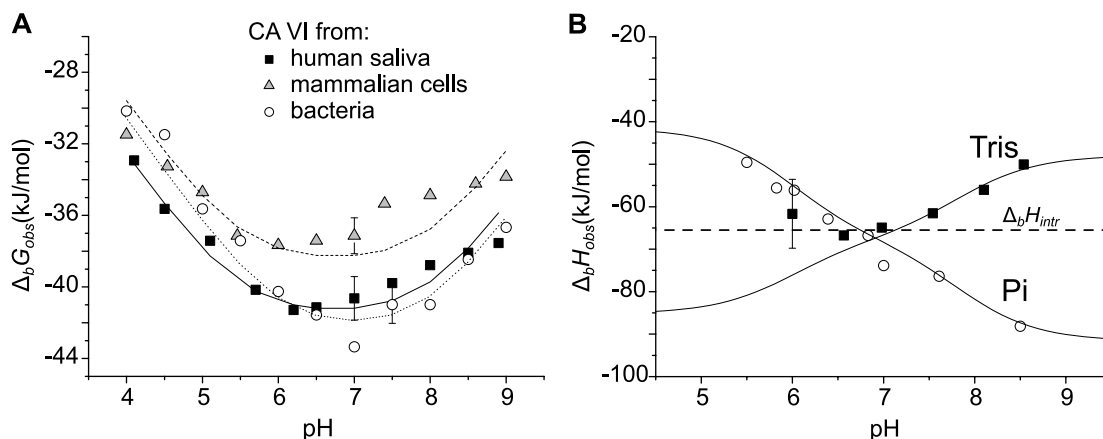
Figure 9: (A) Comparison of $\Delta_b G_{obs}$ of EZA binding to CA VI purified from three sources (human saliva, mammalian FreeStyle 293-F cells, and bacteria *E. coli*) as a function of pH (extrapolated to 37 °C). Solid and dashed curves were fitted according to equation 1 recalculated to Gibbs energies. Experiments were performed in universal buffer prepared of 50 mM sodium phosphate, 50 mM sodium acetate, and 25 mM sodium borate. (B) The $\Delta_b H_{obs}$ of EZA binding to the recombinant CA VI from bacteria as a function of pH in two different buffers (sodium phosphate (Pi) and Tris), which have different protonation enthalpies. Experiments were carried out by ITC at 37 °C. The dashed line shows the intrinsic binding enthalpy, which is independent of pH. Solid curves were fitted according to equation 6.

The $\Delta_b H_{obs}$ depended on the buffer and pH of the experiments, as shown in Figure 9B. More than $20\,\mathrm{kJ\,mol^{-1}}$ differences in binding enthalpies were observed in same buffer at different pHs (at 25 °C using Tris: $-65.7\,\mathrm{kJ\,mol^{-1}}$ at pH 5.6, $-45.3\,\mathrm{kJ\,mol^{-1}}$ at pH 9.2 (data not shown); at 25 °C using sodium phosphate: $-38.4\,\mathrm{kJ\,mol^{-1}}$ at pH 5.2, $-67.0\,\mathrm{kJ\,mol^{-1}}$ at pH 7.9 (data not shown); at 37 °C using Tris: $-66.8\,\mathrm{kJ\,mol^{-1}}$ at pH 6.5, $-50.0\,\mathrm{kJ\,mol^{-1}}$ at pH 8.5; at 37 °C using sodium phosphate: $-49.5\,\mathrm{kJ\,mol^{-1}}$ at pH 5.5, $-88.2\,\mathrm{kJ\,mol^{-1}}$ at pH 8.5). A slight inconsistency between the model and observed values of binding enthalpy at lower pHs in Tris buffer, especially at 37 °C, was due to pH instability and low buffering capacity of Tris in acidic solution.

Intrinsic thermodynamics of inhibitor binding to CA VI

To investigate the structure-activity relationships, pH-independent, intrinsic parameters must be obtained by dissecting protonation and deprotonation contributions. The K_{d_intr} values for interactions between the recombinant CA VI and investigated series of compounds were calculated using equation 1 in subsection 7.3. They are shown in Figure 8 in the order of decreasing intrinsic affinity and listed in the last column of Table 5.

The largest differences between the K_{d_obs} and K_{d_intr} values were observed for nonfluorinated benzenesulfonamides (6a, 6b, and 6c), where the binding to CA VI

differed $14\,000$, $32\,000$, and $22\,000$-fold, respectively. The most potent inhibitors according to their K_{d_obs} were 3e, 3p, and 3j, while the strongest binders were respective nonfluorinated compounds according to calculated intrinsic data. The K_{d_intr} for 3e, 3p, and 3j binding to CA VI spanned the range of $0.59\,\text{nM}$ to $2.7\,\text{nM}$, whereas K_{d_intr} for 6a, 6b, and 6c binding to same CA VI were in the range of $0.11\,\text{nM}$ to $0.39\,\text{nM}$. The 3b and 3r were the weakest binders not only according to observed thermodynamics (K_{d_obs} $25\,000\,\text{nM}$ and $12\,000\,\text{nM}$, respectively), but also by intrinsic parameters (K_{d_intr} $70\,\text{nM}$ and $110\,\text{nM}$, respectively). Only three compounds (1, 3j, and 3p) exhibited lower than 100-fold difference between the K_{d_obs} and K_{d_intr}.

The chemical structure analysis of compound binding to CA VI showed that fluorinated compounds 3a-3w bearing different substituents at *para* position bound to CA VI stronger than BSA itself. Intrinsic parameters indicated that fluorination of benzenesulfonamide ring weakened compound binding to CA VI. The strongest intrinsic interaction between inhibitor and CA VI was obtained when inhibitor did not possess any fluorine in benzenesulfonamide scaffold and contained a hydrophobic substituent in its *para* position, such as $SCH_2CH_2CH_3$ (6b) and SCH_2CH_2Ph (6c). Replacement of the methyl group by hydrophilic hydroxyl group (6a) weakened the interaction more than 3-fold. Considering the intrinsic parameters of fluorinated 3a-3w binding to CA VI, the hydrophobic contacts between chemical compound and CA VI appeared to be significant. The strongest binder from a series of 3a-3w compounds was identified to be 3e with $SCH_2CH_2CH_3$ group on *para* position. The exchange of methyl group by hydroxyl group made the interaction between inhibitor 3d and protein approximately twice weaker. Moreover, a significant decrease of binding affinity was observed for interactions between inhibitors bearing hydrophilic carboxyl groups (3f, 3g, and 3h) and CA VI. Apparently, the size of *para* substituent had no relevant influence on binding affinity. Inhibitor 3u bearing a large 1-adamantylamino group exhibited similar binding affinity as 3e possessing a small $SCH_2CH_2CH_3$ group, as found from the intrinsic parameters that differed less than 2-fold ($0.59\,\text{nM}$ for 3e and $0.90\,\text{nM}$ for 3u), whereas the observed parameters differed more than 3-fold ($180\,\text{nM}$ for 3e and $610\,\text{nM}$ for 3u). These results demonstrated that the intrinsic thermodynamics could lead to the design of more potent inhibitors of CA VI.

To evaluate intrinsic thermodynamics of an inhibitor binding to the recombinant CA VI from bacteria, it is also necessary to determine the enthalpy of deprotonation of sulfonamide ($\Delta_p H_{SA}$) in addition to its pK_a and the enthalpy of protonation of zinc-bound hydroxide ion in CA active site ($\Delta_p H_{CA}$) and its pK_a. Table 6 lists the thermodynamic parameters of protonation of EZA sulfonamide group and zinc-bound hydroxide anion of CA VI. The $\Delta_p H_{CA}$ was determined by performing ITC titrations of the recombinant CA VI from *E. coli* with EZA as a

function of pH in two buffers of highly different protonation enthalpies, namely, sodium phosphate and Tris (Figure 9B). This entire ITC procedure using two buffers of a series of pHs for the titration of CA VI with EZA was repeated at 25 °C and 37 °C to get an estimate of the heat capacity of EZA binding (ΔC_p = -0.63 kJ mol^{-1} K^{-1}). More than 30 mg of CA VI was required to titrate one inhibitor at various pH in at least two buffer systems at two different temperatures, while the purification yield of CA VI from bacteria usually did not exceed 10 mg from 15 g–20 g of biomass. The $\Delta_p H_{CA}$ was determined to be exothermic (-32.0 kJ mol^{-1} at 25 °C, -29.0 kJ mol^{-1} at 37 °C).

The pK_a values of zinc-bound hydroxide/water molecule of CA VI from human saliva and mammalian FreeStyle 293-F cells matched each other (5.5 at 37 °C). Due to low yield of the native CA VI and the recombinant CA VI from mammalian cells, the pK_a values were determined only by FTSA. However, the pK_a for CA VI from *E. coli* was found to be higher (6.0 at 37 °C), as determined by both FTSA and ITC. The differences in pK_a of zinc-bound hydroxide anion in CA active site from different sources could be influenced by protein length as well as post-translational modifications, which are absent in bacteria.

Table 6: Thermodynamic parameters of protonation of EZA sulfonamide group and zinc-bound hydroxide anion of CA VI isolated from three sources. The pK_a values for the zinc-bound hydroxide anion of CA VI from both mammalian FreeStyle 293-F cells and human saliva were determined by FTSA. The data for CA VI from *E. coli* were confirmed by both FTSA and ITC. ND - not determined.

Protein/ inhibitor	Source	T (°C)	pK_a	$\Delta_p G$ (kJ mol^{-1})	$\Delta_p H$ (kJ mol^{-1})	$T\Delta_p S$ (kJ mol^{-1})
CA VI	Human saliva	37	5.5	-31.4	ND	ND
CA VI	Mammalian cells	37	5.5	-31.4	ND	ND
CA VI	Bacteria	25	6.2	-35.4	-32.0	3.4
CA VI	Bacteria	37	6.0	-34.2	-29.0	5.2
EZA*	-	25	8.0	-45.7	-29.5	16.2

* Data reported previously [341]

Intrinsic thermodynamic parameters of EZA binding to the recombinant CA VI from bacteria are listed in Table 7. According to intrinsic values, the binding of EZA to CA VI was enthalpy driven as compared with the entropic contribution ($T\Delta_b S$).

Table 7: Intrinsic thermodynamics of the deprotonated EZA anion binding to CA VI containing a water molecule (protonated hydroxide ion) in the active site.

Protein	T (°C)	$\Delta_b H_{intr}$ (kJ mol^{-1})	K_{b_intr} (M^{-1})	$\Delta_b G_{intr}$ (kJ mol^{-1})	$T\Delta_b S_{intr}$ (kJ mol^{-1})
CA VI	25	-58.0	2.8×10^9	-53.9	-4.1
CA VI	37	-65.5	1.3×10^9	-54.1	-11.4

Thermal stability profiles

Figure 10 shows that the thermal stability of CA VI from *E. coli* and human saliva was highly affected by the buffer and its pH. The higher T_m shows the conditions when the protein is thermally more stable. The native salivary CA VI was more stable than recombinant CA VI from *E. coli* in most buffers and pH by 4 °C to 6 °C. The proteins were the most stable in sodium acetate buffers at pH 5.0–5.5. Similar effect was observed in Mes buffers at pH 5.0–6.0. The CA VI isozymes were significantly destabilized toward alkaline pH, especially in Hepes and Tris buffers at pH 8.0–9.0.
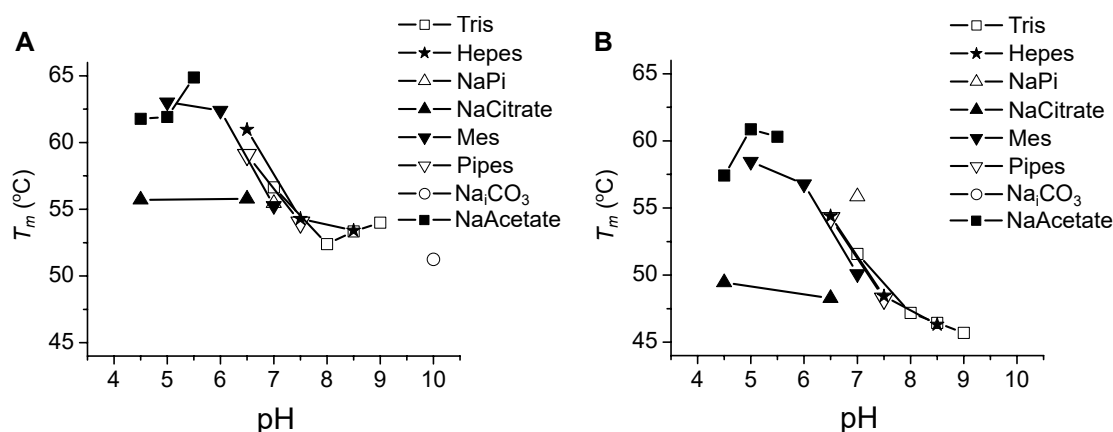

Figure 10: Thermal stabilities of native CA VI from human saliva (A) and recombinant CA VI from *E. coli* (B) in various solution conditions. The dependence of protein melting temperature (T_m) on pH was determined in various buffers (100 mM): Tris, Hepes, sodium phosphate (NaPi), sodium citrate (NaCitrate), Mes, Pipes, sodium carbonate (NaiCO$_3$), and sodium acetate (NaAcetate).

10   Action of inhibitors in biological systems

By routinely producing the recombinant CA VI from bacteria and performing FTSA experiments to measure CA VI-inhibitor binding, I contributed to the screening of over 200 compounds designed at the Department of Biothermodynamics and Drug Design (Institute of Biotechnology, Vilnius university). The aim was to discover the compound exhibiting the most favorable properties against CA IX, the anti-cancer target, and low affinity toward other CA isoforms, such as CA VI. This collaborative work of chemists, biochemist, and biophysicists led to the important publication describing two lead fluorinated benzenesulfonamides, named VD11-4-2 and VD12-09, as extraordinary strong picomolar binders and selective inhibitors of CA IX [342]. Their structures and binding affinities are shown in Table 8. For further development of lead compounds, it was crucial to involve diverse biological model systems to confirm their *in vitro* efficacy. Thus, studies

applying zebrafish embryos/larvae, *Xenopus* oocytes, and human cancer cells were conducted for the biological evaluation of discovered lead CA IX inhibitors.

Table 8: Structures and binding affinities of compounds applied in biological assays of this study. K_{d_obs} values of VD11-4-2, VD12-09, and VR16-09 for the binding with twelve human recombinant CA isoforms were determined by FTSA (extrapolated to 37 °C, performed at pH 7.0). The synthesis, binding and inhibition profiles of compounds VD11-4-2 and VD12-09 were previously published [342].

CA isoform	K_{d_obs} (nM)		
	VD11-4-2	VD12-09	VR16-09
CA I	710	50 000	$\geq$ 200 000
CA II	60	1300	$\geq$ 200 000
CA III	40 000	$\geq$ 200 000	$\geq$ 200 000
CA IV	25	1700	$\geq$ 200 000
CA VA	2500	3300	$\geq$ 200 000
CA VB	5.6	210	45 000
CA VI	95	4300	$\geq$ 200 000
CA VII	9.8	330	37 000
CA IX	**0.05**	**1.1**	**0.16**
CA XII	3.3	330	710
CA XIII	3.6	140	20
CA XIV	1.6	170	170

10.1 Toxic effects of inhibitors on zebrafish embryos/larvae

Lethal concentrations

Results of five experiments employing over 2300 zebrafish embryos showed the dose-dependent lethal effects of VD11-4-2, VD12-09, and EZA (a non-selective CA inhibitor) on the development of 120 hpf zebrafish after treatment for 5 days. VD12-09 had a significant impact on zebrafish mortality, which was comparable to EZA (LC_{50} were 13 µM and 9 µM, respectively). VD11-4-2 exhibited the highest LC_{50} value (120 µM) among the tested compounds (Figure 11).

Phenotype defects

Zebrafish embryos were exposed to diverse doses of VD11-4-2, VD12-09, and EZA at 0 hpf–2 hpf and their phenotypes were observed after 24 h (Figure 12). The highest concentration of compounds in this study was 1000 µM. This dose of the
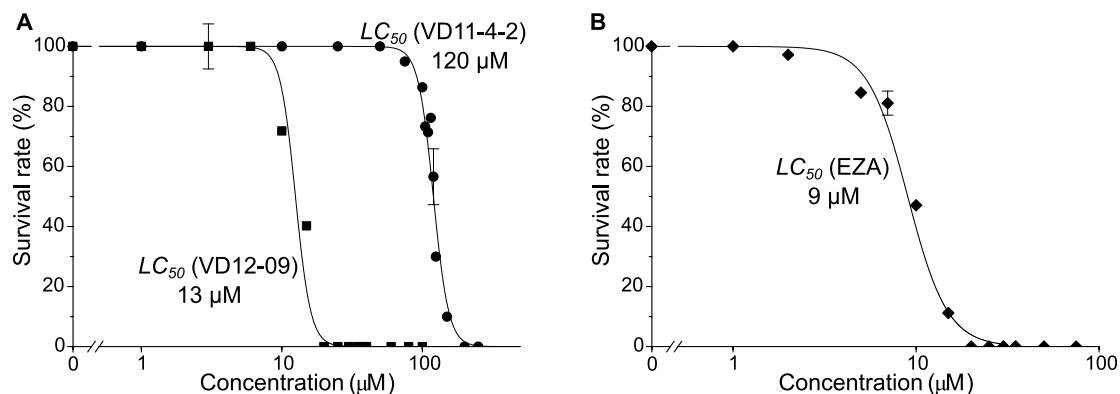
Figure 11: The dependence of zebrafish survival at 120 hpf on the dose of inhibitors: (A) VD11-4-2 (●), VD12-09 (■); (B) EZA. Data points were obtained experimentally, while the solid lines were simulated according to the Hill model (Hill coefficient 4–8).

tested compounds had a significant impact on the survival of zebrafish embryos. Even though this concentration of VD11-4-2 and VD12-09 was lethal, the appearances of dead embryos were observed to be variable. The appearance of dead embryos exposed to 1000 µM VD11-4-2 was completely dark, while dead embryos were partially transparent after the treatment with 1000 µM VD12-09.

Lower than 1000 µM doses of tested compounds also significantly affected zebrafish development. The lethal impact on zebrafish embryos was found using 500 µM VD11-4-2. Several phenotype defects, such as abnormal body shape and reduction of the body pigmentation, were observed when embryos were exposed to 100 µM–250 µM VD11-4-2. The inhibitor VD12-09 appeared to be more lethal than VD11-4-2. Zebrafish embryos treated with the concentration higher than 60 µM VD12-09 were dead at 24 hpf. No abnormalities were found when 20 µM VD12-09 was applied. Moreover, EZA influenced the survival of embryos at 24 hpf. The coagulations and dark debris were detected when embryos were treated with 1000 µM of EZA. Lower concentrations, such as 100 µM EZA, slightly affected the phenotypic appearance of embryos and reduced their pigmentation. The lowest investigated concentration of 1 µM VD11-4-2, VD12-09, or EZA did not cause any mortality in zebrafish embryos and their phenotype appeared normal.

The impact of tested inhibitors on the zebrafish exposed for 5 days was determined. The phenotypes of 120 hpf alive zebrafish larvae were found to be less severe when treated with VD11-4-2 or VD12-09 than EZA. Zebrafish larvae exposed to 10 µM EZA showed severe developmental abnormalities, such as pericardial edema, unutilized yolk, and abnormal body shape (Figure 13A). These defects of zebrafish larvae were not found after the treatment with VD compounds (13B for VD11-4-2).

Interestingly, the hatching rate of 48 hpf zebrafish embryos was affected by one
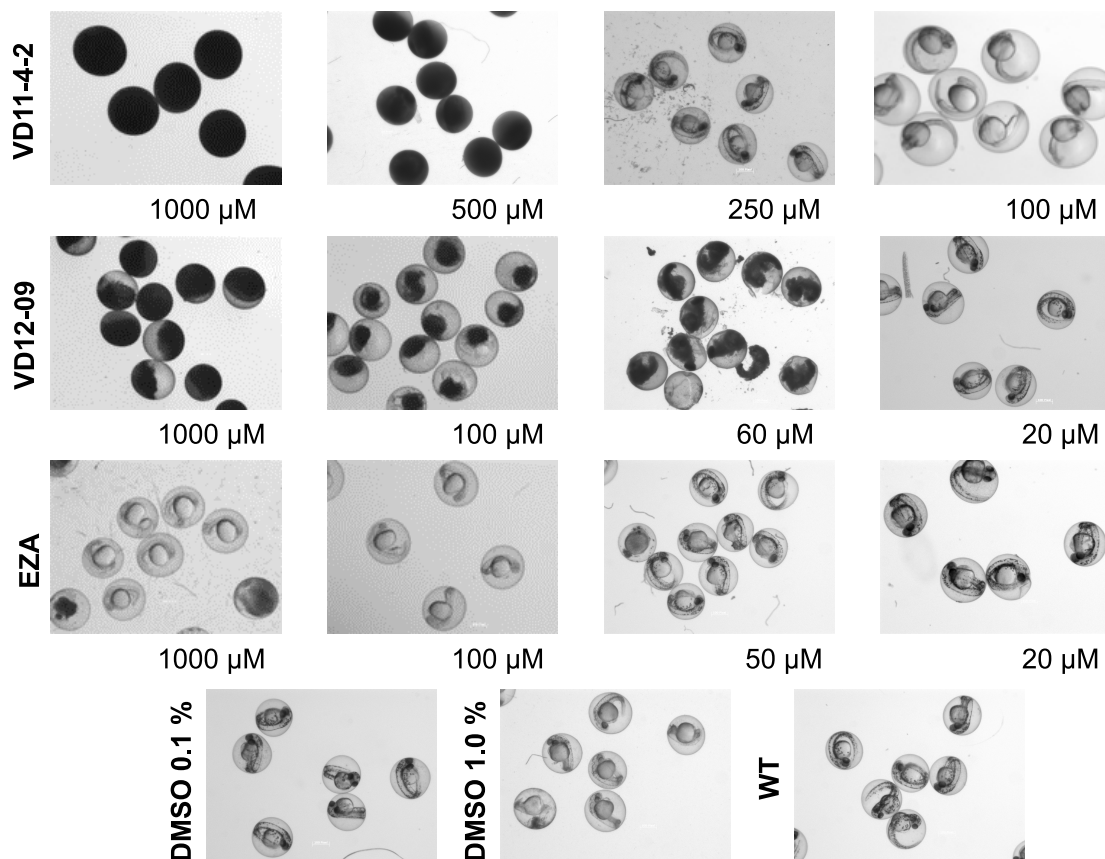
Figure 12: The phenotype of zebrafish embryos exposed to VD11-4-2, VD12-09, or EZA at 24 hpf.
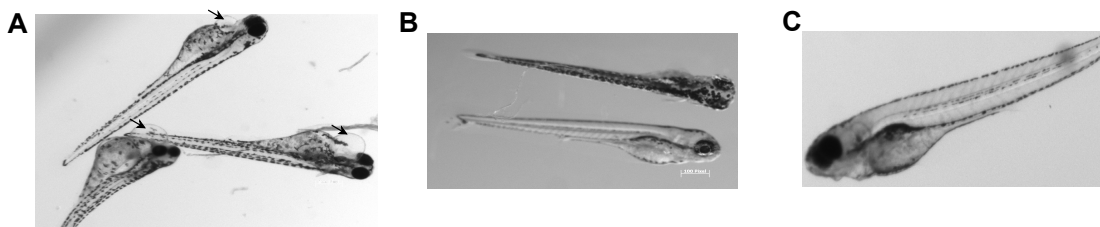
Figure 13: The phenotype of 120 hpf zebrafish larvae after the treatment with 10 µM EZA (A) or 100 µM VD11-4-2 (B) for 5 days and untreated WT control (C). Arrows in panel A indicate pericardial edema.

of the tested inhibitors. Figure 14 shows that 10 µM VD12-09 delayed the hatching time, whereas 120 µM VD11-4-2 and 10 µM EZA did not affect the hatching significantly as compared with the hatching times of WT zebrafish. The fractions of embryos that came out of the chorion at 72 hpf did not vary significantly after the treatment with VD11-4-2, VD12-09, and EZA. Thus, VD12-09 caused a temporary delay in hatching time, while other inhibitors did not exhibit the same effect.
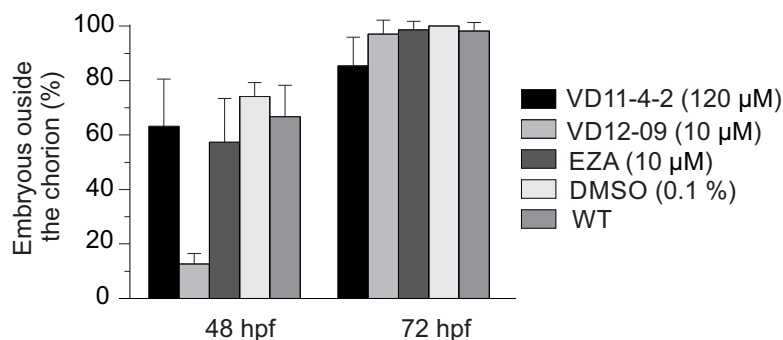
Figure 14: Hatching rates of 48 hpf and 72 hpf zebrafish embryos, which were untreated or exposed to the inhibitors or 0.1 % DMSO. VD12-09 delayed the hatching time at 48 hpf.

Morphological changes

To identify tissue alterations, the morphological changes were studied in 5 dpf larvae treated with 15 µM VD12-09 and 125 µM VD11-4-2 and compared with DMSO-, 20 µM EZA-treated, and untreated WT controls (Figure 15). After staining with hematoxylin and eosin, the Semithin sagittal sections of the larvae, previously exposed to VD11-4-2 and VD12-09, did not show any apparent morphological changes as compared with the DMSO-treated and untreated WT control larvae.
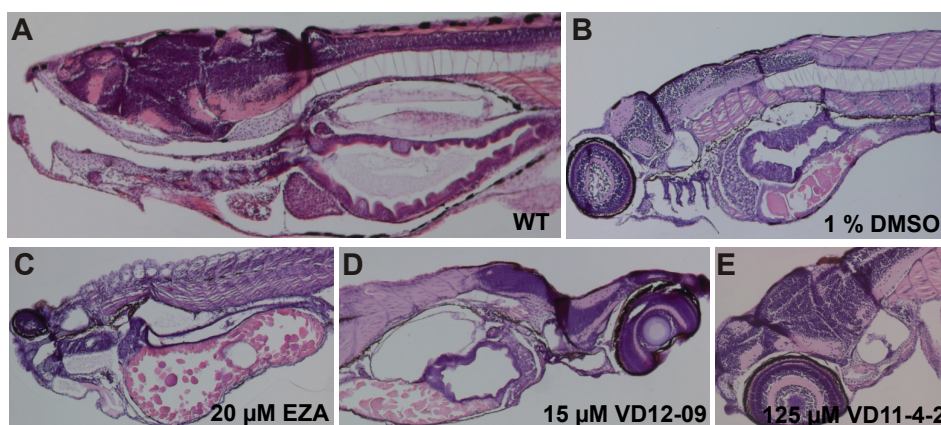
Figure 15: Histochemical images of the 5 dpf zebrafish larvae. The hematoxylin and eosin staining of WT zebrafish (A) and zebrafish exposed to 1 % DMSO (B), 20 µM EZA (C), 15 µM VD12-09 (D), or 125 µM VD11-4-2 (E). Images were selected from five independent groups of experiments. The sagittal sections showed no apparent morphological changes of zebrafish larvae treated with VD11-4-2, VD12-09, or EZA.

10.2 Affinity and selectivity properties of inhibitors in *Xenopus* oocytes

Microelectrode-monitored inhibition of intracellular CA IX

Klier and colleagues previously showed that $\sim 80\%$ of the heterologous CA IX is located inside the *Xenopus* oocyte [292]. Therefore, the inhibitory potencies of compounds VD11-4-2 and VD12-09 against the heterologous intracellular CA IX and CA II were determined by measuring $\Delta[\text{H}^+]_i/\Delta t$ with single-barreled pH-sensitive microelectrodes during repeated application of CO_2/HCO_3^- solution. Acid transients were recorded in native oocytes and oocytes injected with 5 ng CA IX-cRNA or 6 ng CA II-cRNA in the absence and presence of each inhibitor.

Panels A and B of Figure 16 show the acid transients during application of 5 % $CO_2/$ 25 mM HCO_3^- buffer in the oocytes injected with CA II-cRNA or CA IX-cRNA, respectively. Compared with native oocytes, the rate of acidification increased from $25.4 \pm 2.9 \, \text{nM min}^{-1}$ to $82.0 \pm 8.8 \, \text{nM min}^{-1}$ and $137.5 \pm 14.7 \, \text{nM min}^{-1}$ for CA IX and CA II cRNA injected oocytes, respectively (Figure 16C–16E). No impact of 10 µM VD11-4-2 on $\Delta[\text{H}^+]_i/\Delta t$ in CA II expressing oocytes was detected and $\Delta[\text{H}^+]_i/\Delta t$ was evaluated to be $137.1 \pm 17.1 \, \text{nM min}^{-1}$ (Figure 16D). A different effect was observed in CA IX-expressing oocytes. The $\Delta[\text{H}^+]_i/\Delta t$ was reduced from $82.0 \pm 8.8 \, \text{nM min}^{-1}$ down to $20.3 \pm 3.5 \, \text{nM min}^{-1}$ upon administration of 10 µM VD11-4-2 (Figure 16E). This value ($20.3 \pm 3.5 \, \text{nM min}^{-1}$) matched the rate of $20.2 \pm 1.4 \, \text{nM min}^{-1}$ obtained in native cells (w/o any CAs) treated with the same dose of VD11-4-2 (Figure 16C). Moreover, VD11-4-2 was characterized to be not washable from CA IX after exposure to the inhibitor for 15 min and 45 min ($\Delta[\text{H}^+]_i/\Delta t$ were $26.4 \pm 2.9 \, \text{nM min}^{-1}$ and $27.7 \pm 3.5 \, \text{nM min}^{-1}$, respectively). Thus, VD11-4-2 was shown to be membrane-permeable inhibitor that completely blocked the CA IX-generated rate of acidification at 10 µM in *Xenopus* oocytes.

In order to find the correlation between the cytosolic CA IX activity and the amount of VD11-4-2 necessary for inhibition, the experiments of treating CA IX-expressing oocytes with various VD11-4-2 concentrations and measuring $\Delta[\text{H}^+]_i/\Delta t$ were carried out (repeated 4 times). The lowest dose of VD11-4-2 was 1 nM. It was increased by 10-fold until 10 µM. Each concentration was tested on two CO_2/HCO_3^- applications (Figure 17). Average values were determined and used for IC_{50} determination. The IC_{50} value for VD11-4-2 to inhibit intracellular CA IX was determined using the sigmoidal dose-response Hill model (Figure 18). Data points were obtained experimentally and represent the values of changes in $[\text{H}^+]_i$ when doses of 1 nM–10 µM VD11-4-2 were applied on CA IX-expressing oocytes. The rate of change in $[\text{H}^+]_i$ from the first pulse in the absence of VD11-4-2 was defined as 100 % CA IX activity. The $[\text{H}^+]_i/\Delta t$ during the pulse in the
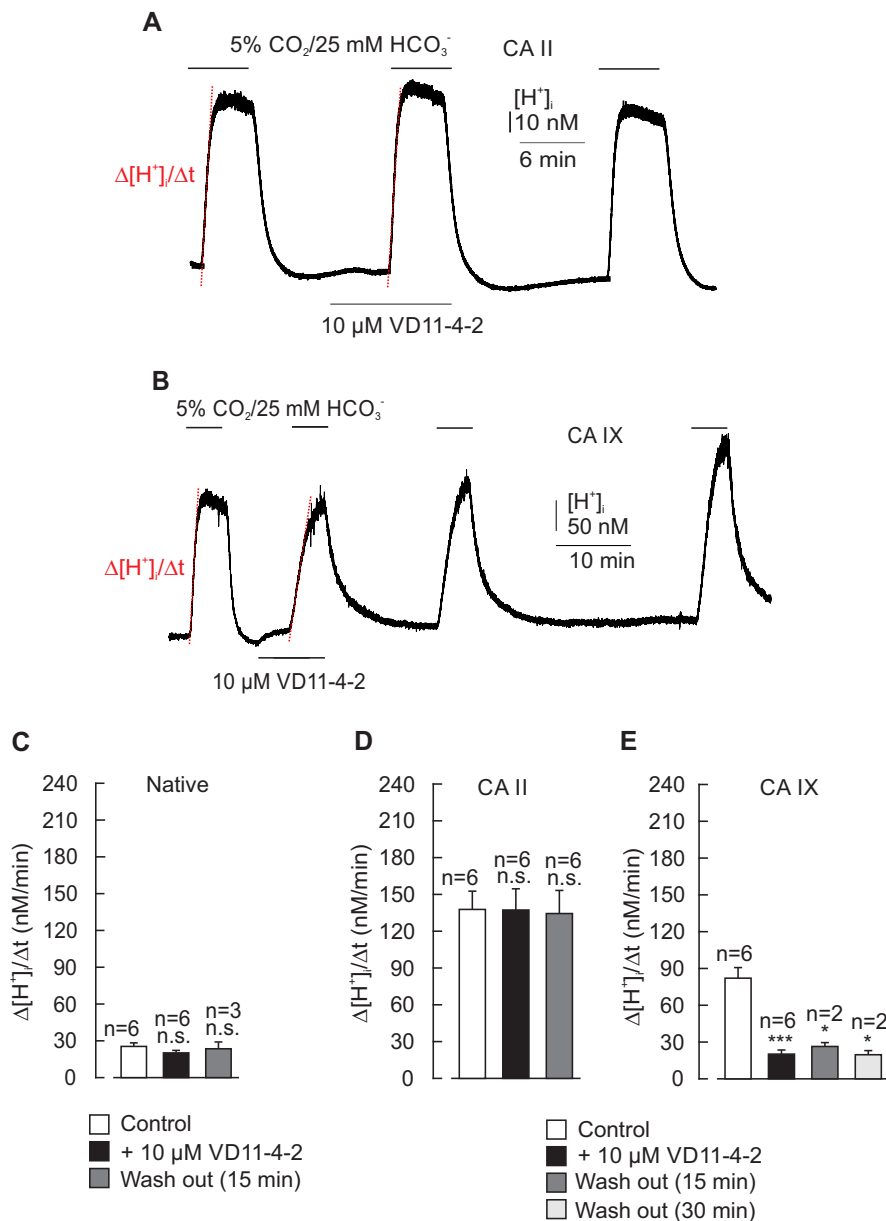
Figure 16: Measurements of cytosolic H^+ changes in native *Xenopus* oocytes (C) and oocytes expressing target CA isoform (A, B, D, E). Cells were injected with CA II-cRNA (A, D) or CA IX-cRNA (B, E) during application of CO_2/HCO_3^- (from a nominally CO_2-free, Hepes-buffered solution) in the absence and presence of $10\,\mu M$ VD11-4-2 and after $15\,min$ or $45\,min$ of washing out. Red lines represent slopes which were used for the evaluation of $\Delta[H^+]_i/\Delta t$. Asterisks indicate significant difference between CA activity before and after addition of inhibitor or washing it out (*$p<0.05$, ***$p<0.001$, n.s.: not significant).

presence of $10\,\mu M$ VD11-4-2 was evaluated to be $0\,\%$ due to the complete inhibition of CA IX catalytic activity using $10\,\mu M$ VD11-4-2 as shown in the Figure 16E. The intracellular pH in CA IX expressing oocytes was already affected by $1\,nM$ VD11-4-2 and $[H^+]_i/\Delta t$ decreased by $\sim20\,\%$. The fast rise of cytosolic $[H^+]$ upon the exposure of CO_2/HCO_3^- was reduced when the concentration of VD11-
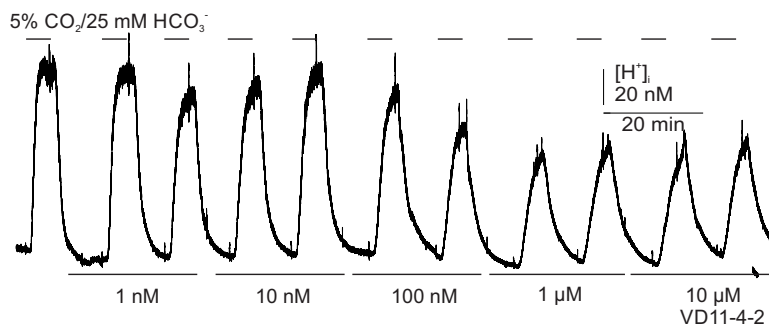
Figure 17: Recordings of $[H^+]_i$ in oocytes injected with CA IX-cRNA during application of CO_2/HCO_3^- (from a nominally CO_2-free, Hepes-buffered solution) in the absence and presence of 1 nM to 10 nM of VD11-4-2.
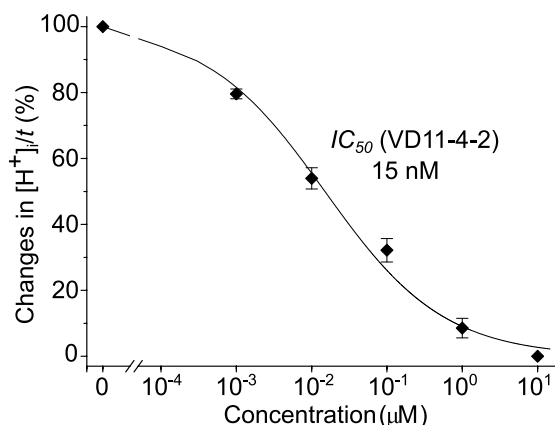
Figure 18: The dependence of changes in $[H^+]_i/t$ on the dose of VD11-4-2. Black data points were obtained experimentally. The solid line was simulated according to the Hill model (Hill coefficient 0.5).

4-2 was increased. The IC_{50} was found to be 15 nM. Thus, VD11-4-2 exhibited the significant inhibitory potential toward the intracellular CA IX.

The inhibitor VD12-09 exhibited lower potential to inhibit activity of heterologous CA IX than VD11-4-2. Panels A and B in Figure 19 show the acid transients representing the oocytes injected with CA II-cRNA or CA IX-cRNA, respectively. The fast rise of $[H^+]_i$ was not affected by 10 µM VD12-09 in CA II-expressing cells (Figure 19A, C) and was inhibited in CA IX-expressing cells from $87.5 \pm 17.8\,\text{nM}\,\text{min}^{-1}$ to $40.6 \pm 6.9\,\text{nM}\,\text{min}^{-1}$ (Figure 19B, D). Even though VD12-09 displayed the selectivity towards CA IX, the CA IX inhibition effect was lower as compared with the one of 10 µM VD11-4-2 and therefore inhibition of the intracellular CA IX by VD12-09 was not further investigated.
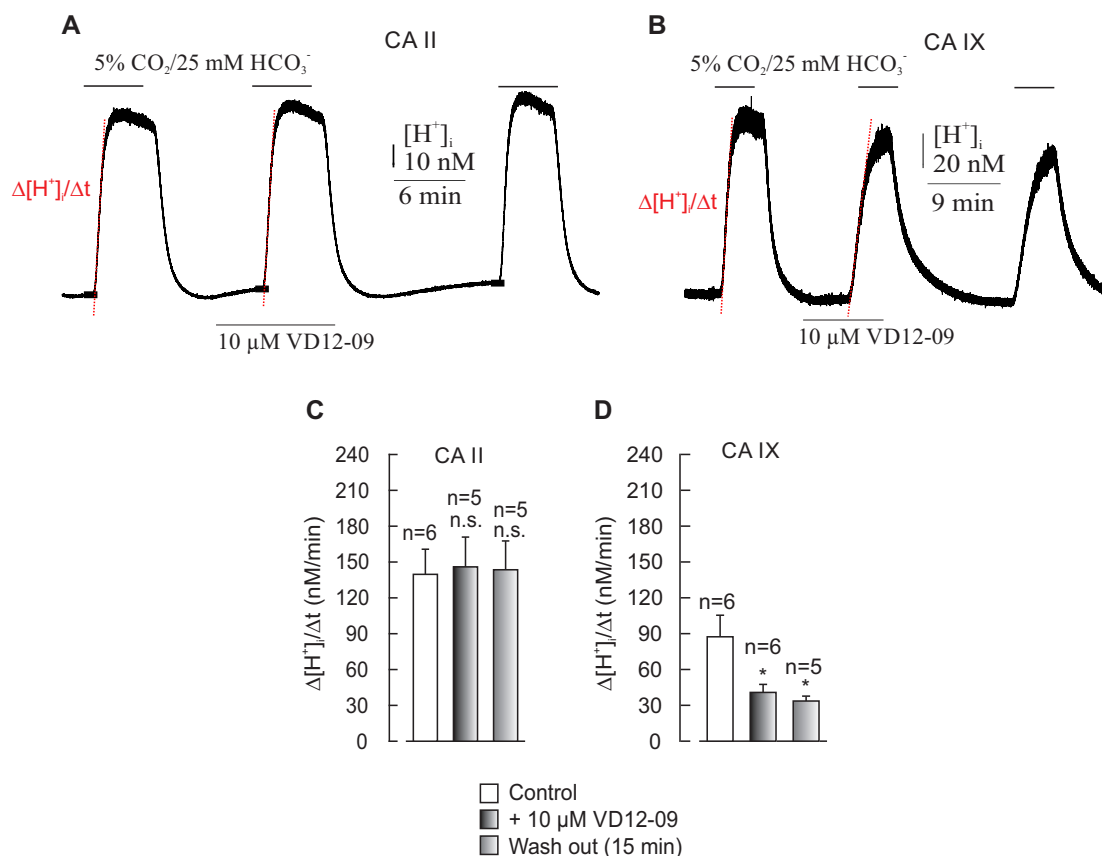
Figure 19: Measurements of cytosolic H^+ changes in *Xenopus* oocytes expressing target CA isoform. Cells were injected with CA II-cRNA (A, C) or CA IX-cRNA (B, D) during application of CO_2/HCO_3^- (from a nominally CO_2-free, Hepes-buffered solution) in the absence and presence of $10\,\mu M$ VD12-09 and after $15\,min$ of washing out. Red lines represent slopes which were used for the evaluation of $\Delta[H^+]_i/\Delta t$. Asterisks indicate significant difference between CA activity before and after addition of inhibitor or washing it out (*$p<0.05$, n.s.: not significant).

Microelectrode-monitored inhibition of extracellular CA IX

Being an important therapeutic target, the mature CA IX is a homodimeric and membrane-anchored protein displaying extracellular catalytic activity [108]. In *Xenopus* oocytes, $\sim20\,\%$ of CA IX is located outside at the membrane [292]. The sensitivity of extracellular CA IX activity to $10\,\mu M$ VD11-4-2 and VD12-09 was evaluated in oocytes by recording $[H^+]_s$ and the reference potential (E_{ref}) using double-barreled pH-sensitive microelectrodes (Figure 20A). Changes in E_{ref} were negligible ($\leq2\,mV$) during the measurements and are not presented here. A transient decrease in $[H^+]_s$ was caused upon addition of CO_2/HCO_3^- and a rise of $[H^+]_s$ was induced upon removal of CO_2/HCO_3^-. The extracellular CA IX activity was assessed by the amplitude of $\Delta[H^+]_s$ during the removal of CO_2/HCO_3^-.

In the absence of inhibitors, $\Delta[H^+]_s$ was determined to be $15.6 \pm 0.4\,nM\,min^{-1}$ in native cells (Figure 20B), which increased to $63.0 \pm 3.1\,nM\,min^{-1}$ in CA IX-

expressing oocytes (Figure 20C). The impact of VD11-4-2 on CA-mediated changes of the extracellular pH in CA IX-expressing oocytes was significant, whereas no significant effect of VD12-09 was found in this case. The amplitude of the acid transient decreased to $22.1 \pm 0.7 \, \mathrm{nM \, min^{-1}}$ with $10 \, \mu\mathrm{M}$ VD11-4-2 (Figure 20C). This $\Delta[\mathrm{H^+}]_s$ correlated with the result of treating native cells with the same dose of VD11-4-2 ($14.5 \pm 0.5 \, \mathrm{nM \, min^{-1}}$, Figure 20B). Similarly to intracellular pH measurements applying VD11-4-2 on CA IX-expressing oocytes, the interaction between the heterologous extracellular CA IX and VD11-4-2 featured great affinity and was shown to be essentially irreversible with $\Delta[\mathrm{H^+}]_s$ of $34.0 \pm 6.0 \, \mathrm{nM \, min^{-1}}$ after 15 min of washing out (Figure 20C).
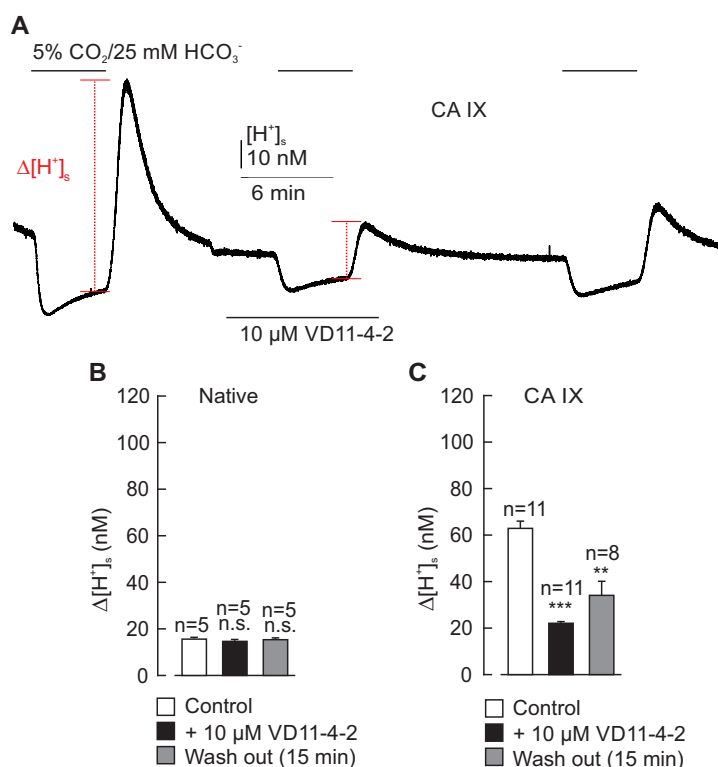
Figure 20: Measurements of $[\mathrm{H^+}]_s$ in *Xenopus* oocytes injected with CA IX-cRNA (A and C) and native oocytes (B) during application of CO_2/HCO_3^- (from a nominally CO_2-free, Hepes-buffered solution) in the absence and in the presence of $10 \, \mu\mathrm{M}$ VD11-4-2 and after 15 min of washing out. Red lines represent amplitudes which were used for the evaluation of $\Delta[\mathrm{H^+}]_s$. Asterisks indicate significant difference between CA activity before and after addition of inhibitor or washing it out (**$p<0.01$, ***$p<0.001$, n.s.: not significant).

The dependence of extracellular CA IX catalytic activity on added VD11-4-2 concentration was determined. The amplitudes of $\Delta[\mathrm{H^+}]_s$ transients after the application of different doses of VD11-4-2 are shown in Figure 21. The highest concentration of VD11-4-2 was $10 \, \mu\mathrm{M}$, which was decreased by 10-fold to $0.1 \, \mathrm{nM}$. Each concentration was applied during two applications of CO_2/HCO_3^-. The av-

erage values were calculated and used for IC_{50} evaluation. Figure 22 shows the
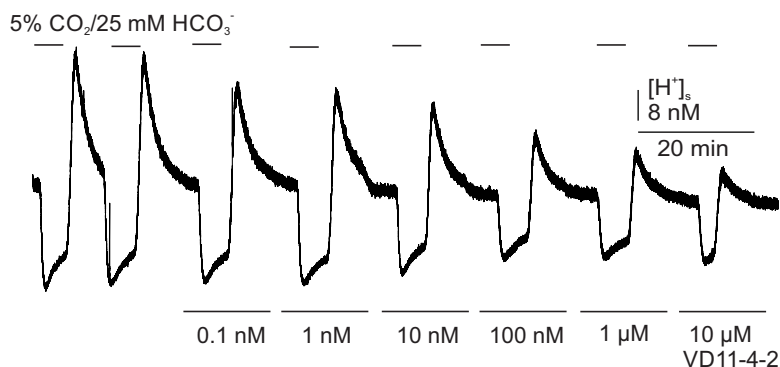
Figure 21: Recordings of $[H^+]_s$ in oocytes injected with CA IX-cRNA during application of CO_2/HCO_3^- (from a nominally CO_2-free, Hepes-buffered solution) in the absence and presence of $0.1\,nM$ to $10\,nM$ of VD11-4-2.

dose-response curve of changes in extracellular $\Delta[H^+]_s$ as a function of added VD11-4-2 concentration. When higher concentrations of the inhibitor were used, the amplitude of $\Delta[H^+]_s$ transient significantly decreased. Simulation of the dependence according to Hill model yielded the extracellular IC_{50} of $25\,nM$, which correlates with the intracellular IC_{50} value for VD11-4-2 (Figure 18). Thus, VD11-4-2 exhibited high inhibitory potential towards both the heterologous intracellular and extracellular CA IX in *Xenopus* oocytes.
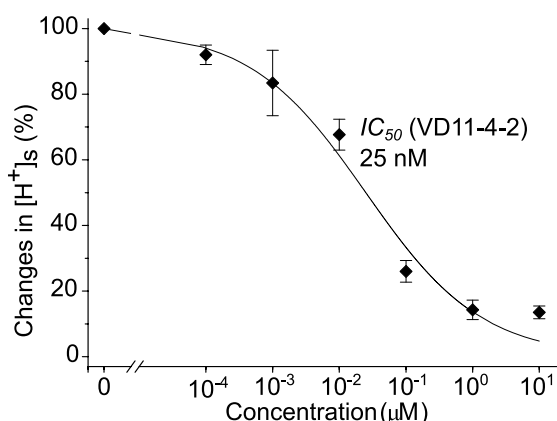
Figure 22: The dependence of changes in $[H^+]_s$ on the dose of VD11-4-2. Black data points were obtained experimentally, while the solid line was simulated according to the Hill model (Hill coefficient 0.5).

Characterization of inhibitor selectivity towards CA IX

The high selectivity of VD11-4-2 toward CA IX was also confirmed by determining the inhibitory potential of the compound towards CA IV and CA XII. VD11-4-2 was shown to have a relatively minor effect on extracellular pH in CA IV-cRNA

(Figure 23A, C) and CA XII-cRNA (Figure 23B, D) injected oocytes at 50 nM concentration. However, the administration of 10 µM of VD11-4-2 resulted in $\Delta[H^+]_s$ of $54.3 \pm 5.7\,\mathrm{nM\,min^{-1}}$ and $26.5 \pm 1.4\,\mathrm{nM\,min^{-1}}$ in oocytes expressing CA IV and CA XII, respectively. Moreover, the effect of VD11-4-2 on CA IV was found to be washable after 15 min, while non-washable for CA XII. These experiments supported the conclusion about the high selectivity of VD11-4-2 towards CA IX, but not CA II, CA IV, or CA XII.
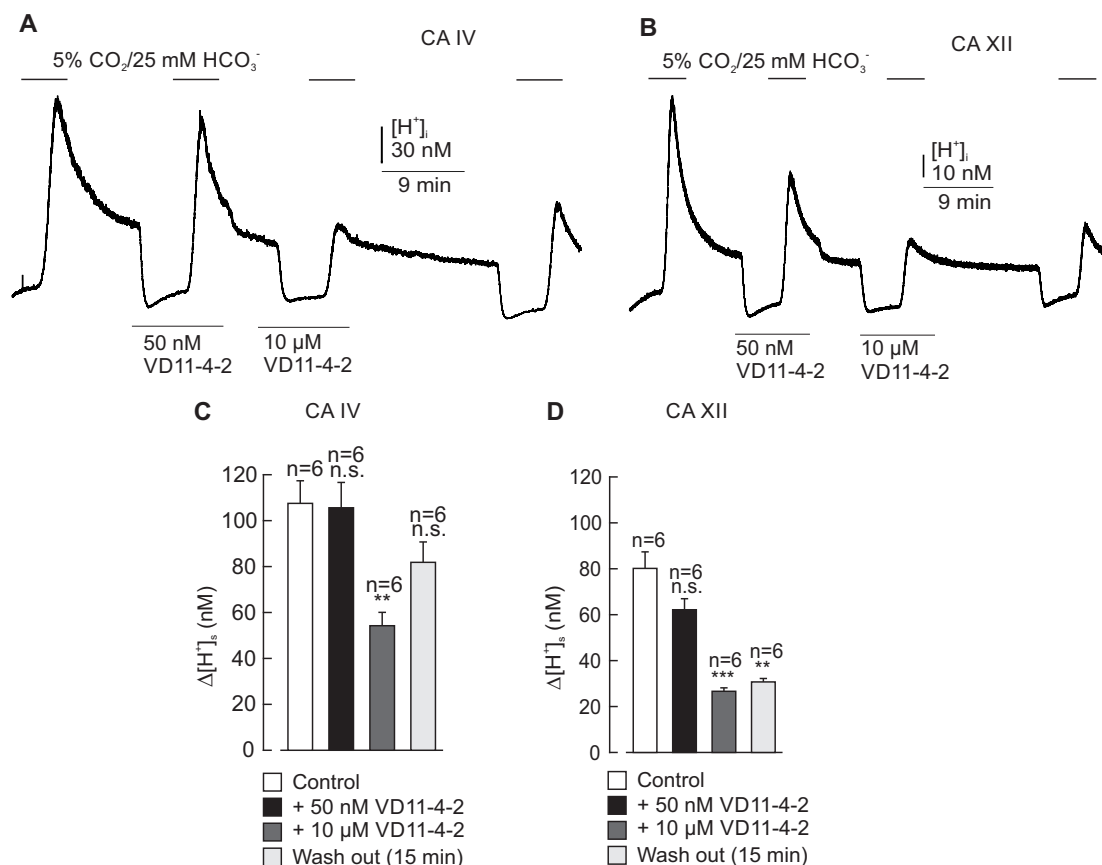
Figure 23: Measurements of $[H^+]_s$ in oocytes injected with 1 ng CA IV-cRNA (A, C) or 5 ng CA XII-cRNA (B, D) during application of CO_2/HCO_3^- (from a nominally CO_2-free, Hepes-buffered solution) in the absence and presence of 50 nM and 10 µM VD11-4-2 and after 15 min of washing out. Asterisks indicate significant difference between CA activity before and after addition of inhibitor or washing it out (**$p<0.01$, ***$p<0.001$, n.s.: not significant).

Inhibition of CA IX evaluated by mass spectrometry

The activity of CA IX decreased by 25 % after the addition of 1 nM VD11-4-2 to oocyte lysate according to MS measurements (Figure 24A and 24B). In the lysate of oocytes expressing CA IX, which was exposed to 10 nM of VD11-4-2, the rate of ^{18}O enrichment did not differ from the rate in the lysate of native cells treated with the same dose of inhibitor. Therefore, the complete inhibition of

CA IX activity was identified using 10 nM of VD11-4-2. These results confirmed the outcome from intracellular and extracellular pH measurements highlighting the nanomolar affinity of VD11-4-2 against CA IX.
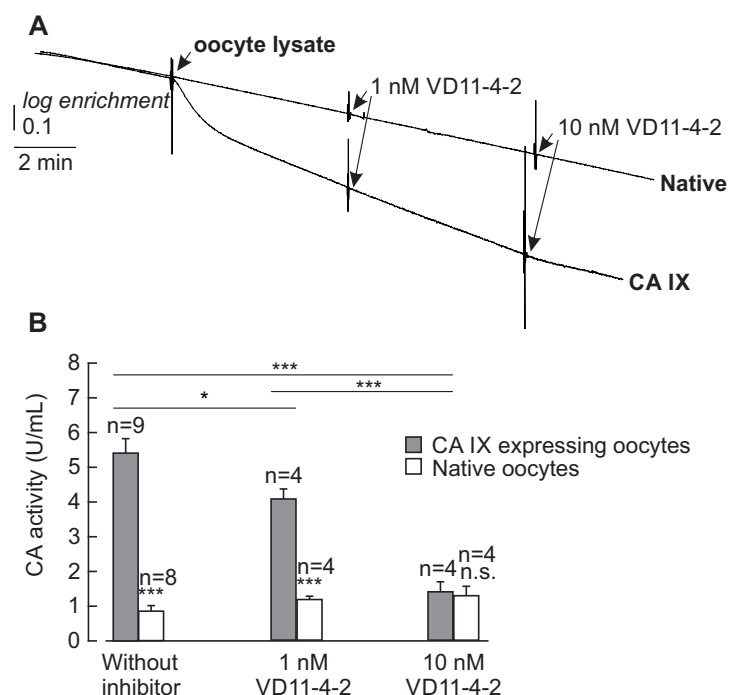
Figure 24: Recordings of the degradation of ^{18}O-labeled CO_2 (A) and evaluations of CA IX activity (B) in the absence and presence of 1 nM and 10 nM VD11-4-2 in lysed oocytes as measured by MS. The addition of oocyte lysate made from 20 cells and different concentrations of VD11-4-2 are shown by arrows. Asterisks in the upper part of the graph in panel B indicate significant difference between CA activity before and after addition of inhibitor using CA IX-expressing oocytes, while asterisks above the bars show difference between CA activity in native and CA IX-expressing oocytes applying the same dose of inhibitor (*$p<0.05$, ***$p<0.001$, n.s.: not significant).

10.3 Anti-proliferative and functional activities of inhibitors in cancer cells

In addition to compounds VD11-4-2 and VD12-09, another discovered inhibitor VR16-09 was included in the study. The structure and binding affinities of VR16-09 to the recombinant human CA isoforms are indicated in Table 8. VR16-09 exhibited the high affinity in combination with greater selectivity than VD11-4-2 and VD12-09 towards CA IX. The inhibitor VR16-09 has not been reported by the publication so far. Therefore it was relevant to involve VR16-09 into the biological investigation, particularly in human cancer cells, of lead CA IX-targeting compounds.

CA IX-dependent functional activities of inhibitors in cancer cells

The compounds VD11-4-2, VD12-09, and VR16-09 were evaluated for their biological functional activities in a panel of human cancer cell lines. The expression of CA IX increased in hypoxic (0.2% O_2) A549 (lung), AsPC-1 (pancreatic), MDA-MB-231 (breast), H460 (lung), and HeLa (cervical) cancer cells (Figure 25A), whereas CA XII expression was similar under normoxia and hypoxia (Figure 25B). First, the impact of compounds on the inhibition of total extracellular CA cat-
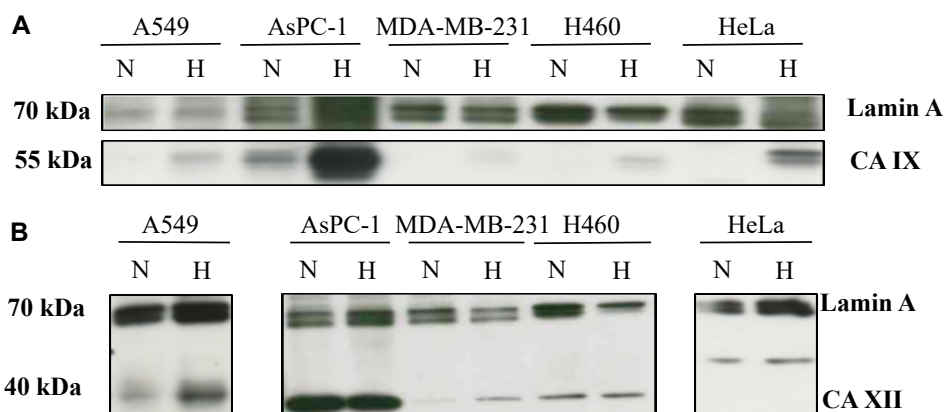
Figure 25: Western blot analysis of CA IX (A) and CA XII (B) expression in A549, AsPC-1, MDA-MB-231, H460, and HeLa cells after exposure to normoxia (N, 21%) or hypoxia (H, 0.2%) for 72 h. The MW of CA XII in HeLa was found to be larger than in other tested cell lines, suggesting variability of CA XII isoforms or their post-translational modifications in different cell lines. Lamin A was used as loading control.

alytic activity in hypoxic MDA-MB-231 cells was evaluated by determining the rate of the CO_2/HCO_3^- hydration/dehydration reaction via ^{18}O depletion from $^{13}C^{18}O_2$, measured by MS. Addition of cell suspension resulted in an acceleration of the reaction indicating the extracellular CA catalytic activity in hypoxic MDA-MB-231 cells (Figure 26A). Pre-incubation of the cell suspension with VR16-09, VD11-4-2, or VD12-09 resulted in a dose-dependent decrease in CA activity with IC_{50} values of 1.29 ± 0.11 nM, 2.95 ± 0.69 nM, and 167.4 ± 1.3 nM, respectively (Figure 26B–26D).

To verify the CA IX-specificity of investigated inhibitors, HeLa CA IX KO cells were generated using CRISPR-Cas9 genome editing. Two clones of HeLa cells with knocked out CA IX were selected according to Western blot analysis (Figure 27), followed by the genetic confirmation of KO-causing mutations in the *CA9* gene in two alleles per clone using single allele sequencing. Two HeLa CA IX KO clones and HeLa WT cells were exposed to VR16-09, VD11-4-2, or VD12-09 at concentrations of near maximum inhibition of extracellular CA activity in hypoxic MDA-MB-231 cells. In both HeLa CA IX KO clones, VR16-09 (300 nM), VD11-4-2 (300 nM), or VD12-09 (30 µM) did not alter CA activity (Figure 28). However,
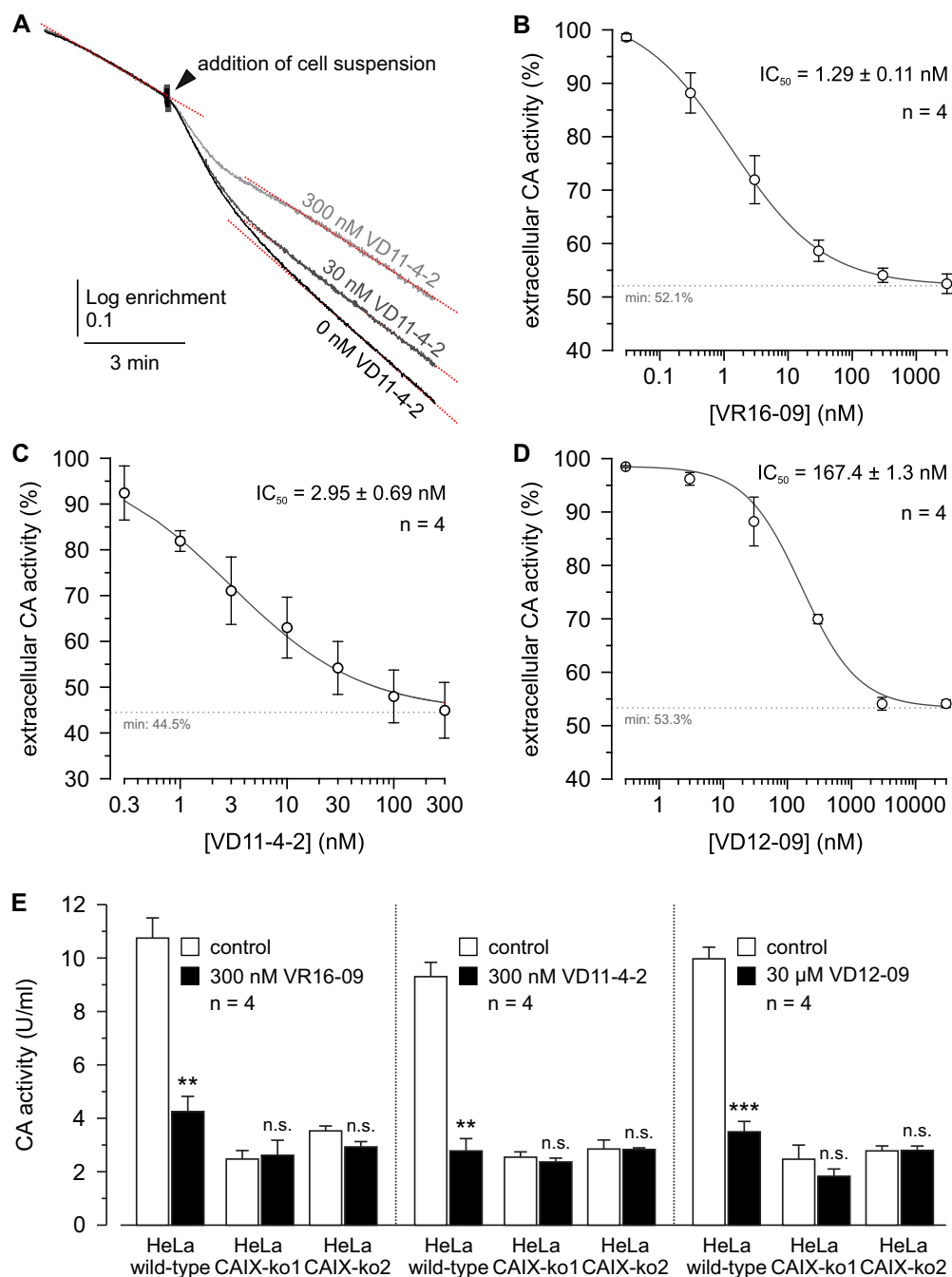
Figure 26: *IC*$_{50}$ determination of VR16-09, VD11-4-2, and VD12-09 in hypoxic MDA-MB-231 cells. (A) Original recordings of the log enrichment of MDA-MB-231 cells pre-incubated with VD11-4-2 for up to 3 h. The beginning of each trace shows the rate of degradation of the ^{18}O-labeled substrate in the non-catalyzed reaction. (B-D) Relative CA activity in MDA-MB-231 cells, incubated under hypoxia (1 % O$_2$) for 3 days. Cells were pre-incubated with VR16-09 (B), VD11-4-2 (C), or VD12-09 (D) for up to 3 h. CA activity was determined by MS gas-analysis from the increase in the rate of log enrichment after addition of cell suspension. CA activity in the presence of inhibitor was normalized to the activity in the absence of inhibitor. Average ± SD of four independent experiments per cell line are shown.

the considerable CA activity remained in HeLa CA IX KO cells, indicating activity of other extracellular CA isoforms. In HeLa WT cells, CA activity decreased to 30 %–40 % after the treatment with tested inhibitors. These values did not significantly differ from CA activity of the untreated HeLa CA IX KO clones. Thus, VR16-09, VD11-4-2, and VD12-09 specifically targeted CA IX, while other extracellular CA isoforms remained unaffected.
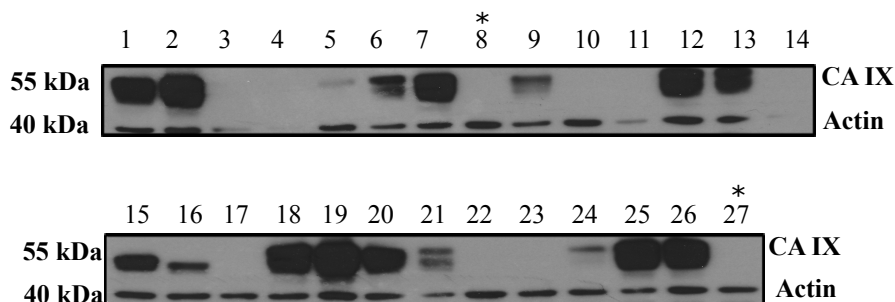
Figure 27: Western blot analysis of CA IX expression in a panel of expected HeLa CA IX KO clones after exposure to hypoxia (0.2 %) for 24 h. Clones 8 and 27, marked by asterisks, were selected as HeLa CA IX KO clones 1 and 2, respectively, and used in experiments. The growth rate of clones 8 and 27 were similar as compared to HeLa WT cells. Actin was used as loading control.
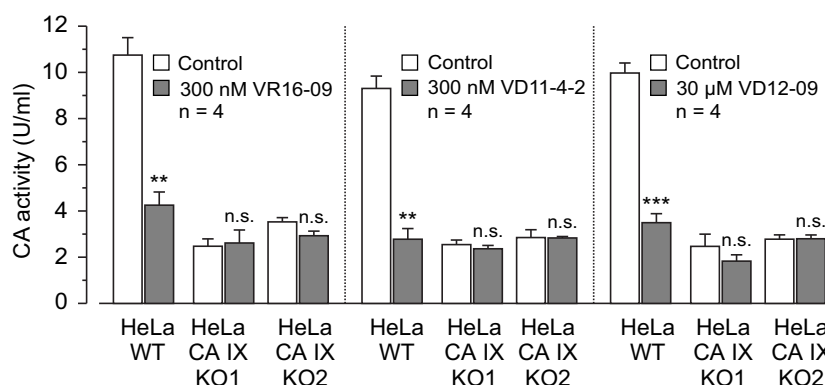
Figure 28: CA IX-dependent mode of action for inhibitors in hypoxic HeLa cells. CA activity in HeLa WT and two HeLa CA IX KO clones, before (white bars) and after addition of VR16-09, VD11-4-2, or VD12-09 (grey bars), was determined by MS gas-analysis from the increase in the rate of log enrichment after addition of cell suspension. CA activity in the presence of inhibitor was normalized to the activity in the absence of inhibitor. Average $\pm$ SD of four independent experiments per cell line are shown. Asterisks indicate significant difference between CA activity before and after addition of inhibitor (**$p < 0.01$, ***$p < 0.001$, n.s.: not significant).

Second, the functional activity of compounds was further confirmed by measuring the rise in extracellular pH directly inside a hypoxic chamber. VR16-09, VD11-4-2, and VD12-09 significantly reduced hypoxia-induced acidification of HeLa cells in a dose-dependent manner, while the effect on cells exposed to

normoxia was negligible (Figure 29A). This functional activity was the most pronounced for VR16-09 at 50 µM, whereas VD12-09 exhibited the lowest functional activity of tested compounds in HeLa cells. Hypoxia-induced acidosis of other
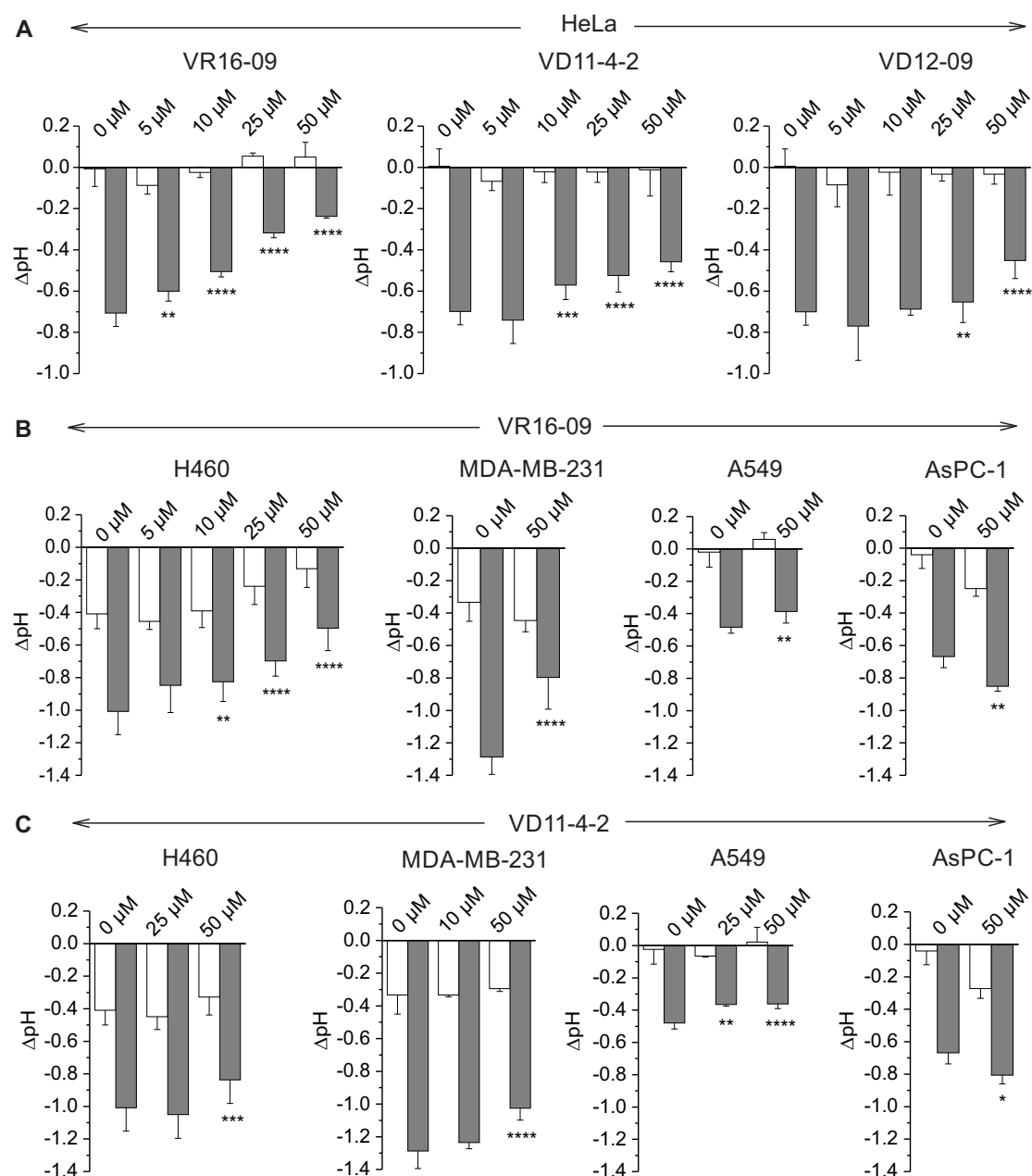
Figure 29: (A) Changes in extracellular acidification of HeLa cells after the treatment with VR16-09, VD11-4-2 or VD12-09 for 72 h under normoxia (21 % O_2; white bars) or hypoxia (0.2 % O_2; grey bars). Effect of VR16-09 (B) and VD11-4-2 (C) on the hypoxia-induced extracellular acidification of H460, MDA-MB-231, A549, and AsPC-1 after the exposure for 72 h. Average ± SD of at least three independent experiments is shown. Asterisks indicate significant difference between medium pH of cells exposed to DMSO and cells treated with various doses of inhibitor under hypoxic conditions (*$p<0.05$, **$p<0.01$, ***$p<0.001$, ****$p<0.0001$).

three investigated cell lines was significantly reduced by $10\,\mu M$ to $50\,\mu M$ VR16-09 (Figures 29B). The extracellular pH of cells, treated with DMSO and in parallel with $50\,\mu M$ VR16-09, was elevated from 6.97 ± 0.06 to 7.44 ± 0.06 for HeLa, from 6.67 ± 0.13 to 7.19 ± 0.14 for H460, from pH 6.37 ± 0.11 to 6.83 ± 0.20 for MDA-MB-231, and from pH 6.70 ± 0.04 to 6.79 ± 0.07 for A549 cells. A 4-fold lower concentration of sodium bicarbonate in the medium was used for A549 to determine the functional effects of the compounds due to relatively low levels of hypoxia-induced CA IX (Figure 25A).

The inhibitor VD11-4-2 also significantly affected hypoxic acidification (Figure 29A, 29C) and the exposure of cells to $50\,\mu M$ VD11-4-2, as compared with DMSO control, caused the increase of pH from 6.97 ± 0.06 to 7.21 ± 0.05 for HeLa, from 6.67 ± 0.13 to 6.84 ± 0.14 for H460, from pH 6.37 ± 0.11 to 6.63 ± 0.07 for MDA-MB-231, and from pH 6.70 ± 0.04 to 6.81 ± 0.03 for A549 cells.

However, acidosis of AsPC-1 cells in hypoxia increased after exposure to VR16-09 and VD11-4-2 from 6.99 ± 0.07 to 6.81 ± 0.03 and to 6.85 ± 0.05, respectively (Figure 29B, 29C). AsPC-1 cells were unique among tested human cancer cell lines due to expression of MCT1 under both normoxic and hypoxic conditions (Figure 30A), whereas MCT4 was expressed in all tested cell lines and was up-regulated in response to hypoxia (Figure 30B). The link between increased acidosis of AsPC-1 by inhibitors under hypoxia and the MCT1 expression is discussed in the next chapter.
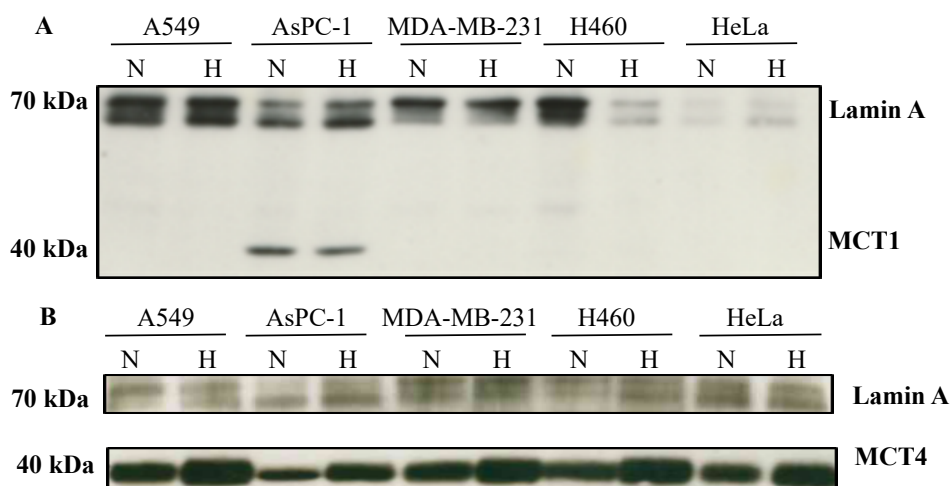
Figure 30: Western blot analysis of MCT1 expression in A549, AsPC-1, MDA-MB-231, H460, and HeLa cell lines after exposure to normoxia (N, 21 %) or hypoxia (H, 0.2 %) for 72 h. Lamin A was used as loading control.

Inhibitor-induced cytotoxicity

Cytotoxicity of tested compounds was higher in normoxic than hypoxic cell monolayers, as determined by cell viability assay using alamarBlue® after treatment for

48 h or 72 h (Table 9). Inhibitors were less effective in reducing viability of CA IX-expressing hypoxic cells than normoxic cells without or with significantly lower CA IX expression.

Table 9: EC_{50} values for VR16-09, VD11-4-2, and VD12-09 evaluated by alamarBlue® cell viability assay. The HeLa, H460, A549, and MDA-MB-231 cells were exposed to the compounds under normoxia (21 % O_2) or hypoxia (0.2 % O_2) for 72 h, while AsPC-1 cells - for 48 h. Results of at least three independent repeats are shown (average ± SD).

| | EC_{50} (µM) | | | | | |
| | VR16-09 | | VD11-4-2 | | VD12-09 | |
O_2	21 %	0.2 %	21 %	0.2 %	21 %	0.2 %
HeLa	20.2 ± 4.3	40.8 ± 9.6	47.8 ± 9.6	92.2 ± 8.3	21.6 ± 4.1	46.9 ± 7.0
H460	19.3 ± 3.6	40.0 ± 9.6	21.4 ± 3.1	44.6 ± 6.4	17.8 ± 2.2	37.0 ± 7.6
A549	17.0 ± 1.0	76.7 ± 2.9	43.8 ± 2.5	105 ± 6	33.8 ± 2.5	98.8 ± 8.5
MDA-MB-231	74.2 ± 3.8	84.2 ± 4.9	52.8 ± 7.1	64.3 ± 11.5	55.4 ± 6.6	67.6 ± 7.1
AsPC-1	153 ± 23	160 ± 17	165 ± 6	145 ± 6	100 ± 20	83.3 ± 5.8

Similarly, tested compounds VR16-09 and VD12-09 were more effective in reducing clonogenic survival in normoxic compared to hypoxic monolayer HeLa cells after exposure for 72 h (Figure 31).
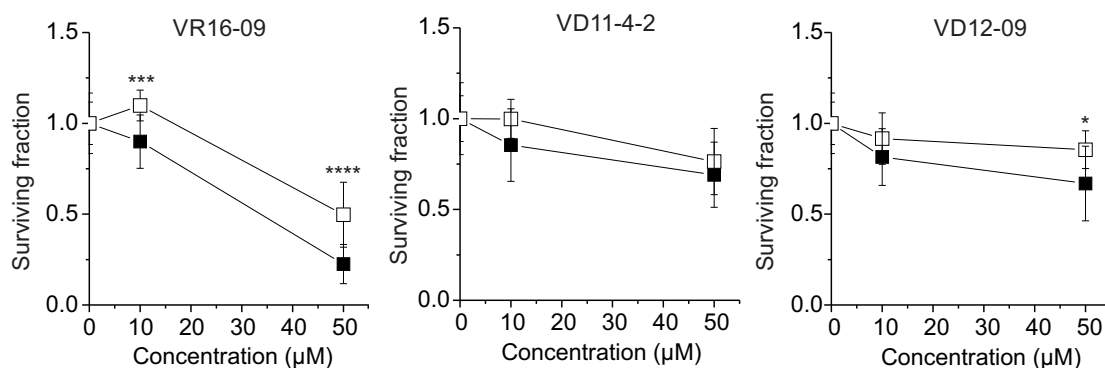
Figure 31: Clonogenic survival of monolayer HeLa cells after the exposure to compounds for 72 h under normoxia (21 % O_2; ■) or hypoxia (0.2 % O_2; □). Surviving fraction was normalized to vehicle control. Average ± SD of three independent repeats is shown. Asterisks indicate statistically significant differences between the surviving fractions of normoxic and hypoxic clonogenic cells after exposure to the same dose of inhibitor (*p<0.05, ***p<0.001, ****p<0.0001).

Hypoxia-dependent effect on spheroid clonogenic survival

To confirm the hypoxia-dependent efficacy of the compounds, H460 spheroids were employed. Immunofluorescence analysis confirmed overlap between CA IX expression and PIMO-positive hypoxia in sections of H460 spheroids grown for 11 days, whereas neither CA IX nor hypoxia were found in spheroids grown for

7 days (Figure 32A). Therefore, non-hypoxic (grown for 4 days) and hypoxic (grown for 11 days) H460 spheroids were exposed to VR16-09 using effective doses based on extracellular pH assays (Figure 29A, 29B) for 24 h and afterwards plated for clonogenic survival. In contrast to two-dimensional (2D) cell viability and clonogenic survival assays, the impact of VR16-09 on clonogenic cell survival was observed to be dependent on hypoxia, correlating with CA IX expression, in H460 3D spheroids (Figure 32B).
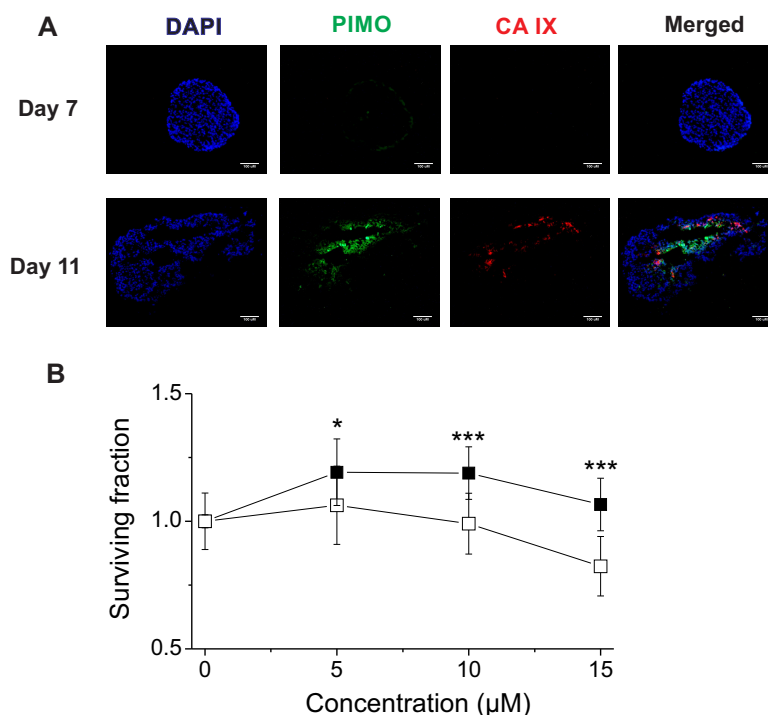
Figure 32: The impact of VR16-09 on H460 spheroid clonogenic survival. (A) Immunofluorescence images of H460 spheroids stained for DAPI (blue), PIMO (green), and CA IX (red). The scale bar indicates $100\,\mu$M. (B) Survival of clonogenic cells derived from non-hypoxic (■) and hypoxic (□) H460 spheroids exposed to VR16-09 for 24 h on day 4 or day 11, respectively. Asterisks indicate statistically significant differences between the surviving fractions of clonogenic cells derived from normoxic or hypoxic spheroids after exposure to the same dose of inhibitor (*$p<0.05$, ***$p<0.001$).

Discussion

The first critical step toward developing novel drugs is identification of the compound that induces a therapeutically relevant response by acting on the macromolecule, such as the enzyme, linked with the disease. Understanding the role of enzymes in pathological states and the implementation of strategies to modulate their activities remains a key focus for drug discovery [1]. Despite the recent advances in molecular sciences, the development of numerous therapeutics often fail in clinical trials most likely due to the insufficient characterization during preclinical research [343]. Thus, the wide collaboration across various disciplines is crucial to improve the combination of biochemical, biophysical, and cell biology assays and thus provide the deeper insight into the efficacy of drug candidates.

Human CA isoforms play important physiological functions, while the abnormal levels or activities of these enzymes are associated with various diseases. Therefore, diverse human CA isozymes have emerged as relevant targets for diagnostics and targeted drug delivery applications. However, the design of CA isoform-selective compounds has been a challenging goal for many researchers over the last several decades because of the structural homology among human CA isoforms. The main and most investigated class of CA inhibitors is composed of sulfonamide-based compounds. To date, there are nine clinically available sulfonamides targeting CAs and they are known to induce undesired side effects due to nonspecific CA inhibition [344]. Therefore, there is a need to improve the *in vitro* characterization of compounds leading to more efficient CA-targeting strategies.

Different expression systems have been investigated for the production of soluble and active recombinant proteins required for the *in vitro* analysis of protein-inhibitor binding in the initial stages of drug discovery. Due to low cost and quick procedure, microbial systems, such as *E. coli*, are a preferred choice. Mammalian cells are competing with bacteria as a host system because bacteria lack the post-translational modifications and often exhibit improper protein folding [345]. Such structural differences can influence the affinity of inhibitor binding to the target protein expressed in model systems as compared with human body. Therefore, it is of fundamental importance to ensure the suitability of the recombinant isozyme representing the native target of human body for *in vitro* approaches.

In this study, the binding of a series of sulfonamides to three forms of CA VI was evaluated. CA VI was obtained by three different procedures: the native CA VI was purified from human saliva, the recombinant CA VI was expressed in *E. coli* bacteria, and another recombinant CA VI was expressed in mammalian FreeStyle 293-F suspension cells. The inhibitors bound with essentially identical affinities to CA VI purified from three different sources, as determined by FTSA and ITC. Therefore, the recombinant CA VI from *E. coli* was characterized to be a suitable model of human native CA VI for the *in vitro* investigation of inhibitors binding to CA VI by applied biophysical approaches. Moreover, the profiles of thermal stability by FTSA showed that CA VI from bacteria was less stable than CA VI from mammalian cells and human saliva most likely due to the absence of glycosylation that is found in eukaryotic CA VI [72, 73]. FTSA also revealed that the pH and buffer conditions to purify and store the recombinant CA VI may be improved by using pH 5.0–6.0 rather than pH 7.0. It correlates with the previous study showing the retained enzymatic activity of CA VI in the acidic environment [85].

The importance of dissecting the linked protonation-deprotonation reactions occurring upon compound binding to CA isoforms has been reviewed by White-side's group [346]. Protonation events occurring upon the inhibitor binding to the active site of CA have been recently confirmed by neutron crystallography [347]. To generate compounds with great affinities by rational design, it is important to distinguish the intrinsic binding thermodynamic parameters from the observed ones by subtracting the linked protonation events occurring in conjunction with the binding reaction between the CA and inhibitor. Here, intrinsic binding constants of nonfluorinated compounds showed stronger binding than of fluorinated benzenesulfonamides. However, the higher observed affinity of fluorinated compounds than nonfluorinated ones was determined. This significant difference between intrinsic and observed parameters was caused by the fluorine effect on diminishing the pK_a of sulfonamide group but not due to the direct recognition of the CA VI by fluorine atoms of inhibitor. The reduced pK_a of fluorinated compounds resulted in the elevated observed affinity because of the increased inhibitor fraction in the deprotonated form that can bind to CA VI containing the protonated zinc-bound hydroxide ion (water molecule) in the active site. This finding confirmed that only intrinsic parameters should be applied to analyze the interaction mode and correlate the binding energetics with the chemical structure for the rational drug design.

Among fifteen human CA isoforms, CA IX is of particular interest due to its high expression in tumors and low levels in normal tissues [99]. The relevant association between CA IX expression and worse prognosis of patients having diverse cancer types has been demonstrated [112], thereby confirming the clinical

importance of CA IX. Recently, several compounds, VD11-4-2 and VD12-09, were designed at the Department of Biothermodynamics and Drug Design (Institute of Biotechnology, Vilnius university) and reported as highly potent and selective inhibitors of recombinant CA IX according to enzymatic and biophysical methods [342]. Therefore, there was a demand to further develop these compounds by assessing their efficacy using biological assays. In this study, model systems of zebrafish, *Xenopus* oocytes, and human cancer cells were involved to determine the effects of CA IX-targeting lead compounds designed by our group.

Zebrafish has emerged as a promising vertebrate animal model for chemical screenings [272]. Here toxic effects of three compounds on zebrafish embryonic development were determined. Both CA IX-selective inhibitors VD11-4-2 and VD12-09 and a non-selective CA inhibitor EZA, a commonly used drug in clinics [348,349], were applied. According to LC_{50} values, VD11-4-2 exhibited 10-fold lower toxicity than EZA. VD12-09 and EZA had a strong effect on the zebrafish mortality represented by steep dose response curves (Figure 11), which can be compared with ones reported in the recent investigation of the toxicity of anti-cancer compounds in zebrafish [350]. VD11-4-2 exhibited a milder systematic impact on the zebrafish survival as represented by the gradual dose response curve. These results suggested that VD12-09 and EZA are more toxic than VD11-4-2 and may exhibit lower excretion and cause severe effects on multiple organ systems.

Moreover, changes in zebrafish larvae treated with inhibitors were studied by light-field microscopy and histological analysis. The exposure of zebrafish to VD11-4-2 and VD12-09, using the same or lower doses as their exhibited LC_{50} values, did not lead to deleterious effects on the zebrafish embryonic development, whereas EZA induced severe phenotypic defects, such as pericardial edema and abnormal appearance of the body. Histochemical studies did not show any morphological changes of zebrafish exposed to tested compounds. To summarize, both VD11-4-2 and VD12-09 caused lower toxicity than EZA in zebrafish and therefore were suitable for the further development.

The heterologous protein expression in *Xenopus* oocytes has emerged as a promising tool in molecular and physiological research. Here the catalytic activities of diverse CA isoforms heterologously expressed in *Xenopus* oocytes were evaluated in the presence of VD11-4-2 and VD12-09. Measurements of the rate of cytosolic pH changes and the amplitude of pH changes at the outer membrane surface during addition/removal of CO_2/HCO_3^- revealed the best balance of VD11-4-2 affinity and selectivity towards the heterologous CA IX in oocytes. The IC_{50} values for the inhibition of both intracellular and extracellular CA IX varied in range of 15 nM–25 nM resulting in the similar inhibition dose response curves (Figures 18 and 22). The high affinity of VD11-4-2 against CA IX was confirmed by MS method following the ^{18}O depletion of doubly labeled $^{13}C^{18}O_2$.

Results of MS experiments demonstrated the complete block of CA IX catalytic activity upon administration of 10 nM VD11-4-2 into lysate of CA IX-expressing oocytes. Importantly, intracellular CA II and extracellular CA IV and CA XII were not significantly affected by the administration of VD11-4-2 at nanomolar concentrations (Figure 23). Therefore, this study for the first time showed the high selectivity and nanomolar affinity of VD11-4-2 towards CA IX in a biological model system. In addition, we indicated here the irreversibility of interaction between VD11-4-2 and CA IX after 45 min. This result is in line with recent investigations [351, 352], which described VD11-4-2 as a tight binder of recombinant CA IX with dissociation rates too slow to be determined by surface plasmon resonance.

The impact of VD12-09 on the catalytic activity of heterologous CA IX was lower than VD11-4-2 in *Xenopus* oocytes. VD12-09 exhibited high affinity and selectivity against intracellular CA IX as compared with negligible effects on the intracellular CA II activity (Figure 19). However, VD12-09 did not influence the amplitude of pH changes at the outer oocyte membrane surface. Possibly, VD12-09 was not able to accommodate in the active site of the mature membrane-anchored CA IX with extracellular catalytic domain. It may be caused by structural differences in intracellular and extracellular CA IX due to incomplete protein folding and the lack of post-translation modifications in the intracellular CA IX structure.

The concentration-dependent inhibition of intracellular and extracellular CA IX catalytic activity in *Xenopus* oocytes by EZA has been recently investigated [292]. Results demonstrated that 30 µM EZA induced slow rates of cytosolic pH changes and small amplitudes of pH changes at the outer membrane side in CA IX-expressing oocytes, which were analogous to the respective parameters of native oocytes, when only the spontaneous, non-catalyzed reaction of CO_2 hydration to H^+ and HCO_3^- occurred. In this study, 1 µM VD11-4-2 resulted in the complete inhibition of CA IX catalytic activity. The amount of VD11-4-2 was 30-fold lower than EZA, which induced the same effect using the same method. Thus, VD11-4-2 was more potent inhibitor against CA IX than EZA according to studies using *Xenopus* oocytes.

Since the compounds are expected to be membrane-permeable, it was difficult to be certain that extracellular measurements reflect inhibition of only extracellularly expressed CA IX. However, around 20 % of CA IX in oocytes is located outside at the membrane and 80 % inside the oocyte, as previously shown [292]. Thus, the applied inhibitors would primarily inhibit an outside-located CA IX.

The characterization of compound anti-tumor properties is the essential step during preclinical evaluation of novel anti-cancer agents. Therefore, five human cancer cell lines were involved in this study to determine functional and anti-

proliferative effects of the lead CA IX inhibitors. In addition to compounds VD11-4-2 and VR12-09, the newly designed inhibitor VR16-09 was included due to the combination of its high affinity and greater selectivity than VD11-4-2 and VD12-09 towards the recombinant CA IX.

The functional activities of three tested inhibitors to reduce hypoxia-induced acidosis of human cancer cells was confirmed by two methods: MS following the ^{18}O depletion of doubly labeled $^{13}C^{18}O_2$ (Figure 26) and extracellular acidification assay of measuring pH directly inside a hypoxic chamber (Figure 29). Hypoxia-induced extracellular acidification of human cervical (HeLa), lung (H460, A549), and breast (MDA-MB-231) cancer cells was significantly reduced in the dose-dependent manner with the IC_{50} values up to 1.29 nM, as determined for the inhibitor VR16-09. Moreover, MS confirmed the CA IX-based mechanism of the inhibitors in a CRISPR-Cas9-mediated HeLa CA IX KO cells (Figure 28). By using the same ^{18}O exchange assay, Li and colleagues previously reported K_i value of 85.3 nM for the fluorescent sulfonamide Cpd 5c to diminish the total extracellular CA acitivity of intact hypoxic MDA-MB-231 cells [353], while another study revealed the significant reduction of extracellular CA activity of MDA-MB-231 cells by 1 µM AZM [354]. Furthermore, several CA IX-targeting agents, such as fluorescent sulfonamide [128] and nitroimidazole-based inhibitors [355, 356], have been previously reported and their activities were determined by the extracellular acidification assay. Results of this thesis showed that the investigated inhibitors, especially VR16-09 and VD11-4-2, were more efficacious in decreasing extracellular acidification than previously described compounds because of their significant functionality at lower concentrations (5 µM–50 µM), emphasizing the potential for CA IX-targeting therapy.

Interestingly, hypoxia-induced acidosis of pancreatic AsPC-1 cells increased after exposure to VR16-09 or VD11-4-2 (Figure 29B, 29C), related to the unique expression of MCT1 under both normoxic and hypoxic conditions in these cells (Figure 30A). Recently, CA IX was proposed to be a "H$^+$-distributing antenna" for MCT1 to facilitate rapid extrusion of lactate and H$^+$ from the cell [295]. Even though the catalytic activity of CA IX was inhibited in AsPC-1 by compounds, the rise of acidification might be caused by MCT1 which was further non-catalytically stimulated by CA IX and this interaction was enhanced by tested inhibitors. In contrast, MCT4 was expressed in all tested cell lines and was up-regulated in response to hypoxia (Figure 30B), in line with previously confirmed HIF-1α-dependent mechanism of MCT4 expression in cancer cells [357].

The inhibitor-induced cytotoxicty was investigated by the alamarBlue® cell viability assay and further confirmed by clonogenic cell survival assay, considered as the gold standard because of possibility to determine both early and late impacts of compound on cell death, such as delayed growth arrest [358]. When tradi-

tional 2D monolayer cells were employed, all three tested inhibitors were more effective in reducing viability and clonogenic cell survival of normoxic cells without or with significantly lower CA IX expression than hypoxic CA IX-expressing cells (Table 9). This result correlates with previously published cytotoxicity profiles of benzenesulfonamides, including SLC-0111 [359], sulfamate S4 [360], and dual-target compounds bearing various CA IX-targeting moieties combined with different anti-cancer drugs [361], which showed more effective cell kill in normoxia than hypoxia. We hypothesize that higher cytotoxicity of inhibitors in normoxic cells as compared with hypoxic cells could be due to the affinity of tested compounds towards CA XII, expressed in all cell lines investigated here and shown previously to be up-regulated to compensate the CA IX knockdown [126,133,135]. Thus, new cellular models with both CA IX and CA XII KOs would be crucial to determine the link between functional activity of compounds and CA IX- or CA XII-dependent cellular mechanisms.

To confirm the hypoxia-dependent efficacy of the compounds, 3D cell models were involved in this study. They reflect important properties of *in vivo* tumors, such as interactions between cells, oxygen gradients, and penetration of drugs, which are absent in rapidly and uncontrollably growing 2D cells [362–364]. According to immunofluorescence analysis, hypoxic regions and CA IX expression were found in sections of H460 spheroids grown for 11 days. Therefore, non-hypoxic and hypoxic H460 spheroids grown for 4 and 11 days, respectively, were exposed to different doses of VR16-09, which was the most effective compound on reducing extracellular acidification under hypoxia, and thereafter plated for evaluation by clonogenic cell survival. Different from results obtained by using 2D cells, a hypoxia-dependent effect on clonogenic survival of VR16-09 was found in H460 spheroids (Figure 32). This finding highlights the importance of explore CA IX-targeting compounds in 3D cell models resembling the naturally occurring hypoxic microenvironment with clonogenic survival as endpoint.

Overall the integrative set of biophysical, biochemical, and cell biology-based approaches is described in this thesis. Novel inhibitors of CA IX exhibited low toxicity in zebrafish embryos/larvae, high affinity and selectivity towards heterologous CA IX in *Xenopus* oocytes, and reached CA IX-dependent nanomolar functional effects in hypoxic human cancer cells. Therefore, these newly designed compounds, especially VD11-4-2 and VR16-09, appear to be promising agents for CA IX-specific therapy.

For future directions, the design of dual targeting compounds based on the conjugation of CA IX inhibitors with various derivatives, such as nitroimidazoles, would be worth pursuing. This strategy was previously reported to be effective in reducing tumor growth and sensitizing only CA IX-expressing tumors to irradiation without systemic toxicity [356]. Moreover, combinatorial approaches of

applying tested CA IX inhibitors with the standard treatment modalities, such as doxorubicin, in human cancer cells may lead to the improved *in vitro* biological efficacies. Prior to clinical applications, the exploration on anti-cancer activities of CA IX-targeting compounds *in vivo* using tumor-bearing mice would be relevant for further development.

Conclusions

- There are no significant differences in affinities of tested sulfonamide inhibitor binding to recombinant and native CA VI.

- Based on the intrinsic binding parameters, compound 6b is the strongest binder of CA VI among the tested inhibitors, while the corresponding fluorinated compound 3e exhibits weaker intrinsic but stronger observed affinities, thereby emphasizing the impact of fluorine electronegativity on the lowering of the pK_a of inhibitor sulfonamide group.

- The protonation pK_a values for the zinc-bound hydroxide anion of CA VI purified from bacteria *E. coli* Rosetta™ 2 (DE3) strain, mammalian FreeStyle 293-F cells, and human saliva are 5.5, 6.0, and 6.0, respectively (37 °C). The enthalpy of protonation of hydroxide bound to zinc ion in the active site of CA VI from *E. coli* is equal to -29.0 kJ mol^{-1} at 37 °C.

- The compound VD11-4-2 at lower than LC_{50} concentrations does not lead to deleterious effects on the zebrafish embryonic development and exhibits IC_{50} of 15 nM to inhibit heterologous CA IX in *Xenopus* oocytes.

- Compounds VR16-09, VD11-4-2, and VD12-09 significantly reduce hypoxia-induced extracellular acidification of HeLa, H460, MDA-MB-231, and A549 cancer cells with the IC_{50} values up to 1.29 nM and their action mechanism is based on CA IX inhibition.

- Compound VR16-09 decreases the clonogenic survival of H460 cells cultivated under 3D conditions in hypoxia-dependent manner.

Bibliography

[1] Holdgate, G.A., Meek, T.D., Grimley, R.L.: Mechanistic enzymology in drug discovery: A fresh perspective. Nature Reviews Drug Discovery **17**(2), 115–132 (2018)

[2] Meldrum, N., Roughton, F.: Some properties of carbonic anhydrase, the CO2 enzyme present in blood. J Physiol **75**, 15–6 (1932)

[3] Smirnovienė, J., Smirnovas, V., Matulis, D.: Picomolar inhibitors of carbonic anhydrase: Importance of inhibition and binding assays. Anal. Biochem. **522**, 61–72 (2017)

[4] Jemal, A., Bray, F., Center, M.M., Ferlay, J., Ward, E., Forman, D.: Global cancer statistics. CA Cancer J Clin **61**(2), 69–90 (2011 Mar-Apr)

[5] Hanahan, D., Coussens, L.M.: Accessories to the crime: Functions of cells recruited to the tumor microenvironment. Cancer Cell **21**(3), 309–322 (2012)

[6] Junttila, M.R., de Sauvage, F.J.: Influence of tumour micro-environment heterogeneity on therapeutic response. Nature **501**(7467), 346–354 (2013)

[7] Lu, P., Weaver, V.M., Werb, Z.: The extracellular matrix: A dynamic niche in cancer progression. J Cell Biol **196**(4), 395–406 (2012)

[8] Quail, D.F., Joyce, J.A.: Microenvironmental regulation of tumor progression and metastasis. Nat. Med. **19**(11), 1423–1437 (2013)

[9] Pastorek, J., Pastorekova, S.: Hypoxia-induced carbonic anhydrase IX as a target for cancer therapy: From biology to clinical use. Seminars in Cancer Biology **31**, 52–64 (2015)

[10] Zheng, S.-S., Chen, X.-H., Yin, X., Zhang, B.-H.: Prognostic Significance of HIF-1 alpha Expression in Hepatocellular Carcinoma: A Meta-Analysis. PLOS ONE **8**(6), 65753 (2013)

[11] Semenza, G.L.: Oxygen sensing, hypoxia-inducible factors, and disease pathophysiology. Annu Rev Pathol **9**, 47–71 (2014)

[12] Wang, G.L., Jiang, B.H., Rue, E.A., Semenza, G.L.: Hypoxia-inducible factor 1 is a basic-helix-loop-helix-PAS heterodimer regulated by cellular O2 tension. Proc Natl Acad Sci U S A **92**(12), 5510–5514 (1995)

[13] Wang, G.L., Semenza, G.L.: Purification and Characterization of Hypoxia-inducible Factor 1. J. Biol. Chem. **270**(3), 1230–1237 (1995)

[14] Luan, Y., Gao, C., Miao, Y., Li, Y., Wang, Z., Qiu, X.: Clinicopathological and prognostic significance of HIF-1 alpha and HIF-2 alpha expression in small cell lung cancer. Pathology - Research and Practice **209**(3), 184–189 (2013)

[15] Kroeger, N., Seligson, D.B., Signoretti, S., Yu, H., Magyar, C.E., Huang, J., Belldegrun, A.S., Pantuck, A.J.: Poor prognosis and advanced clinicopathological features of clear cell renal cell carcinoma (ccRCC) are associated with cytoplasmic subcellular localisation of Hypoxia inducible factor-2α. European Journal of Cancer **50**(8), 1531–1540 (2014)

[16] Ku, J.H., Park, Y.H., Myung, J.K., Moon, K.C., Kwak, C., Kim, H.H.: Expression of hypoxia inducible factor-1 alpha and 2 alpha in conventional renal cell carcinoma with or without sarcomatoid differentiation. Urologic Oncology: Seminars and Original Investigations **29**(6), 731–737 (2011)

[17] Hara, S., Hamada, J., Kobayashi, C., Kondo, Y., Imura, N.: Expression and Characterization of Hypoxia-Inducible Factor (HIF)-3α in Human Kidney: Suppression of HIF-Mediated Gene Expression by HIF-3α. Biochemical and Biophysical Research Communications **287**(4), 808–813 (2001)

[18] Augstein, A., Poitz, D.M., Braun-Dullaeus, R.C., Strasser, R.H., Schmeisser, A.: Cell-specific and hypoxia-dependent regulation of human HIF-3alpha: Inhibition of the expression of HIF target genes in vascular cells. Cell. Mol. Life Sci. **68**(15), 2627–2642 (2011)

[19] Zhang, P., Yao, Q., Lu, L., Li, Y., Chen, P.-J., Duan, C.: Hypoxia-inducible factor 3 is an oxygen-dependent transcription activator and regulates a distinct transcriptional response to hypoxia. Cell Rep **6**(6), 1110–1121 (2014)

[20] Huang, Y., Kapere Ochieng, J., Kempen, M.B.-v., Munck, A.B.-d., Swagemakers, S., van Ijcken, W., Grosveld, F., Tibboel, D., Rottier, R.J.: Hypoxia inducible factor 3α plays a critical role in alveolarization and distal epithelial cell differentiation during mouse lung development. PLoS ONE **8**(2), 57695 (2013)

[21] Metzen, E., Berchner-Pfannschmidt, U., Stengel, P., Marxsen, J.H., Stolze, I., Klinger, M., Huang, W.Q., Wotzlaw, C., Hellwig-Bürgel, T., Jelkmann, W., Acker, H., Fandrey, J.: Intracellular localisation of human HIF-1 alpha hydroxylases: Implications for oxygen sensing. J. Cell. Sci. **116**(Pt 7), 1319–1326 (2003)

[22] Lieb, M.E., Menzies, K., Moschella, M.C., Ni, R., Taubman, M.B.: Mammalian EGLN genes have distinct patterns of mRNA expression and regulation. Biochem. Cell Biol. **80**(4), 421–426 (2002)

[23] Ivan, M., Kondo, K., Yang, H., Kim, W., Valiando, J., Ohh, M., Salic, A., Asara, J.M., Lane, W.S., Kaelin, W.G.: HIFalpha targeted for VHL-mediated destruction by proline hydroxylation: Implications for O2 sensing. Science **292**(5516), 464–468 (2001)

[24] Jaakkola, P., Mole, D.R., Tian, Y.M., Wilson, M.I., Gielbert, J., Gaskell, S.J., von Kriegsheim, A., Hebestreit, H.F., Mukherji, M., Schofield, C.J., Maxwell, P.H., Pugh, C.W., Ratcliffe, P.J.: Targeting of HIF-alpha to the von Hippel-Lindau ubiquitylation complex by O2-regulated prolyl hydroxylation. Science **292**(5516), 468–472 (2001)

[25] Yu, F., White, S.B., Zhao, Q., Lee, F.S.: HIF-1alpha binding to VHL is regulated by stimulus-sensitive proline hydroxylation. Proc. Natl. Acad. Sci. U.S.A. **98**(17), 9630–9635 (2001)

[26] Lando, D., Peet, D.J., Whelan, D.A., Gorman, J.J., Whitelaw, M.L.: Asparagine hydroxylation of the HIF transactivation domain a hypoxic switch. Science **295**(5556), 858–861 (2002)

[27] Lando, D., Peet, D.J., Gorman, J.J., Whelan, D.A., Whitelaw, M.L., Bruick, R.K.: FIH-1 is an asparaginyl hydroxylase enzyme that regulates the transcriptional activity of hypoxia-inducible factor. Genes Dev. **16**(12), 1466–1471 (2002)

[28] Samanta, D., Semenza, G.L.: Maintenance of redox homeostasis by hypoxia-inducible factors. Redox Biology **13**(Supplement C), 331–335 (2017)

[29] Xia, X., Lemieux, M.E., Li, W., Carroll, J.S., Brown, M., Liu, X.S., Kung, A.L.: Integrative analysis of HIF binding and transactivation reveals its role in maintaining histone methylation homeostasis. Proc. Natl. Acad. Sci. U.S.A. **106**(11), 4260–4265 (2009)

[30] Schödel, J., Oikonomopoulos, S., Ragoussis, J., Pugh, C.W., Ratcliffe, P.J., Mole, D.R.: High-resolution genome-wide mapping of HIF-binding sites by ChIP-seq. Blood **117**(23), 207–217 (2011)

[31] Semenza, G.L.: HIF-1 mediates metabolic responses to intratumoral hypoxia and oncogenic mutations. J. Clin. Invest. **123**(9), 3664–3671 (2013)

[32] Pescador, N., Villar, D., Cifuentes, D., Garcia-Rocha, M., Ortiz-Barahona, A., Vazquez, S., Ordoñez, A., Cuevas, Y., Saez-Morales, D., Garcia-Bermejo, M.L., Landazuri, M.O., Guinovart, J., del Peso, L.: Hypoxia Promotes Glycogen Accumulation through Hypoxia Inducible Factor (HIF)-Mediated Induction of Glycogen Synthase 1. PLoS One **5**(3) (2010)

[33] Favaro, E., Bensaad, K., Chong, M.G., Tennant, D.A., Ferguson, D.J.P., Snell, C., Steers, G., Turley, H., Li, J.-L., Günther, U.L., Buffa, F.M., McIntyre, A., Harris, A.L.: Glucose utilization via glycogen phosphorylase sustains proliferation and prevents premature senescence in cancer cells. Cell Metab. **16**(6), 751–764 (2012)

[34] Denko, N.C.: Hypoxia, HIF1 and glucose metabolism in the solid tumour. Nat. Rev. Cancer **8**(9), 705–713 (2008)

[35] Payen, V.L., Porporato, P.E., Baselet, B., Sonveaux, P.: Metabolic changes associated with tumor metastasis, part 1: Tumor pH, glycolysis and the pentose phosphate pathway. Cell. Mol. Life Sci. **73**(7), 1333–1348 (2016)

[36] Warburg, O.: On the origin of cancer cells. Science **123**(3191), 309–314 (1956)

[37] Hanahan, D., Weinberg, R.A.: Hallmarks of cancer: The next generation. Cell **144**(5), 646–674 (2011)

[38] Gao, P., Tchernyshyov, I., Chang, T.-C., Lee, Y.-S., Kita, K., Ochi, T., Zeller, K.I., De Marzo, A.M., Van Eyk, J.E., Mendell, J.T., Dang, C.V.: C-Myc suppression of miR-23a/b enhances mitochondrial glutaminase expression and glutamine metabolism. Nature **458**(7239), 762–765 (2009)

[39] Levine, A.J., Puzio-Kuter, A.M.: The Control of the Metabolic Switch in Cancers by Oncogenes and Tumor Suppressor Genes. Science **330**(6009), 1340–1344 (2010)

[40] Webb, B.A., Chimenti, M., Jacobson, M.P., Barber, D.L.: Dysregulated pH: A perfect storm for cancer progression. Nat. Rev. Cancer **11**(9), 671–677 (2011)

[41] Gallagher, F.A., Kettunen, M.I., Day, S.E., Hu, D.-E., Ardenkjær-Larsen, J.H., Zandt, R.i.t., Jensen, P.R., Karlsson, M., Golman, K., Lerche, M.H., Brindle, K.M.: Magnetic resonance imaging of pH in vivo using hyperpolarized 13C-labelled bicarbonate. Nature **453**(7197), 940–943 (2008)

[42] Mazzio, E.A., Smith, B., Soliman, K.F.A.: Evaluation of endogenous acidic metabolic products associated with carbohydrate metabolism in tumor cells. Cell Biol Toxicol **26**(3), 177–188 (2010)

[43] Hashim, A.I., Zhang, X., Wojtkowiakk, J.W., Gillies, R.J.: Imaging pH and Metastasis. NMR Biomed **24**(6), 582–591 (2011)

[44] Gillies, R.J., Verduzco, D., Gatenby, R.A.: Evolutionary Dynamics Unifies Carcinogenesis and Cancer Therapy. Nat Rev Cancer **12**(7), 487–493 (2012)

[45] Pouysségur, J., Franchi, A., Pagès, G.: pHi, aerobic glycolysis and vascular endothelial growth factor in tumour growth. Novartis Found. Symp. **240**, 186–196196198 (2001)

[46] Hinton, A., Sennoune, S.R., Bond, S., Fang, M., Reuveni, M., Sahagian, G.G., Jay, D., Martinez-Zaguilan, R., Forgac, M.: Function of a subunit isoforms of the V-ATPase in pH homeostasis and in vitro invasion of MDA-MB231 human breast cancer cells. J. Biol. Chem. **284**(24), 16400–16408 (2009)

[47] Nishisho, T., Hata, K., Nakanishi, M., Morita, Y., Sun-Wada, G.-H., Wada, Y., Yasui, N., Yoneda, T.: The a3 isoform vacuolar type H^+-ATPase promotes distant metastasis in the mouse B16 melanoma cells. Mol. Cancer Res. **9**(7), 845–855 (2011)

[48] Capecci, J., Forgac, M.: The function of vacuolar ATPase (V-ATPase) a subunit isoforms in invasiveness of MCF10a and MCF10CA1a human breast cancer cells. J. Biol. Chem. **288**(45), 32731–32741 (2013)

[49] Parks, S.K., Chiche, J., Pouysségur, J.: Disrupting proton dynamics and energy metabolism for cancer therapy. Nat. Rev. Cancer **13**(9), 611–623 (2013)

[50] Halestrap, A.P.: The monocarboxylate transporter family–Structure and functional characterization. IUBMB Life **64**(1), 1–9 (2012)

[51] Lim, K.S., Lim, K.J., Price, A.C., Orr, B.A., Eberhart, C.G., Bar, E.E.: Inhibition of monocarboxylate transporter-4 depletes stem-like glioblastoma cells and inhibits HIF transcriptional response in a lactate-independent manner. Oncogene **33**(35), 4433–4441 (2014)

[52] Morais-Santos, F., Granja, S., Miranda-Gonçalves, V., Moreira, A.H.J., Queirós, S., Vilaça, J.L., Schmitt, F.C., Longatto-Filho, A., Paredes, J., Baltazar, F., Pinheiro, C.: Targeting lactate transport suppresses in vivo breast tumour growth. Oncotarget **6**(22), 19177–19189 (2015)

[53] Vince, J.W., Reithmeier, R.A.: Carbonic anhydrase II binds to the carboxyl terminus of human band 3, the erythrocyte C1-/HCO3- exchanger. J. Biol. Chem. **273**(43), 28430–28437 (1998)

[54] Svastova, E., Witarski, W., Csaderova, L., Kosik, I., Skvarkova, L., Hulikova, A., Zatovicova, M., Barathova, M., Kopacek, J., Pastorek, J., Pastorekova, S.: Carbonic anhydrase IX interacts with bicarbonate transporters in lamellipodia and increases cell migration via its catalytic domain. J. Biol. Chem. **287**(5), 3392–3402 (2012)

[55] Parks, S.K., Pouyssegur, J.: The Na(+)/HCO3(-) Co-Transporter SLC4A4 Plays a Role in Growth and Migration of Colon and Breast Cancer Cells. J. Cell. Physiol. **230**(8), 1954–1963 (2015)

[56] McIntyre, A., Hulikova, A., Ledaki, I., Snell, C., Singleton, D., Steers, G., Seden, P., Jones, D., Bridges, E., Wigfield, S., Li, J.-L., Russell, A., Swietach, P., Harris, A.L.: Disrupting Hypoxia-Induced Bicarbonate Transport Acidifies Tumor Cells and Suppresses Tumor Growth. Cancer Res **76**(13), 3744–3755 (2016)

[57] Zhang, L.-J., Lu, R., Song, Y.-N., Zhu, J.-Y., Xia, W., Zhang, M., Shao, Z.-Y., Huang, Y., Zhou, Y., Zhang, H., Guo, L., Zhang, M., Zhang, H.: Knockdown of anion exchanger 2 suppressed the growth of ovarian cancer cells via mTOR/p70S6K1 signaling. Scientific Reports **7**(1), 6362 (2017)

[58] Del Prete, S., Vullo, D., De Luca, V., Supuran, C.T., Capasso, C.: Biochemical characterization of the delta-carbonic anhydrase from the marine diatom Thalassiosira weissflogii, TweCA. J Enzyme Inhib Med Chem **29**(6), 906–911 (2014)

[59] Samukawa, M., Shen, C., Hopkinson, B.M., Matsuda, Y.: Localization of putative carbonic anhydrases in the marine diatom, Thalassiosira pseudonana. Photosyn. Res. **121**(2-3), 235–249 (2014)

[60] Supuran, C.T., Capasso, C.: The η-class carbonic anhydrases as drug targets for antimalarial agents. Expert Opin. Ther. Targets **19**(4), 551–563 (2015)

[61] Kikutani, S., Nakajima, K., Nagasato, C., Tsuji, Y., Miyatake, A., Matsuda, Y.: Thylakoid luminal theta-carbonic anhydrase critical for growth and photosynthesis in the marine diatom Phaeodactylum tricornutum. Proc. Natl. Acad. Sci. U.S.A. **113**(35), 9828–9833 (2016)

[62] Zolfaghari Emameh, R., Barker, H.R., Syrjänen, L., Urbański, L., Supuran, C.T., Parkkila, S.: Identification and inhibition of carbonic anhydrases from nematodes. J Enzyme Inhib Med Chem **31**(sup4), 176–184 (2016)

[63] Zolfaghari Emameh, R., Barker, H.R., Tolvanen, M.E.E., Parkkila, S., Hytönen, V.P.: Horizontal transfer of β-carbonic anhydrase genes from prokaryotes to protozoans, insects, and nematodes. Parasit Vectors **9** (2016)

[64] Supuran, C.T.: Advances in structure-based drug discovery of carbonic anhydrase inhibitors. Expert Opin Drug Discov **12**(1), 61–88 (2017)

[65] Aggarwal, M., Boone, C.D., Kondeti, B., McKenna, R.: Structural annotation of human carbonic anhydrases. J Enzyme Inhib Med Chem **28**(2), 267–277 (2013)

[66] Frost, S.C.: Physiological functions of the alpha class of carbonic anhydrases. Subcell. Biochem. **75**, 9–30 (2014)

[67] Pinard, M.A., Mahon, B., McKenna, R.: Probing the surface of human carbonic anhydrase for clues towards the design of isoform specific inhibitors. Biomed Res Int **2015**, 453543 (2015)

[68] Rapp, G.W.: The biochemistry of oral calculus the presence of carbonic anhydrase in human saliva. J Am Dent Assoc **33**, 191–194 (1946)

[69] Henkin, R.I., Lippoldt, R.E., Bilstad, J., Edelhoch, H.: A zinc protein isolated from human parotid saliva. Proc. Natl. Acad. Sci. U.S.A. **72**(2), 488–492 (1975)

[70] Fernley, R.T., Wright, R.D., Coghlan, J.P.: A novel carbonic anhydrase from the ovine parotid gland. FEBS Lett. **105**(2), 299–302 (1979)

[71] Feldstein, J.B., Silverman, D.N.: Purification and characterization of carbonic anhydrase from the saliva of the rat. J. Biol. Chem. **259**(9), 5447–5453 (1984)

[72] Murakami, H., Sly, W.S.: Purification and characterization of human salivary carbonic anhydrase. J. Biol. Chem. **262**(3), 1382–1388 (1987)

[73] Thatcher, B.J., Doherty, A.E., Orvisky, E., Martin, B.M., Henkin, R.I.: Gustin from human parotid saliva is carbonic anhydrase VI. Biochem. Biophys. Res. Commun. **250**(3), 635–641 (1998)

[74] Parkkila, S., Kaunisto, K., Rajaniemi, L., Kumpulainen, T., Jokinen, K., Rajaniemi, H.: Immunohistochemical localization of carbonic anhydrase isoenzymes VI, II, and I in human parotid and submandibular glands. J. Histochem. Cytochem. **38**(7), 941–947 (1990)

[75] Leinonen, J., Parkkila, S., Kaunisto, K., Koivunen, P., Rajaniemi, H.: Secretion of carbonic anhydrase isoenzyme VI (CA VI) from human and rat lingual serous von Ebner's glands. J. Histochem. Cytochem. **49**(5), 657–662 (2001)

[76] Kivelä, J., Parkkila, S., Waheed, A., Parkkila, A.K., Sly, W.S., Rajaniemi, H.: Secretory carbonic anhydrase isoenzyme (CA VI) in human serum. Clin. Chem. **43**(12), 2318–2322 (1997)

[77] Karhumaa, P., Leinonen, J., Parkkila, S., Kaunisto, K., Tapanainen, J., Rajaniemi, H.: The identification of secreted carbonic anhydrase VI as a constitutive glycoprotein of human and rat milk. Proc Natl Acad Sci U S A **98**(20), 11604–11608 (2001)

[78] Ogawa, Y., Matsumoto, K., Maeda, T., Tamai, R., Suzuki, T., Sasano, H., Fernley, R.T.: Characterization of lacrimal gland carbonic anhydrase VI. J. Histochem. Cytochem. **50**(6), 821–827 (2002)

[79] Leinonen, J.S., Saari, K.A., Seppänen, J.M., Myllylä, H.M., Rajaniemi, H.J.: Immunohistochemical demonstration of carbonic anhydrase isoenzyme VI (CA VI) expression in rat lower airways and lung. J. Histochem. Cytochem. **52**(8), 1107–1112 (2004)

[80] Kaseda, M., Ichihara, N., Nishita, T., Amasaki, H., Asari, M.: Immunohistochemistry of the bovine secretory carbonic anhydrase isozyme (CA-VI) in bovine alimentary canal and major salivary glands. J. Vet. Med. Sci. **68**(2), 131–135 (2006)

[81] Parkkila, S., Parkkila, A.K., Rajaniemi, H.: Circadian periodicity in salivary carbonic anhydrase VI concentration. Acta Physiol. Scand. **154**(2), 205–211 (1995)

[82] Sok, J., Wang, X.Z., Batchvarova, N., Kuroda, M., Harding, H., Ron, D.: CHOP-Dependent stress-inducible expression of a novel form of carbonic anhydrase VI. Mol. Cell. Biol. **19**(1), 495–504 (1999)

[83] Matthews, T.A., Abel, A., Demme, C., Sherman, T., Pan, P.-w., Halterman, M.W., Parkkila, S., Nehrke, K.: Expression of the CHOP-inducible carbonic anhydrase CAVI-b is required for BDNF-mediated protection from hypoxia. Brain Res **1543**, 28–37 (2014)

[84] Pilka, E.S., Kochan, G., Oppermann, U., Yue, W.W.: Crystal structure of the secretory isozyme of mammalian carbonic anhydrases CA VI: Implications for biological assembly and inhibitor development. Biochem. Biophys. Res. Commun. **419**(3), 485–489 (2012)

[85] Parkkila, S., Parkkila, A.K., Lehtola, J., Reinilä, A., Södervik, H.J., Rannisto, M., Rajaniemi, H.: Salivary carbonic anhydrase protects gastroesophageal mucosa from acid injury. Dig. Dis. Sci. **42**(5), 1013–1019 (1997)

[86] Oleksiewicz, M.B., Kjeldal, H.O., Klenø, T.G.: Identification of stool proteins in C57BL/6J mice by two-dimensional gel electrophoresis and MALDI-TOF mass spectrometry. Biomarkers **10**(1), 29–40 (2005 Jan-Feb)

[87] The PyMOL Molecular Graphics System, L. Version 1.8 Schrödinger

[88] Nishimori, I., Minakuchi, T., Onishi, S., Vullo, D., Scozzafava, A., Supuran, C.T.: Carbonic anhydrase inhibitors. DNA cloning, characterization, and inhibition studies of the human secretory isoform VI, a new target for sulfonamide and sulfamate inhibitors. J. Med. Chem. **50**(2), 381–388 (2007)

[89] Winum, J.-Y., Montero, J.-L., Vullo, D., Supuran, C.T.: Carbonic anhydrase inhibitors: Glycosylsulfanilamides act as subnanomolar inhibitors of the human secreted isoform VI. Chem Biol Drug Des **74**(6), 636–639 (2009)

[90] Shatzman, A.R., Henkin, R.I.: Gustin concentration changes relative to salivary zinc and taste in humans. Proc. Natl. Acad. Sci. U.S.A. **78**(6), 3867–3871 (1981)

[91] Melis, M., Atzori, E., Cabras, S., Zonza, A., Calò, C., Muroni, P., Nieddu, M., Padiglia, A., Sogos, V., Tepper, B.J., Tomassini Barbarossa, I.: The gustin (CA6) gene polymorphism, rs2274333 (A/G), as a mechanistic link between PROP tasting and fungiform taste papilla density and maintenance. PLoS ONE **8**(9), 74151 (2013)

[92] Patrikainen, M., Pan, P., Kulesskaya, N., Voikar, V., Parkkila, S.: The role of carbonic anhydrase VI in bitter taste perception: Evidence from the Car6-/- mouse model. J Biomed Sci **21**(1), 82 (2014)

[93] Kivela, J., Parkkila, S., Parkkila, A.K., Leinonen, J., Rajaniemi, H.: Salivary carbonic anhydrase isoenzyme VI. J. Physiol. (Lond.) **520 Pt 2**, 315–320 (1999)

[94] Kimoto, M., Kishino, M., Yura, Y., Ogawa, Y.: A role of salivary carbonic anhydrase VI in dental plaque. Arch. Oral Biol. **51**(2), 117–122 (2006)

[95] Imtaiyaz Hassan, M., Shajee, B., Waheed, A., Ahmad, F., Sly, W.S.: Structure, function and applications of carbonic anhydrase isozymes. Bioorg. Med. Chem. **21**(6), 1570–1582 (2013)

[96] Pan, P.-w., Käyrä, K., Leinonen, J., Nissinen, M., Parkkila, S., Rajaniemi, H.: Gene expression profiling in the submandibular gland, stomach, and duodenum of CAVI-deficient mice. Transgenic Res. **20**(3), 675–698 (2011)

[97] Patrikainen, M.S., Pan, P., Barker, H.R., Parkkila, S.: Altered gene expression in the lower respiratory tract of Car6 (-/-) mice. Transgenic Res. **25**(5), 649–664 (2016)

[98] Pastoreková, S., Závadová, Z., Kostál, M., Babusíková, O., Závada, J.: A novel quasi-viral agent, MaTu, is a two-component system. Virology **187**(2), 620–626 (1992)

[99] Pastorek, J., Pastoreková, S., Callebaut, I., Mornon, J.P., Zelník, V., Opavský, R., Zat'ovicová, M., Liao, S., Portetelle, D., Stanbridge, E.J.: Cloning and characterization of MN, a human tumor-associated protein with a domain homologous to carbonic anhydrase and a putative helix-loop-helix DNA binding segment. Oncogene **9**(10), 2877–2888 (1994)

[100] Opavský, R., Pastoreková, S., Zelník, V., Gibadulinová, A., Stanbridge, E.J., Závada, J., Kettmann, R., Pastorek, J.: Human MN/CA9 gene, a novel member of the carbonic anhydrase family: Structure and exon to protein domain relationships. Genomics **33**(3), 480–487 (1996)

[101] Oosterwijk, E., Ruiter, D.J., Hoedemaeker, P.J., Pauwels, E.K., Jonas, U., Zwartendijk, J., Warnaar, S.O.: Monoclonal antibody G 250 recognizes a determinant present in renal-cell carcinoma and absent from normal kidney. Int. J. Cancer **38**(4), 489–494 (1986)

[102] Grabmaier, K., Vissers, J.L., De Weijert, M.C., Oosterwijk-Wakka, J.C., Van Bokhoven, A., Brakenhoff, R.H., Noessner, E., Mulders, P.A., Merkx, G., Figdor, C.G., Adema, G.J., Oosterwijk, E.: Molecular cloning and immunogenicity of renal cell carcinoma-associated antigen G250. Int. J. Cancer **85**(6), 865–870 (2000)

[103] Závada, J., Závadová, Z., Pastorek, J., Biesová, Z., Jezek, J., Velek, J.: Human tumour-associated cell adhesion protein MN/CA IX: Identification of M75 epitope and of the region mediating cell adhesion. Br. J. Cancer **82**(11), 1808–1813 (2000)

[104] Dorai, T., Sawczuk, I.S., Pastorek, J., Wiernik, P.H., Dutcher, J.P.: The role of carbonic anhydrase IX overexpression in kidney cancer. Eur. J. Cancer **41**(18), 2935–2947 (2005)

[105] Ditte, P., Dequiedt, F., Svastova, E., Hulikova, A., Ohradanova-Repic, A., Zatovicova, M., Csaderova, L., Kopacek, J., Supuran, C.T., Pastorekova, S., Pastorek, J.: Phosphorylation of carbonic anhydrase IX controls its ability to mediate extracellular acidification in hypoxic tumors. Cancer Res. **71**(24), 7558–7567 (2011)

[106] Barathova, M., Takacova, M., Holotnakova, T., Gibadulinova, A., Ohradanova, A., Zatovicova, M., Hulikova, A., Kopacek, J., Parkkila, S., Supuran, C.T., Pastorekova, S., Pastorek, J.: Alternative splicing variant of the hypoxia marker carbonic anhydrase IX expressed independently of hypoxia and tumour phenotype. British Journal of Cancer **98**(1), 129 (2008)

[107] Malentacchi, F., Simi, L., Nannelli, C., Andreani, M., Janni, A., Pastorekova, S., Orlando, C.: Alternative splicing variants of carbonic anhydrase IX in human non-small cell lung cancer. Lung Cancer **64**(3), 271–276 (2009)

[108] Alterio, V., Hilvo, M., Fiore, A.D., Supuran, C.T., Pan, P., Parkkila, S., Scaloni, A., Pastorek, J., Pastorekova, S., Pedone, C., Scozzafava, A., Monti, S.M., Simone, G.D.: Crystal structure of the catalytic domain of the tumor-associated human carbonic anhydrase IX. PNAS **106**(38), 16233–16238 (2009)

[109] Pastorekova, S., Parkkila, S., Parkkila, A., Opavsky, R., Zelnik, V., Saarnio, J., Pastorek, J.: Carbonic anhydrase IX, MN/CA IX: Analysis of stomach complementary DNA sequence and expression in human and rat alimentary tracts. Gastroenterology **112**(2), 398–408 (1997)

[110] Ivanov, S., Liao, S.Y., Ivanova, A., Danilkovitch-Miagkova, A., Tarasova, N., Weirich, G., Merrill, M.J., Proescholdt, M.A., Oldfield, E.H., Lee, J., Zavada, J., Waheed, A., Sly, W., Lerman, M.I., Stanbridge, E.J.: Expression of hypoxia-inducible cell-surface transmembrane carbonic anhydrases in human cancer. Am. J. Pathol. **158**(3), 905–919 (2001)

[111] Leibovich, B.C., Sheinin, Y., Lohse, C.M., Thompson, R.H., Cheville, J.C., Zavada, J., Kwon, E.D.: Carbonic anhydrase IX is not an independent predictor of outcome for patients with clear cell renal cell carcinoma. J. Clin. Oncol. **25**(30), 4757–4764 (2007)

[112] van Kuijk, S.J.A., Yaromina, A., Houben, R., Niemans, R., Lambin, P., Dubois, L.J.: Prognostic Significance of Carbonic Anhydrase IX Expression in Cancer Patients: A Meta-Analysis. Front Oncol **6** (2016)

[113] Wykoff, C.C., Beasley, N.J.P., Watson, P.H., Turner, K.J., Pastorek, J., Sibtain, A., Wilson, G.D., Turley, H., Talks, K.L., Maxwell, P.H., Pugh, C.W., Ratcliffe, P.J., Harris, A.L.: Hypoxia-inducible Expression of Tumor-associated Carbonic Anhydrases. Cancer Res **60**(24), 7075–7083 (2000)

[114] Kopacek, J., Barathova, M., Dequiedt, F., Sepelakova, J., Kettmann, R., Pastorek, J., Pastorekova, S.: MAPK pathway contributes to density- and hypoxia-induced expression of the tumor-associated carbonic anhydrase IX. Biochim. Biophys. Acta **1729**(1), 41–49 (2005)

[115] Simko, V., Takacova, M., Debreova, M., Laposova, K., Ondriskova-Panisova, E., Pastorekova, S., Csaderova, L., Pastorek, J.: Dexamethasone downregulates expression of carbonic anhydrase IX via HIF-1α and NF-κB-dependent mechanisms. Int. J. Oncol. **49**(4), 1277–1288 (2016)

[116] Andreucci, E., Peppicelli, S., Carta, F., Brisotto, G., Biscontin, E., Ruzzolini, J., Bianchini, F., Biagioni, A., Supuran, C.T., Calorini, L.: Carbonic anhydrase IX inhibition affects viability of cancer cells adapted to extracellular acidosis. J. Mol. Med. (2017)

[117] Panisova, E., Kery, M., Sedlakova, O., Brisson, L., Debreova, M., Sboarina, M., Sonveaux, P., Pastorekova, S., Svastova, E.: Lactate stimulates CA IX expression in normoxic cancer cells. Oncotarget **8**(44), 77819–77835 (2017)

[118] Závada, J., Závadová, Z., Zat'ovicová, M., Hyrsl, L., Kawaciuk, I.: Soluble form of carbonic anhydrase IX (CA IX) in the serum and urine of renal carcinoma patients. Br. J. Cancer **89**(6), 1067–1071 (2003)

[119] Zatovicova, M., Sedlakova, O., Svastova, E., Ohradanova, A., Ciampor, F., Arribas, J., Pastorek, J., Pastorekova, S.: Ectodomain shedding of the hypoxia-induced carbonic anhydrase IX is a metalloprotease-dependent process regulated by TACE/ADAM17. Br. J. Cancer **93**(11), 1267–1276 (2005)

[120] Hyrsl, L., Zavada, J., Zavadova, Z., Kawaciuk, I., Vesely, S., Skapa, P.: Soluble form of carbonic anhydrase IX (CAIX) in transitional cell carcinoma of urinary tract. Neoplasma **56**(4), 298–302 (2009)

[121] Ilie, M., Mazure, N.M., Hofman, V., Ammadi, R.E., Ortholan, C., Bonnetaud, C., Havet, K., Venissac, N., Mograbi, B., Mouroux, J., Pouysségur, J., Hofman, P.: High levels of carbonic anhydrase IX in tumour tissue and plasma are biomarkers of poor prognostic in patients with non-small cell lung cancer. Br. J. Cancer **102**(11), 1627–1635 (2010)

[122] Woelber, L., Kress, K., Kersten, J.F., Choschzick, M., Kilic, E., Herwig, U., Lindner, C., Schwarz, J., Jaenicke, F., Mahner, S., Milde-Langosch, K., Mueller, V., Ihnen, M.: Carbonic anhydrase IX in tumor tissue and sera of patients with primary cervical cancer. BMC Cancer **11**, 12 (2011)

[123] Schütze, D., Milde-Langosch, K., Witzel, I., Rody, A., Karn, T., Schmidt, M., Choschzick, M., Jänicke, F., Müller, V.: Relevance of cellular and serum carbonic anhydrase IX in primary breast cancer. J. Cancer Res. Clin. Oncol. **139**(5), 747–754 (2013)

[124] Svastová, E., Hulíková, A., Rafajová, M., Zat'ovicová, M., Gibadulinová, A., Casini, A., Cecchi, A., Scozzafava, A., Supuran, C.T., Pastorek, J., Pastoreková, S.: Hypoxia activates the capacity of tumor-associated carbonic anhydrase IX to acidify extracellular pH. FEBS Lett. **577**(3), 439–445 (2004)

[125] Swietach, P., Patiar, S., Supuran, C.T., Harris, A.L., Vaughan-Jones, R.D.: The role of carbonic anhydrase 9 in regulating extracellular and intracellular ph in three-dimensional tumor cell growths. J. Biol. Chem. **284**(30), 20299–20310 (2009)

[126] McIntyre, A., Patiar, S., Wigfield, S., Li, J.-l., Ledaki, I., Turley, H., Leek, R., Snell, C., Gatter, K., Sly, W.S., Vaughan-Jones, R.D., Swietach, P., Harris, A.L.: Carbonic anhydrase IX promotes tumour growth and necrosis in vivo and inhibition enhances anti-VEGF therapy. Clin Cancer Res **18**(11), 3100–3111 (2012)

[127] Buanne, P., Renzone, G., Monteleone, F., Vitale, M., Monti, S.M., San-domenico, A., Garbi, C., Montanaro, D., Accardo, M., Troncone, G., Za-tovicova, M., Csaderova, L., Supuran, C.T., Pastorekova, S., Scaloni, A., De Simone, G., Zambrano, N.: Characterization of carbonic anhydrase IX interactome reveals proteins assisting its nuclear localization in hypoxic cells. J. Proteome Res. **12**(1), 282–292 (2013)

[128] Dubois, L., Douma, K., Supuran, C.T., Chiu, R.K., van Zandvoort, M.A.M.J., Pastoreková, S., Scozzafava, A., Wouters, B.G., Lambin, P.: Imaging the hypoxia surrogate marker CA IX requires expression and cat-alytic activity for binding fluorescent sulfonamide inhibitors. Radiother On-col **83**(3), 367–373 (2007)

[129] Li, Y., Qiu, X., Zhang, S., Zhang, Q., Wang, E.: Hypoxia induced CCR7 expression via HIF-1alpha and HIF-2alpha correlates with migration and invasion in lung cancer cells. Cancer Biol. Ther. **8**(4), 322–330 (2009)

[130] Dubois, L., Peeters, S., Lieuwes, N.G., Geusens, N., Thiry, A., Wigfield, S., Carta, F., McIntyre, A., Scozzafava, A., Dogné, J.-M., Supuran, C.T., Harris, A.L., Masereel, B., Lambin, P.: Specific inhibition of carbonic anhy-drase IX activity enhances the in vivo therapeutic effect of tumor irradiation. Radiother Oncol **99**(3), 424–431 (2011)

[131] Cianchi, F., Vinci, M.C., Supuran, C.T., Peruzzi, B., De Giuli, P., Fasolis, G., Perigli, G., Pastorekova, S., Papucci, L., Pini, A., Masini, E., Puccetti, L.: Selective inhibition of carbonic anhydrase IX decreases cell proliferation and induces ceramide-mediated apoptosis in human cancer cells. J. Phar-macol. Exp. Ther. **334**(3), 710–719 (2010)

[132] Robertson, N., Potter, C., Harris, A.L.: Role of carbonic anhydrase IX in human tumor cell growth, survival, and invasion. Cancer Res. **64**(17), 6160–6165 (2004)

[133] Chiche, J., Ilc, K., Laferrière, J., Trottier, E., Dayan, F., Mazure, N.M., Brahimi-Horn, M.C., Pouysségur, J.: Hypoxia-inducible carbonic anhydrase IX and XII promote tumor cell growth by counteracting acidosis through the regulation of the intracellular pH. Cancer Res. **69**(1), 358–368 (2009)

[134] Lou, Y., McDonald, P.C., Oloumi, A., Chia, S., Ostlund, C., Ahmadi, A., Kyle, A., Auf dem Keller, U., Leung, S., Huntsman, D., Clarke, B., Suther-land, B.W., Waterhouse, D., Bally, M., Roskelley, C., Overall, C.M., Minch-inton, A., Pacchiano, F., Carta, F., Scozzafava, A., Touisni, N., Winum, J.-Y., Supuran, C.T., Dedhar, S.: Targeting tumor hypoxia: Suppression of breast tumor growth and metastasis by novel carbonic anhydrase IX in-hibitors. Cancer Res. **71**(9), 3364–3376 (2011)

[135] Parks, S.K., Cormerais, Y., Durivault, J., Pouyssegur, J.: Genetic disruption of the pHi-regulating proteins Na+/H+ exchanger 1 (SLC9A1) and carbonic anhydrase 9 severely reduces growth of colon cancer cells. Oncotarget **8**(6), 10225–10237 (2016)

[136] Currie, M.J., Beardsley, B.E., Harris, G.C., Gunningham, S.P., Dachs, G.U., Dijkstra, B., Morrin, H.R., Wells, J.E., Robinson, B.A.: Immunohistochemical analysis of cancer stem cell markers in invasive breast carcinoma and associated ductal carcinoma in situ: Relationships with markers of tumor hypoxia and microvascularity. Hum. Pathol. **44**(3), 402–411 (2013)

[137] Lock, F.E., McDonald, P.C., Lou, Y., Serrano, I., Chafe, S.C., Ostlund, C., Aparicio, S., Winum, J.-Y., Supuran, C.T., Dedhar, S.: Targeting carbonic anhydrase IX depletes breast cancer stem cells within the hypoxic niche. Oncogene **32**(44), 5210–5219 (2013)

[138] Stock, C., Schwab, A.: Protons make tumor cells move like clockwork. Pflugers Arch. **458**(5), 981–992 (2009)

[139] Swayampakula, M., McDonald, P.C., Vallejo, M., Coyaud, E., Chafe, S.C., Westerback, A., Venkateswaran, G., Shankar, J., Gao, G., Laurent, E.M.N., Lou, Y., Bennewith, K.L., Supuran, C.T., Nabi, I.R., Raught, B., Dedhar, S.: The interactome of metabolic enzyme carbonic anhydrase IX reveals novel roles in tumor cell migration and invadopodia/MMP14-mediated invasion. Oncogene **36**(45), 6244 (2017)

[140] Svastová, E., Zilka, N., Zat'ovicová, M., Gibadulinová, A., Ciampor, F., Pastorek, J., Pastoreková, S.: Carbonic anhydrase IX reduces E-cadherin-mediated adhesion of MDCK cells via interaction with beta-catenin. Exp. Cell Res. **290**(2), 332–345 (2003)

[141] Kim, B.-R., Shin, H.-J., Kim, J.-Y., Byun, H.-J., Lee, J.H., Sung, Y.K., Rho, S.B.: Dickkopf-1 (DKK-1) interrupts FAK/PI3K/mTOR pathway by interaction of carbonic anhydrase IX (CA9) in tumorigenesis. Cell. Signal. **24**(7), 1406–1413 (2012)

[142] Shin, H.-J., Rho, S.B., Jung, D.C., Han, I.-O., Oh, E.-S., Kim, J.-Y.: Carbonic anhydrase IX (CA9) modulates tumor-associated cell migration and invasion. J. Cell. Sci. **124**(Pt 7), 1077–1087 (2011)

[143] Sansone, P., Piazzi, G., Paterini, P., Strillacci, A., Ceccarelli, C., Minni, F., Biasco, G., Chieco, P., Bonafè, M.: Cyclooxygenase-2/carbonic anhydrase-IX up-regulation promotes invasive potential and hypoxia survival in colorectal cancer cells. J Cell Mol Med **13**(9b), 3876–3887 (2009)

[144] Radvak, P., Repic, M., Svastova, E., Takacova, M., Csaderova, L., Strnad, H., Pastorek, J., Pastorekova, S., Kopacek, J.: Suppression of carbonic anhydrase IX leads to aberrant focal adhesion and decreased invasion of tumor cells. Oncol. Rep. **29**(3), 1147–1153 (2013)

[145] Supuran, C.T.: Carbonic anhydrases–an overview. Curr. Pharm. Des. **14**(7), 603–614 (2008)

[146] Kuo, W.-H., Yang, S.-F., Hsieh, Y.-S., Tsai, C.-S., Hwang, W.-L., Chu, S.-C.: Differential expression of carbonic anhydrase isoenzymes in various types of anemia. Clin. Chim. Acta **351**(1-2), 79–86 (2005)

[147] Gao, B.-B., Clermont, A., Rook, S., Fonda, S.J., Srinivasan, V.J., Wojtkowski, M., Fujimoto, J.G., Avery, R.L., Arrigg, P.G., Bursell, S.-E., Aiello, L.P., Feener, E.P.: Extracellular carbonic anhydrase mediates hemorrhagic retinal and cerebral vascular permeability through prekallikrein activation. Nat. Med. **13**(2), 181–188 (2007)

[148] Chang, X., Han, J., Zhao, Y., Yan, X., Sun, S., Cui, Y.: Increased expression of carbonic anhydrase I in the synovium of patients with ankylosing spondylitis. BMC Musculoskelet Disord **11**, 279 (2010)

[149] Chang, X., Zheng, Y., Yang, Q., Wang, L., Pan, J., Xia, Y., Yan, X., Han, J.: Carbonic anhydrase I (CA1) is involved in the process of bone formation and is susceptible to ankylosing spondylitis. Arthritis Res Ther **14**(4), 176 (2012)

[150] Takakura, M., Yokomizo, A., Tanaka, Y., Kobayashi, M., Jung, G., Banno, M., Sakuma, T., Imada, K., Oda, Y., Kamita, M., Honda, K., Yamada, T., Naito, S., Ono, M.: Carbonic Anhydrase I as a New Plasma Biomarker for Prostate Cancer. ISRN Oncol **2012** (2012)

[151] Gramlich, T.L., Hennigar, R.A., Spicer, S.S., Schulte, B.A.: Immunohistochemical localization of sodium-potassium-stimulated adenosine triphosphatase and carbonic anhydrase in human colon and colonic neoplasms. Arch. Pathol. Lab. Med. **114**(4), 415–419 (1990)

[152] Mincione, F., Starnotti, M., Masini, E., Bacciottini, L., Scrivanti, C., Casini, A., Vullo, D., Scozzafava, A., Supuran, C.T.: Carbonic anhydrase inhibitors: Design of thioureido sulfonamides with potent isozyme II and XII inhibitory properties and intraocular pressure lowering activity in a rabbit model of glaucoma. Bioorg. Med. Chem. Lett. **15**(17), 3821–3827 (2005)

[153] Carta, F., Aggarwal, M., Maresca, A., Scozzafava, A., McKenna, R., Masini, E., Supuran, C.T.: Dithiocarbamates strongly inhibit carbonic anhydrases and show antiglaucoma action in vivo. J. Med. Chem. **55**(4), 1721–1730 (2012)

[154] Lönnerholm, G., Wistrand, P.J., Bárány, E.: Carbonic anhydrase isoenzymes in the rat kidney. Effects of chronic acetazolamide treatment. Acta Physiol. Scand. **126**(1), 51–60 (1986)

[155] Carta, F., Akdemir, A., Scozzafava, A., Masini, E., Supuran, C.T.: Xanthates and trithiocarbonates strongly inhibit carbonic anhydrases and show antiglaucoma effects in vivo. J. Med. Chem. **56**(11), 4691–4700 (2013)

[156] Thiry, A., Dogné, J.-M., Supuran, C.T., Masereel, B.: Anticonvulsant sulfonamides/sulfamates/sulfamides with carbonic anhydrase inhibitory activity: Drug design and mechanism of action. Curr. Pharm. Des. **14**(7), 661–671 (2008)

[157] Aggarwal, M., Boone, C.D., Kondeti, B., McKenna, R.: Structural annotation of human carbonic anhydrases. J Enzyme Inhib Med Chem **28**(2), 267–277 (2013)

[158] Oksala, N., Levula, M., Pelto-Huikko, M., Kytömäki, L., Soini, J.T., Salenius, J., Kähönen, M., Karhunen, P.J., Laaksonen, R., Parkkila, S., Lehtimäki, T.: Carbonic anhydrases II and XII are up-regulated in osteoclast-like cells in advanced human atherosclerotic plaques-Tampere Vascular Study. Ann. Med. **42**(5), 360–370 (2010)

[159] Kenny, A.D.: Role of carbonic anhydrase in bone: Plasma acetazolamide concentrations associated with inhibition of bone loss. Pharmacology **31**(2), 97–107 (1985)

[160] Kayser, B., Hulsebosch, R., Bosch, F.: Low-dose acetylsalicylic acid analog and acetazolamide for prevention of acute mountain sickness. High Alt. Med. Biol. **9**(1), 15–23 (2008)

[161] Kayser, B., Dumont, L., Lysakowski, C., Combescure, C., Haller, G., Tramèr, M.R.: Reappraisal of acetazolamide for the prevention of acute mountain sickness: A systematic review and meta-analysis. High Alt. Med. Biol. **13**(2), 82–92 (2012)

[162] Parkkila, S., Lasota, J., Fletcher, J.A., Ou, W.-B., Kivelä, A.J., Nuorva, K., Parkkila, A.-K., Ollikainen, J., Sly, W.S., Waheed, A., Pastorekova, S., Pastorek, J., Isola, J., Miettinen, M.: Carbonic anhydrase II. A novel biomarker for gastrointestinal stromal tumors. Mod. Pathol. **23**(5), 743–750 (2010)

[163] Hynninen, P., Parkkila, S., Huhtala, H., Pastorekova, S., Pastorek, J., Waheed, A., Sly, W.S., Tomas, E.: Carbonic anhydrase isozymes II, IX, and XII in uterine tumors. APMIS **120**(2), 117–129 (2012)

[164] Sly, W.S., Hewett-Emmett, D., Whyte, M.P., Yu, Y.S., Tashian, R.E.: Carbonic anhydrase II deficiency identified as the primary defect in the autosomal recessive syndrome of osteopetrosis with renal tubular acidosis and cerebral calcification. Proc. Natl. Acad. Sci. U.S.A. **80**(9), 2752–2756 (1983)

[165] Räisänen, S.R., Lehenkari, P., Tasanen, M., Rahkila, P., Härkönen, P.L., Väänänen, H.K.: Carbonic anhydrase III protects cells from hydrogen peroxide-induced apoptosis. FASEB J. **13**(3), 513–522 (1999)

[166] Roy, P., Reavey, E., Rayne, M., Roy, S., Abed El Baky, M., Ishii, Y., Bartholomew, C.: Enhanced sensitivity to hydrogen peroxide-induced apoptosis in Evi1 transformed Rat1 fibroblasts due to repression of carbonic anhydrase III. FEBS J. **277**(2), 441–452 (2010)

[167] Heath, R., Schwartz, M.S., Brown, I.R., Carter, N.D.: Carbonic anhydrase III in neuromuscular disorders. J. Neurol. Sci. **59**(3), 383–388 (1983)

[168] Elchuri, S., Naeemuddin, M., Sharpe, O., Robinson, W.H., Huang, T.-T.: Identification of biomarkers associated with the development of hepatocellular carcinoma in CuZn superoxide dismutase deficient mice. Proteomics **7**(12), 2121–2129 (2007)

[169] Kuhara, M., Wang, J., Flores, M.J., Qiao, Z., Koizumi, Y., Koyota, S., Taniguchi, N., Sugiyama, T.: Sexual dimorphism in LEC rat liver: Suppression of carbonic anhydrase III by copper accumulation during hepatocarcinogenesis. Biomed. Res. **32**(2), 111–117 (2011)

[170] Mitterberger, M.C., Kim, G., Rostek, U., Levine, R.L., Zwerschke, W.: Carbonic anhydrase III regulates peroxisome proliferator-activated receptor-$\gamma 2$. Exp. Cell Res. **318**(8), 877–886 (2012)

[171] Whitney, P.L., Briggle, T.V.: Membrane-associated carbonic anhydrase purified from bovine lung. J. Biol. Chem. **257**(20), 12056–12059 (1982)

[172] Waheed, A., Okuyama, T., Heyduk, T., Sly, W.S.: Carbonic anhydrase IV: Purification of a secretory form of the recombinant human enzyme and identification of the positions and importance of its disulfide bonds. Arch. Biochem. Biophys. **333**(2), 432–438 (1996)

[173] Rebello, G., Ramesar, R., Vorster, A., Roberts, L., Ehrenreich, L., Oppon, E., Gama, D., Bardien, S., Greenberg, J., Bonapace, G., Waheed, A., Shah, G.N., Sly, W.S.: Apoptosis-inducing signal sequence mutation in carbonic anhydrase IV identified in patients with the RP17 form of retinitis pigmentosa. Proc. Natl. Acad. Sci. U.S.A. **101**(17), 6617–6622 (2004)

[174] Datta, R., Waheed, A., Bonapace, G., Shah, G.N., Sly, W.S.: Pathogenesis of retinitis pigmentosa associated with apoptosis-inducing mutations in carbonic anhydrase IV. Proc. Natl. Acad. Sci. U.S.A. **106**(9), 3437–3442 (2009)

[175] Datta, R., Shah, G.N., Rubbelke, T.S., Waheed, A., Rauchman, M., Goodman, A.G., Katze, M.G., Sly, W.S.: Progressive renal injury from transgenic expression of human carbonic anhydrase IV folding mutants is enhanced by deficiency of p58IPK. Proc Natl Acad Sci U S A **107**(14), 6448–6452 (2010)

[176] Zhang, J., Tsoi, H., Li, X., Wang, H., Gao, J., Wang, K., Go, M.Y., Ng, S.C., Chan, F.K., Sung, J.J., Yu, J.: Carbonic anhydrase IV inhibits colon cancer development by inhibiting the Wnt signalling pathway through targeting the WTAP-WT1-TBL1 axis. Gut **65**(9), 1482–1493 (2016)

[177] Barker, H., Aaltonen, M., Pan, P., Vähätupa, M., Kaipiainen, P., May, U., Prince, S., Uusitalo-Järvinen, H., Waheed, A., Pastoreková, S., Sly, W.S., Parkkila, S., Järvinen, T.A.: Role of carbonic anhydrases in skin wound healing. Exp. Mol. Med. **49**(5), 334 (2017)

[178] Chandrashekar, J., Yarmolinsky, D., von Buchholtz, L., Oka, Y., Sly, W., Ryba, N.J.P., Zuker, C.S.: The taste of carbonation. Science **326**(5951), 443–445 (2009)

[179] Amor-Gueret, M., Levi-Strauss, M.: Nucleotide and derived amino-acid sequence of a cDNA encoding a new mouse carbonic anhydrase. Nucleic Acids Res. **18**(6), 1646 (1990)

[180] Shah, G.N., Hewett-Emmett, D., Grubb, J.H., Migas, M.C., Fleming, R.E., Waheed, A., Sly, W.S.: Mitochondrial carbonic anhydrase CA VB: Differences in tissue distribution and pattern of evolution from those of CA VA suggest distinct physiological roles. Proc. Natl. Acad. Sci. U.S.A. **97**(4), 1677–1682 (2000)

[181] Dodgson, S.J., Forster, R.E., Storey, B.T., Mela, L.: Mitochondrial carbonic anhydrase. Proc. Natl. Acad. Sci. U.S.A. **77**(9), 5562–5566 (1980)

[182] Lynch, C.J., Fox, H., Hazen, S.A., Stanley, B.A., Dodgson, S., Lanoue, K.F.: Role of hepatic carbonic anhydrase in de novo lipogenesis. Biochem. J. **310** **(Pt 1)**, 197–202 (1995)

[183] Dodgson, S.J., Forster, R.E.: Carbonic anhydrase: Inhibition results in decreased urea production by hepatocytes. J. Appl. Physiol. **60**(2), 646–652 (1986)

[184] Dodgson, S.J., Forster, R.E.: Inhibition of CA V decreases glucose synthesis from pyruvate. Arch. Biochem. Biophys. **251**(1), 198–204 (1986)

[185] Scozzafava, A., Supuran, C.T., Carta, F.: Antiobesity carbonic anhydrase inhibitors: A literature and patent review. Expert Opinion on Therapeutic Patents **23**(6), 725–735 (2013)

[186] Parkkila, A.-K., Scarim, A.L., Parkkila, S., Waheed, A., Corbett, J.A., Sly, W.S.: Expression of Carbonic Anhydrase V in Pancreatic Beta Cells Suggests Role for Mitochondrial Carbonic Anhydrase in Insulin Secretion. J. Biol. Chem. **273**(38), 24620–24623 (1998)

[187] Price, T.O., Eranki, V., Banks, W.A., Ercal, N., Shah, G.N.: Topiramate treatment protects blood-brain barrier pericytes from hyperglycemia-induced oxidative damage in diabetic mice. Endocrinology **153**(1), 362–372 (2012)

[188] Shah, G.N., Rubbelke, T.S., Hendin, J., Nguyen, H., Waheed, A., Shoemaker, J.D., Sly, W.S.: Targeted mutagenesis of mitochondrial carbonic anhydrases VA and VB implicates both enzymes in ammonia detoxification and glucose metabolism. Proc. Natl. Acad. Sci. U.S.A. **110**(18), 7423–7428 (2013)

[189] Bootorabi, F., Jänis, J., Smith, E., Waheed, A., Kukkurainen, S., Hytönen, V., Valjakka, J., Supuran, C.T., Vullo, D., Sly, W.S., Parkkila, S.: Analysis of a shortened form of human carbonic anhydrase VII expressed in vitro compared to the full-length enzyme. Biochimie **92**(8), 1072–1080 (2010)

[190] Truppo, E., Supuran, C.T., Sandomenico, A., Vullo, D., Innocenti, A., Di Fiore, A., Alterio, V., De Simone, G., Monti, S.M.: Carbonic anhydrase VII is S-glutathionylated without loss of catalytic activity and affinity for sulfonamide inhibitors. Bioorg. Med. Chem. Lett. **22**(4), 1560–1564 (2012)

[191] Ruusuvuori, E., Li, H., Huttu, K., Palva, J.M., Smirnov, S., Rivera, C., Kaila, K., Voipio, J.: Carbonic anhydrase isoform VII acts as a molecular switch in the development of synchronous gamma-frequency firing of hippocampal CA1 pyramidal cells. J. Neurosci. **24**(11), 2699–2707 (2004)

[192] Rivera, C., Voipio, J., Kaila, K.: Two developmental switches in GABAergic signalling: The K+-Cl- cotransporter KCC2 and carbonic anhydrase CAVII. J. Physiol. (Lond.) **562**(Pt 1), 27–36 (2005)

[193] Thiry, A., Dogné, J.-M., Supuran, C.T., Masereel, B.: Carbonic anhydrase inhibitors as anticonvulsant agents. Curr Top Med Chem **7**(9), 855–864 (2007)

[194] Asiedu, M., Ossipov, M.H., Kaila, K., Price, T.J.: Acetazolamide and midazolam act synergistically to inhibit neuropathic pain. Pain **148**(2), 302–308 (2010)

[195] Whittington, D.A., Waheed, A., Ulmasov, B., Shah, G.N., Grubb, J.H., Sly, W.S., Christianson, D.W.: Crystal structure of the dimeric extracellular domain of human carbonic anhydrase XII, a bitopic membrane protein overexpressed in certain cancer tumor cells. Proc. Natl. Acad. Sci. U.S.A. **98**(17), 9545–9550 (2001)

[196] Creighton, C.J., Cordero, K.E., Larios, J.M., Miller, R.S., Johnson, M.D., Chinnaiyan, A.M., Lippman, M.E., Rae, J.M.: Genes regulated by estrogen in breast tumor cells in vitro are similarly regulated in vivo in tumor xenografts and human breast tumors. Genome Biol **7**(4), 28 (2006)

[197] Barnett, D.H., Sheng, S., Charn, T.H., Waheed, A., Sly, W.S., Lin, C.-Y., Liu, E.T., Katzenellenbogen, B.S.: Estrogen receptor regulation of carbonic anhydrase XII through a distal enhancer in breast cancer. Cancer Res. **68**(9), 3505–3515 (2008)

[198] Türeci, O., Sahin, U., Vollmar, E., Siemer, S., Göttert, E., Seitz, G., Parkkila, A.K., Shah, G.N., Grubb, J.H., Pfreundschuh, M., Sly, W.S.: Human carbonic anhydrase XII: cDNA cloning, expression, and chromosomal localization of a carbonic anhydrase gene that is overexpressed in some renal cell cancers. Proc. Natl. Acad. Sci. U.S.A. **95**(13), 7608–7613 (1998)

[199] Parkkila, S., Parkkila, A.K., Saarnio, J., Kivelä, J., Karttunen, T.J., Kaunisto, K., Waheed, A., Sly, W.S., Türeci, O., Virtanen, I., Rajaniemi, H.: Expression of the membrane-associated carbonic anhydrase isozyme XII in the human kidney and renal tumors. J. Histochem. Cytochem. **48**(12), 1601–1608 (2000)

[200] Kivelä, A., Parkkila, S., Saarnio, J., Karttunen, T.J., Kivelä, J., Parkkila, A.-K., Waheed, A., Sly, W.S., Grubb, J.H., Shah, G., Türeci, Ö., Rajaniemi, H.: Expression of a Novel Transmembrane Carbonic Anhydrase Isozyme XII in Normal Human Gut and Colorectal Tumors. Am J Pathol **156**(2), 577–584 (2000)

[201] Karhumaa, P., Parkkila, S., Türeci, O., Waheed, A., Grubb, J.H., Shah, G., Parkkila, A., Kaunisto, K., Tapanainen, J., Sly, W.S., Rajaniemi, H.: Identification of carbonic anhydrase XII as the membrane isozyme expressed in the normal human endometrial epithelium. Mol. Hum. Reprod. **6**(1), 68–74 (2000)

[202] Watson, P.H., Chia, S.K., Wykoff, C.C., Han, C., Leek, R.D., Sly, W.S., Gatter, K.C., Ratcliffe, P., Harris, A.L.: Carbonic anhydrase XII is a marker of good prognosis in invasive breast carcinoma. Br J Cancer **88**(7), 1065–1070 (2003)

[203] Haapasalo, J., Hilvo, M., Nordfors, K., Haapasalo, H., Parkkila, S., Hyrsky-luoto, A., Rantala, I., Waheed, A., Sly, W.S., Pastorekova, S., Pastorek, J., Parkkila, A.-K.: Identification of an alternatively spliced isoform of carbonic anhydrase XII in diffusely infiltrating astrocytic gliomas. Neuro-oncology **10**(2), 131–138 (2008)

[204] Hsieh, M.-J., Chen, K.-S., Chiou, H.-L., Hsieh, Y.-S.: Carbonic anhydrase XII promotes invasion and migration ability of MDA-MB-231 breast cancer cells through the p38 MAPK signaling pathway. Eur. J. Cell Biol. **89**(8), 598–606 (2010)

[205] Doyen, J., Parks, S.K., Marcié, S., Pouysségur, J., Chiche, J.: Knock-down of hypoxia-induced carbonic anhydrases IX and XII radiosensitizes tumor cells by increasing intracellular acidosis. Front Oncol **2** (2013)

[206] Liao, S.-Y., Ivanov, S., Ivanova, A., Ghosh, S., Cote, M.A., Keefe, K., Coca-Prados, M., Stanbridge, E.J., Lerman, M.I.: Expression of cell surface transmembrane carbonic anhydrase genes CA9 and CA12 in the human eye: Overexpression of CA12 (CAXII) in glaucoma. J. Med. Genet. **40**(4), 257–261 (2003)

[207] Power, K.A., Grad, S., Rutges, J.P.H.J., Creemers, L.B., van Rijen, M.H.P., O'Gaora, P., Wall, J.G., Alini, M., Pandit, A., Gallagher, W.M.: Identification of cell surface-specific markers to target human nucleus pulposus cells: Expression of carbonic anhydrase XII varies with age and degeneration. Arthritis Rheum. **63**(12), 3876–3886 (2011)

[208] Lee, M., Vecchio-Pagán, B., Sharma, N., Waheed, A., Li, X., Raraigh, K.S., Robbins, S., Han, S.T., Franca, A.L., Pellicore, M.J., Evans, T.A., Arcara, K.M., Nguyen, H., Luan, S., Belchis, D., Hertecant, J., Zabner, J., Sly, W.S., Cutting, G.R.: Loss of carbonic anhydrase XII function in individuals with elevated sweat chloride concentration and pulmonary airway disease. Hum. Mol. Genet. **25**(10), 1923–1933 (05 15, 2016)

[209] Feldshtein, M., Elkrinawi, S., Yerushalmi, B., Marcus, B., Vullo, D., Romi, H., Ofir, R., Landau, D., Sivan, S., Supuran, C.T., Birk, O.S.: Hyper-chlorhidrosis caused by homozygous mutation in CA12, encoding carbonic anhydrase XII. Am. J. Hum. Genet. **87**(5), 713–720 (2010)

[210] Muhammad, E., Leventhal, N., Parvari, G., Hanukoglu, A., Hanukoglu, I., Chalifa-Caspi, V., Feinstein, Y., Weinbrand, J., Jacoby, H., Manor, E., Nagar, T., Beck, J.C., Sheffield, V.C., Hershkovitz, E., Parvari, R.: Autosomal recessive hyponatremia due to isolated salt wasting in sweat associated with a mutation in the active site of Carbonic Anhydrase 12. Hum. Genet. **129**(4), 397–405 (2011)

[211] Di Fiore, A., Monti, S.M., Hilvo, M., Parkkila, S., Romano, V., Scaloni, A., Pedone, C., Scozzafava, A., Supuran, C.T., De Simone, G.: Crystal structure of human carbonic anhydrase XIII and its complex with the inhibitor acetazolamide. Proteins **74**(1), 164–175 (2009)

[212] Lehtonen, J., Shen, B., Vihinen, M., Casini, A., Scozzafava, A., Supuran, C.T., Parkkila, A.-K., Saarnio, J., Kivelä, A.J., Waheed, A., Sly, W.S., Parkkila, S.: Characterization of CA XIII, a novel member of the carbonic anhydrase isozyme family. J. Biol. Chem. **279**(4), 2719–2727 (2004)

[213] Kummola, L., Hämäläinen, J.M., Kivelä, J., Kivelä, A.J., Saarnio, J., Karttunen, T., Parkkila, S.: Expression of a novel carbonic anhydrase, CA XIII, in normal and neoplastic colorectal mucosa. BMC Cancer **5**, 41 (2005)

[214] Alterio, V., Pan, P., Parkkila, S., Buonanno, M., Supuran, C.T., Monti, S.M., De Simone, G.: The structural comparison between membrane-associated human carbonic anhydrases provides insights into drug design of selective inhibitors. Biopolymers **101**(7), 769–778 (2014)

[215] Parkkila, S., Parkkila, A.-K., Rajaniemi, H., Shah, G.N., Grubb, J.H., Waheed, A., Sly, W.S.: Expression of membrane-associated carbonic anhydrase XIV on neurons and axons in mouse and human brain. PNAS **98**(4), 1918–1923 (2001)

[216] Ashida, S., Nishimori, I., Tanimura, M., Onishi, S., Shuin, T.: Effects of von Hippel-Lindau gene mutation and methylation status on expression of transmembrane carbonic anhydrases in renal cell carcinoma. J. Cancer Res. Clin. Oncol. **128**(10), 561–568 (2002)

[217] Parkkila, S., Kivelä, A.J., Kaunisto, K., Parkkila, A.-K., Hakkola, J., Rajaniemi, H., Waheed, A., Sly, W.S.: The plasma membrane carbonic anhydrase in murine hepatocytes identified as isozyme XIV. BMC Gastroenterol **2**, 13 (2002)

[218] Ogilvie, J.M., Ohlemiller, K.K., Shah, G.N., Ulmasov, B., Becker, T.A., Waheed, A., Hennig, A.K., Lukasiewicz, P.D., Sly, W.S.: Carbonic anhydrase XIV deficiency produces a functional defect in the retinal light response. PNAS **104**(20), 8514–8519 (2007)

[219] Svichar, N., Waheed, A., Sly, W.S., Hennings, J.C., Hübner, C.A., Chesler, M.: Carbonic anhydrases CA4 and CA14 both enhance AE3-mediated Cl–HCO3- exchange in hippocampal neurons. J. Neurosci. **29**(10), 3252–3258 (2009)

[220] Shah, G.N., Ulmasov, B., Waheed, A., Becker, T., Makani, S., Svichar, N., Chesler, M., Sly, W.S.: Carbonic anhydrase IV and XIV knockout mice: Roles of the respective carbonic anhydrases in buffering the extracellular space in brain. Proc. Natl. Acad. Sci. U.S.A. **102**(46), 16771–16776 (2005)

[221] Vargas, L.A., Alvarez, B.V.: Carbonic anhydrase XIV in the normal and hypertrophic myocardium. J. Mol. Cell. Cardiol. **52**(3), 741–752 (2012)

[222] Tashian, R.E., Hewett-Emmett, D., Carter, N., Bergenhem, N.C.: Carbonic anhydrase (CA)-related proteins (CA-RPs), and transmembrane proteins with CA or CA-RP domains. EXS (90), 105–120 (2000)

[223] Aspatwar, A., Tolvanen, M.E.E., Parkkila, S.: An update on carbonic anhydrase-related proteins VIII, X and XI. J Enzyme Inhib Med Chem **28**(6), 1129–1142 (2013)

[224] Kato, K.: Sequence of a novel carbonic anhydrase-related polypeptide and its exclusive presence in Purkinje cells. FEBS Lett. **271**(1-2), 137–140 (1990)

[225] Aspatwar, A., Tolvanen, M.E., Parkkila, S.: Phylogeny and expression of carbonic anhydrase-related proteins. BMC Mol Biol **11**, 25 (2010)

[226] Türkmen, S., Guo, G., Garshasbi, M., Hoffmann, K., Alshalah, A.J., Mischung, C., Kuss, A., Humphrey, N., Mundlos, S., Robinson, P.N.: CA8 Mutations Cause a Novel Syndrome Characterized by Ataxia and Mild Mental Retardation with Predisposition to Quadrupedal Gait. PLOS Genetics **5**(5), 1000487 (2009)

[227] Jiao, Y., Yan, J., Zhao, Y., Donahue, L.R., Beamer, W.G., Li, X., Roe, B.A., Ledoux, M.S., Gu, W.: Carbonic anhydrase-related protein VIII deficiency is associated with a distinctive lifelong gait disorder in waddles mice. Genetics **171**(3), 1239–1246 (2005)

[228] Aspatwar, A., Tolvanen, M.E.E., Jokitalo, E., Parikka, M., Ortutay, C., Harjula, S.-K.E., Rämet, M., Vihinen, M., Parkkila, S.: Abnormal cerebellar development and ataxia in CARP VIII morphant zebrafish. Hum. Mol. Genet. **22**(3), 417–432 (2013)

[229] Ishihara, T., Takeuchi, T., Nishimori, I., Adachi, Y., Minakuchi, T., Fujita, J., Sonobe, H., Ohtsuki, Y., Onishi, S.: Carbonic anhydrase-related protein VIII increases invasiveness of non-small cell lung adenocarcinoma. Virchows Arch. **448**(6), 830–837 (2006)

[230] Lu, S.-h., Takeuchi, T., Fujita, J., Ishida, T., Akisawa, Y., Nishimori, I., Kohsaki, T., Onishi, S., Sonobe, H., Ohtsuki, Y.: Effect of carbonic anhydrase-related protein VIII expression on lung adenocarcinoma cell growth. Lung Cancer **44**(3), 273–280 (2004)

[231] Morimoto, K., Nishimori, I., Takeuchi, T., Kohsaki, T., Okamoto, N., Taguchi, T., Yunoki, S., Watanabe, R., Ohtsuki, Y., Onishi, S.: Overexpression of carbonic anhydrase-related protein XI promotes proliferation and

invasion of gastrointestinal stromal tumors. Virchows Arch. **447**(1), 66–73 (2005)

[232] Kleiderlein, J.J., Nisson, P.E., Jessee, J., Li, W.B., Becker, K.G., Derby, M.L., Ross, C.A., Margolis, R.L.: CCG repeats in cDNAs from human brain. Hum. Genet. **103**(6), 666–673 (1998)

[233] Okamoto, N., Fujikawa-Adachi, K., Nishimori, I., Taniuchi, K., Onishi, S.: cDNA sequence of human carbonic anhydrase-related protein, CA-RP X: mRNA expressions of CA-RP X and XI in human brain. Biochim. Biophys. Acta **1518**(3), 311–316 (2001)

[234] Kumar, V., Kannan, K.K.: Enzyme-Substrate Interactions: Structure of Human Carbonic Anhydrase I Complexed with Bicarbonate. Journal of Molecular Biology **241**(2), 226–232 (1994)

[235] Avvaru, B.S., Kim, C.U., Sippel, K.H., Gruner, S.M., Agbandje-McKenna, M., Silverman, D.N., McKenna, R.: A Short, Strong Hydrogen Bond in the Active Site of Human Carbonic Anhydrase II. Biochemistry **49**(2), 249–251 (2010)

[236] Duda, D.M., Tu, C., Fisher, S.Z., An, H., Yoshioka, C., Govindasamy, L., Laipis, P.J., Agbandje-McKenna, M., Silverman, D.N., McKenna, R.: Human Carbonic Anhydrase III: Structural and Kinetic Study of Catalysis and Proton Transfer,. Biochemistry **44**(30), 10046–10053 (2005)

[237] Stams, T., Chen, Y., Boriack-Sjodin, P.A., Hurt, J.D., Liao, J., May, J.A., Dean, T., Laipis, P., Silverman, D.N., Christianson, D.W.: Structures of murine carbonic anhydrase IV and human carbonic anhydrase II complexed with brinzolamide: Molecular basis of isozyme-drug discrimination. Protein Sci **7**(3), 556–563 (1998)

[238] Di Fiore, A., Truppo, E., Supuran, C.T., Alterio, V., Dathan, N., Bootorabi, F., Parkkila, S., Monti, S.M., Simone, G.D.: Crystal structure of the C183S/C217S mutant of human CA VII in complex with acetazolamide. Bioorganic & Medicinal Chemistry Letters **20**(17), 5023–5026 (2010)

[239] Fisher, S.Z., Maupin, C.M., Budayova-Spano, M., Govindasamy, L., Tu, C., Agbandje-McKenna, M., Silverman, D.N., Voth, G.A., McKenna, R.: Atomic Crystal and Molecular Dynamics Simulation Structures of Human Carbonic Anhydrase II: Insights into the Proton Transfer Mechanism,. Biochemistry **46**(11), 2930–2937 (2007)

[240] De Simone, G., Alterio, V., Supuran, C.T.: Exploiting the hydrophobic and hydrophilic binding sites for designing carbonic anhydrase inhibitors. Expert Opin Drug Discov **8**(7), 793–810 (2013)

[241] Aggarwal, M., Kondeti, B., McKenna, R.: Anticonvulsant/antiepileptic carbonic anhydrase inhibitors: A patent review. Expert Opin Ther Pat **23**(6), 717–724 (2013)

[242] Alterio, V., Di Fiore, A., D'Ambrosio, K., Supuran, C.T., De Simone, G.: Multiple Binding Modes of Inhibitors to Carbonic Anhydrases: How to Design Specific Drugs Targeting 15 Different Isoforms? Chem. Rev. **112**(8), 4421–4468 (2012)

[243] Supuran, C.T.: How many carbonic anhydrase inhibition mechanisms exist? J Enzyme Inhib Med Chem **31**(3), 345–360 (2016)

[244] Lomelino, C., McKenna, R.: Carbonic anhydrase inhibitors: A review on the progress of patent literature (2011–2016). Expert Opinion on Therapeutic Patents **26**(8), 947–956 (2016)

[245] Lomelino, C., McKenna, R.: Carbonic anhydrase inhibitors: A review on the progress of patent literature (2011-2016). Expert Opin Ther Pat **26**(8), 947–956 (2016)

[246] Innocenti, A., Vullo, D., Scozzafava, A., Supuran, C.T.: Carbonic anhydrase inhibitors: Interactions of phenols with the 12 catalytically active mammalian isoforms (CA I-XIV). Bioorg. Med. Chem. Lett. **18**(5), 1583–1587 (2008)

[247] Carta, F., Temperini, C., Innocenti, A., Scozzafava, A., Kaila, K., Supuran, C.T.: Polyamines inhibit carbonic anhydrases by anchoring to the zinc-coordinated water molecule. J. Med. Chem. **53**(15), 5511–5522 (2010)

[248] Martin, D.P., Cohen, S.M.: Nucleophile recognition as an alternative inhibition mode for benzoic acid based carbonic anhydrase inhibitors. Chem. Commun. (Camb.) **48**(43), 5259–5261 (2012)

[249] Tanc, M., Carta, F., Bozdag, M., Scozzafava, A., Supuran, C.T.: 7-Substituted-sulfocoumarins are isoform-selective, potent carbonic anhydrase II inhibitors. Bioorg. Med. Chem. **21**(15), 4502–4510 (2013)

[250] Ferraroni, M., Carta, F., Scozzafava, A., Supuran, C.T.: Thioxocoumarins Show an Alternative Carbonic Anhydrase Inhibition Mechanism Compared to Coumarins. J. Med. Chem. **59**(1), 462–473 (2016)

[251] D'Ambrosio, K., Carradori, S., Monti, S.M., Buonanno, M., Secci, D., Vullo, D., Supuran, C.T., De Simone, G.: Out of the active site binding pocket for carbonic anhydrase inhibitors. Chem. Commun. (Camb.) **51**(2), 302–305 (2015)

[252] Maresca, A., Temperini, C., Vu, H., Pham, N.B., Poulsen, S.-A., Scozzafava, A., Quinn, R.J., Supuran, C.T.: Non-zinc mediated inhibition of carbonic anhydrases: Coumarins are a new class of suicide inhibitors. J. Am. Chem. Soc. **131**(8), 3057–3062 (2009)

[253] Nocentini, A., Ceruso, M., Carta, F., Supuran, C.T.: 7-Aryl-triazolyl-substituted sulfocoumarins are potent, selective inhibitors of the tumor-associated carbonic anhydrase IX and XII. J Enzyme Inhib Med Chem, 1–8 (2015)

[254] Métayer, B., Martin-Mingot, A., Vullo, D., Supuran, C.T., Thibaudeau, S.: Superacid synthesized tertiary benzenesulfonamides and benzofuzed sultams act as selective hCA IX inhibitors: Toward understanding a new mode of inhibition by tertiary sulfonamides. Org. Biomol. Chem. **11**(43), 7540–7549 (2013)

[255] Parkkila, S., Innocenti, A., Kallio, H., Hilvo, M., Scozzafava, A., Supuran, C.T.: The protein tyrosine kinase inhibitors imatinib and nilotinib strongly inhibit several mammalian alpha-carbonic anhydrase isoforms. Bioorg. Med. Chem. Lett. **19**(15), 4102–4106 (2009)

[256] Innocenti, A., Scozzafava, A., Supuran, C.T.: Carbonic anhydrase inhibitors. Inhibition of transmembrane isoforms IX, XII, and XIV with less investigated anions including trithiocarbonate and dithiocarbamate. Bioorg. Med. Chem. Lett. **20**(5), 1548–1550 (2010)

[257] Saada, M.-C., Montero, J.-L., Vullo, D., Scozzafava, A., Winum, J.-Y., Supuran, C.T.: Carbonic anhydrase activators: Gold nanoparticles coated with derivatized histamine, histidine, and carnosine show enhanced activatory effects on several mammalian isoforms. J. Med. Chem. **54**(5), 1170–1177 (2011)

[258] Angeli, A., Tanini, D., Peat, T.S., Di Cesare Mannelli, L., Bartolucci, G., Capperucci, A., Ghelardini, C., Supuran, C.T., Carta, F.: Discovery of New Selenoureido Analogues of 4-(4-Fluorophenylureido)benzenesulfonamide as Carbonic Anhydrase Inhibitors. ACS Med Chem Lett **8**(9), 963–968 (2017)

[259] Briganti, F., Mangani, S., Orioli, P., Scozzafava, A., Vernaglione, G., Supuran, C.T.: Carbonic Anhydrase Activators: X-ray Crystallographic and Spectroscopic Investigations for the Interaction of Isozymes I and II with Histamine,. Biochemistry **36**(34), 10384–10392 (1997)

[260] Cecchi, A., Hulikova, A., Pastorek, J., Pastoreková, S., Scozzafava, A., Winum, J.-Y., Montero, J.-L., Supuran, C.T.: Carbonic anhydrase inhibitors. Design of fluorescent sulfonamides as probes of tumor-associated carbonic anhydrase IX that inhibit isozyme IX-mediated acidification of hypoxic tumors. J. Med. Chem. **48**(15), 4834–4841 (2005)

[261] Lau, J., Lin, K.-S., Bénard, F.: Past, Present, and Future: Development of Theranostic Agents Targeting Carbonic Anhydrase IX. Theranostics **7**(17), 4322–4339 (2017)

[262] Pini, R., Ratto, F., Tatini, F., Fusi, F., Centi, S., Scozzafava, A., Supuran, C.T., Carta, F., Capaccioli, S., Witor, E.J.: Assembly Comprising an Absorber of Near Infrared (Nir) Light Covalently Linked to an Inhibitor of Carbonic Anhydrase. US20160015661 A1, January 2016

[263] Kobayashi, H., Ogawa, M., Kosaka, N., Choyke, P.L., Urano, Y.: Multicolor imaging of lymphatic function with two nanomaterials: Quantum dot-labeled cancer cells and dendrimer-based optical agents. Nanomedicine (Lond) **4**(4), 411–419 (2009)

[264] MacRae, C.A., Peterson, R.T.: Zebrafish as tools for drug discovery. Nat Rev Drug Discov **14**(10), 721–731 (2015)

[265] Lawrence, C.: Chapter 24 - New frontiers for zebrafish management. In: William Detrich, H., Westerfield, M., Zon, L.I. (eds.) Methods in Cell Biology. The Zebrafish, vol. 135, pp. 483–508. Academic Press, ??? (2016)

[266] Battle, H.I., Hisaoka, K.K.: Effects of ethyl carbamate (urethan) on the early development of the teleost Brachydanio rerio. Cancer Res. **12**(5), 334–340 (1952)

[267] Gamse, J.T., Gorelick, D.A.: Mixtures, Metabolites, and Mechanisms: Understanding Toxicology Using Zebrafish. Zebrafish **13**(5), 377–378 (2016)

[268] He, J.-H., Gao, J.-M., Huang, C.-J., Li, C.-Q.: Zebrafish models for assessing developmental and reproductive toxicity. Neurotoxicol Teratol **42**, 35–42 (2014 Mar-Apr)

[269] North, T.E., Goessling, W., Walkley, C.R., Lengerke, C., Kopani, K.R., Lord, A.M., Weber, G.J., Bowman, T.V., Jang, I.-H., Grosser, T., Fitzgerald, G.A., Daley, G.Q., Orkin, S.H., Zon, L.I.: Prostaglandin E2 regulates vertebrate haematopoietic stem cell homeostasis. Nature **447**(7147), 1007–1011 (2007)

[270] Peal, D.S., Mills, R.W., Lynch, S.N., Mosley, J.M., Lim, E., Ellinor, P.T., January, C.T., Peterson, R.T., Milan, D.J.: Novel chemical suppressors of long QT syndrome identified by an in vivo functional screen. Circulation **123**(1), 23–30 (2011)

[271] Gutierrez, A., Pan, L., Groen, R.W.J., Baleydier, F., Kentsis, A., Marineau, J., Grebliunaite, R., Kozakewich, E., Reed, C., Pflumio, F., Poglio, S., Uzan, B., Clemons, P., VerPlank, L., An, F., Burbank, J., Norton, S., Tolliday, N., Steen, H., Weng, A.P., Yuan, H., Bradner, J.E., Mitsiades, C., Look, A.T., Aster, J.C.: Phenothiazines induce PP2A-mediated apoptosis in T cell acute lymphoblastic leukemia. J. Clin. Invest. **124**(2), 644–655 (2014)

[272] Rennekamp, A.J., Peterson, R.T.: 15 years of zebrafish chemical screening. Curr Opin Chem Biol **24**, 58–70 (2015)

[273] Collins, J.E., White, S., Searle, S.M.J., Stemple, D.L.: Incorporating RNA-seq data into the zebrafish Ensembl genebuild. Genome Res. **22**(10), 2067–2078 (2012)

[274] Vilella, A.J., Severin, J., Ureta-Vidal, A., Heng, L., Durbin, R., Birney, E.: EnsemblCompara GeneTrees: Complete, duplication-aware phylogenetic trees in vertebrates. Genome Res. **19**(2), 327–335 (2009)

[275] Esbaugh, A.J., Perry, S.F., Gilmour, K.M.: Hypoxia-inducible carbonic anhydrase IX expression is insufficient to alleviate intracellular metabolic acidosis in the muscle of zebrafish, Danio rerio. Am. J. Physiol. Regul. Integr. Comp. Physiol. **296**(1), 150–160 (2009)

[276] Postel, R., Sonnenberg, A.: Carbonic anhydrase 5 regulates acid-base homeostasis in zebrafish. PLoS ONE **7**(6), 39881 (2012)

[277] Matsumoto, H., Fujiwara, S., Miyagi, H., Nakamura, N., Shiga, Y., Ohta, T., Tsuzuki, M.: Carbonic Anhydrase Inhibitors Induce Developmental Toxicity During Zebrafish Embryogenesis, Especially in the Inner Ear. Mar. Biotechnol. **19**(5), 430–440 (2017)

[278] Aspatwar, A., Tolvanen, M.E.E., Ojanen, M.J.T., Barker, H.R., Saralahti, A.K., Bäuerlein, C.A., Ortutay, C., Pan, P., Kuuslahti, M., Parikka, M., Rämet, M., Parkkila, S.: Inactivation of ca10a and ca10b Genes Leads to Abnormal Embryonic Development and Alters Movement Pattern in Zebrafish. PLoS ONE **10**(7), 0134263 (2015)

[279] Lin, T.-Y., Liao, B.-K., Horng, J.-L., Yan, J.-J., Hsiao, C.-D., Hwang, P.-P.: Carbonic anhydrase 2-like a and 15a are involved in acid-base regulation and Na+ uptake in zebrafish H+-ATPase-rich cells. Am. J. Physiol., Cell Physiol. **294**(5), 1250–1260 (2008)

[280] Ito, Y., Kobayashi, S., Nakamura, N., Miyagi, H., Esaki, M., Hoshijima, K., Hirose, S.: Close Association of Carbonic Anhydrase (CA2a and CA15a), Na(+)/H(+) Exchanger (Nhe3b), and Ammonia Transporter Rhcg1 in Zebrafish Ionocytes Responsible for Na(+) Uptake. Front Physiol **4**, 59 (2013)

[281] Miller, S., Pollack, J., Bradshaw, J., Kumai, Y., Perry, S.F.: Cardiac responses to hypercapnia in larval zebrafish (Danio rerio): The links between CO2 chemoreception, catecholamines and carbonic anhydrase. J. Exp. Biol. **217**(Pt 19), 3569–3578 (2014)

[282] Patrikainen, M.S., Tolvanen, M.E.E., Aspatwar, A., Barker, H.R., Ortutay, C., Jänis, J., Laitaoja, M., Hytönen, V.P., Azizi, L., Manandhar, P., Jáger, E., Vullo, D., Kukkurainen, S., Hilvo, M., Supuran, C.T., Parkkila, S.: Identification and characterization of a novel zebrafish (Danio rerio) pentraxin-carbonic anhydrase. PeerJ **5**, 4128 (2017)

[283] Shapiro, H.A., Zwarenstein, H.: A Rapid Test for Pregnancy on *Xenopus lævis*. Nature **133**(3368), 762 (1934)

[284] Becker, H.M.: Transport of Lactate: Characterization of the Transporters Involved in Transport at the Plasma Membrane by Heterologous Protein Expression in Xenopus Oocytes. In: Hirrlinger, J., Waagepetersen, H.S. (eds.) Brain Energy Metabolism vol. 90, Us edn., pp. 25–43. Springer, New York (2014)

[285] Geib, S., Sandoz, G., Carlier, E., Cornet, V., Cheynet-Sauvion, V., De Waard, M.: A novel Xenopus oocyte expression system based on cytoplasmic coinjection of T7-driven plasmids and purified T7-RNA polymerase. Recept. Channels **7**(5), 331–343 (2001)

[286] Taylor, M.A., Johnson, A.D., Smith, L.D.: Growing Xenopus oocytes have spare translational capacity. Proc Natl Acad Sci U S A **82**(19), 6586–6589 (1985)

[287] Terhag, J., Cavara, N.A., Hollmann, M.: Cave Canalem: How endogenous ion channels may interfere with heterologous expression in Xenopus oocytes. Methods **51**(1), 66–74 (2010)

[288] Weber, W.: Ion currents of Xenopus laevis oocytes: State of the art. Biochim. Biophys. Acta **1421**(2), 213–233 (1999)

[289] Nakhoul, N.L., Davis, B.A., Romero, M.F., Boron, W.F.: Effect of expressing the water channel aquaporin-1 on the CO2 permeability of Xenopus oocytes. Am. J. Physiol. **274**(2 Pt 1), 543–548 (1998)

[290] Becker, H.M., Hirnet, D., Fecher-Trost, C., Sültemeyer, D., Deitmer, J.W.: Transport activity of MCT1 expressed in Xenopus oocytes is increased by interaction with carbonic anhydrase. J. Biol. Chem. **280**(48), 39882–39889 (2005)

[291] Schneider, H.-P., Alt, M.D., Klier, M., Spiess, A., Andes, F.T., Waheed, A., Sly, W.S., Becker, H.M., Deitmer, J.W.: GPI-anchored carbonic anhydrase IV displays both intra- and extracellular activity in cRNA-injected oocytes and in mouse neurons. PNAS **110**(4), 1494–1499 (2013)

[292] Klier, M., Jamali, S., Ames, S., Schneider, H.-P., Becker, H.M., Deitmer, J.W.: Catalytic activity of human carbonic anhydrase isoform IX is displayed both extra- and intracellularly. FEBS J **283**(1), 191–200 (2016)

[293] Becker, H.M., Deitmer, J.W.: Nonenzymatic Proton Handling by Carbonic Anhydrase II during H+-Lactate Cotransport via Monocarboxylate Transporter 1. J. Biol. Chem. **283**(31), 21655–21667 (2008)

[294] Klier, M., Schüler, C., Halestrap, A.P., Sly, W.S., Deitmer, J.W., Becker, H.M.: Transport activity of the high-affinity monocarboxylate transporter MCT2 is enhanced by extracellular carbonic anhydrase IV but not by intracellular carbonic anhydrase II. J. Biol. Chem. **286**(31), 27781–27791 (2011)

[295] Jamali, S., Klier, M., Ames, S., Barros, L.F., McKenna, R., Deitmer, J.W., Becker, H.M.: Hypoxia-induced carbonic anhydrase IX facilitates lactate flux in human breast cancer cells by non-catalytic function. Sci Rep **5**, 13605 (2015)

[296] Davis, A.M., Plowright, A.T., Valeur, E.: Directing evolution: The next revolution in drug discovery? Nature Reviews Drug Discovery **16**(10), 681–698 (2017)

[297] Rosier, J.A., Martens, M.A., Thomas, J.R.: Drug Discovery and Design. In: Global New Drug Development, pp. 13–21. John Wiley & Sons, Ltd, UK (2014)

[298] Swinney, D.C.: Phenotypic vs. target-based drug discovery for first-in-class medicines. Clin. Pharmacol. Ther. **93**(4), 299–301 (2013)

[299] Moffat, J.G., Vincent, F., Lee, J.A., Eder, J., Prunotto, M.: Opportunities and challenges in phenotypic drug discovery: An industry perspective. Nat Rev Drug Discov **16**(8), 531–543 (2017)

[300] Swinney, D.C., Anthony, J.: How were new medicines discovered? Nat Rev Drug Discov **10**(7), 507–519 (06 24, 2011)

[301] Eder, J., Sedrani, R., Wiesmann, C.: The discovery of first-in-class drugs: Origins and evolution. Nat Rev Drug Discov **13**(8), 577–587 (2014)

[302] Narang, A.S., Desai, D.S.: Anticancer Drug Development. In: Pharmaceutical Perspectives of Cancer Therapeutics, pp. 49–92. Springer, New York, NY, USA (2009)

[303] Klebe, G.: Applying thermodynamic profiling in lead finding and optimization. Nat Rev Drug Discov **14**(2), 95–110 (2015)

[304] Bajorath, J.: Large-scale SAR analysis. Drug Discov Today Technol **10**(3), 419–426 (2013)

[305] Bola, B.M., Chadwick, A.L., Michopoulos, F., Blount, K.G., Telfer, B.A., Williams, K.J., Smith, P.D., Critchlow, S.E., Stratford, I.J.: Inhibition of monocarboxylate transporter-1 (MCT1) by AZD3965 enhances radiosensitivity by reducing lactate transport. Mol. Cancer Ther. **13**(12), 2805–2816 (2014)

[306] Polański, R., Hodgkinson, C.L., Fusi, A., Nonaka, D., Priest, L., Kelly, P., Trapani, F., Bishop, P.W., White, A., Critchlow, S.E., Smith, P.D., Blackhall, F., Dive, C., Morrow, C.J.: Activity of the monocarboxylate transporter 1 inhibitor AZD3965 in small cell lung cancer. Clin. Cancer Res. **20**(4), 926–937 (2014)

[307] Walsh, M., Fais, S., Spugnini, E.P., Harguindey, S., Abu Izneid, T., Scacco, L., Williams, P., Allegrucci, C., Rauch, C., Omran, Z.: Proton pump inhibitors for the treatment of cancer in companion animals. Journal of Experimental & Clinical Cancer Research **34**, 93 (2015)

[308] Der, G.: An overview of proton pump inhibitors. Gastroenterol Nurs **26**(5), 182–190 (2003 Sep-Oct)

[309] De Milito, A., Canese, R., Marino, M.L., Borghi, M., Iero, M., Villa, A., Venturi, G., Lozupone, F., Iessi, E., Logozzi, M., Mina, P.D., Santinami, M., Rodolfo, M., Podo, F., Rivoltini, L., Fais, S.: pH-dependent antitumor activity of proton pump inhibitors against human melanoma is mediated by inhibition of tumor acidity. Int. J. Cancer **127**(1), 207–219 (2010)

[310] De Milito, A., Marino, M.L., Fais, S.: A rationale for the use of proton pump inhibitors as antineoplastic agents. Curr. Pharm. Des. **18**(10), 1395–1406 (2012)

[311] Luciani, F., Spada, M., De Milito, A., Molinari, A., Rivoltini, L., Montinaro, A., Marra, M., Lugini, L., Logozzi, M., Lozupone, F., Federici, C., Iessi, E., Parmiani, G., Arancia, G., Belardelli, F., Fais, S.: Effect of proton pump inhibitor pretreatment on resistance of solid tumors to cytotoxic drugs. J. Natl. Cancer Inst. **96**(22), 1702–1713 (2004)

[312] Supuran, C.T.: Carbonic Anhydrase Inhibition and the Management of Hypoxic Tumors. Metabolites **7**(3) (2017)

[313] Davis, I.D., Wiseman, G.A., Lee, F.-T., Gansen, D.N., Hopkins, W., Papenfuss, A.T., Liu, Z., Moynihan, T.J., Croghan, G.A., Adjei, A.A., Hoffman, E.W., Ingle, J.N., Old, L.J., Scott, A.M.: A phase I multiple dose, dose escalation study of cG250 monoclonal antibody in patients with advanced renal cell carcinoma. Cancer Immun. **7**, 13 (2007)

[314] Siebels, M., Rohrmann, K., Oberneder, R., Stahler, M., Haseke, N., Beck, J., Hofmann, R., Kindler, M., Kloepfer, P., Stief, C.: A clinical phase I/II trial with the monoclonal antibody cG250 (RENCAREX®) and interferon-alpha-2a in metastatic renal cell carcinoma patients. World J Urol **29**(1), 121–126 (2011)

[315] Chamie, K., Donin, N.M., Klöpfer, P., Bevan, P., Fall, B., Wilhelm, O., Störkel, S., Said, J., Gambla, M., Hawkins, R.E., Jankilevich, G., Kapoor, A., Kopyltsov, E., Staehler, M., Taari, K., Wainstein, A.J.A., Pantuck, A.J., Belldegrun, A.S.: Adjuvant Weekly Girentuximab Following Nephrectomy for High-Risk Renal Cell Carcinoma: The ARISER Randomized Clinical Trial. JAMA Oncol **3**(7), 913–920 (2017)

[316] Divgi, C.R., Uzzo, R.G., Gatsonis, C., Bartz, R., Treutner, S., Yu, J.Q., Chen, D., Carrasquillo, J.A., Larson, S., Bevan, P., Russo, P.: Positron emission tomography/computed tomography identification of clear cell renal cell carcinoma: Results from the REDECT trial. J. Clin. Oncol. **31**(2), 187–194 (2013)

[317] Petrul, H.M., Schatz, C.A., Kopitz, C.C., Adnane, L., McCabe, T.J., Trail, P., Ha, S., Chang, Y.S., Voznesensky, A., Ranges, G., Tamburini, P.P.: Therapeutic Mechanism and Efficacy of the Antibody–Drug Conjugate BAY 79-4620 Targeting Human Carbonic Anhydrase 9. Mol Cancer Ther **11**(2), 340–349 (2012)

[318] Federici, C., Lugini, L., Marino, M.L., Carta, F., Iessi, E., Azzarito, T., Supuran, C.T., Fais, S.: Lansoprazole and carbonic anhydrase IX inhibitors sinergize against human melanoma cells. J Enzyme Inhib Med Chem **31**(sup1), 119–125 (2016)

[319] Kazokaitė, J., Milinavičiūtė, G., Smirnovienė, J., Matulienė, J., Matulis, D.: Intrinsic binding of 4-substituted-2,3,5,6-tetrafluorobenzenesulfonamides to native and recombinant human carbonic anhydrase VI. FEBS J. **282**(5), 972–983 (2015)

[320] Dudutienė, V., Zubrienė, A., Smirnov, A., Gylytė, J., Timm, D., Manakova, E., Gražulis, S., Matulis, D.: 4-Substituted-2,3,5,6-tetrafluorobenzenesulfonamides as inhibitors of carbonic anhydrases I, II, VII, XII, and XIII. Bioorg. Med. Chem. **21**(7), 2093–2106 (2013)

[321] Matulis, D., Kranz, J.K., Salemme, F.R., Todd, M.J.: Thermodynamic stability of carbonic anhydrase: Measurements of binding affinity and stoichiometry using ThermoFluor. Biochemistry **44**(13), 5258–5266 (2005)

[322] Niesen, F.H., Berglund, H., Vedadi, M.: The use of differential scanning fluorimetry to detect ligand interactions that promote protein stability. Nat Protoc **2**(9), 2212–2221 (2007)

[323] Kranz, J.K., Schalk-Hihi, C.: Protein thermal shifts to identify low molecular weight fragments. Meth. Enzymol. **493**, 277–298 (2011)

[324] Layton, C.J., Hellinga, H.W.: Quantitation of protein–protein interactions by thermal stability shift analysis. Protein Science **20**(8), 1439–1450 (2011)

[325] Cimmperman, P., Baranauskiene, L., Jachimoviciūte, S., Jachno, J., Torresan, J., Michailoviene, V., Matuliene, J., Sereikaite, J., Bumelis, V., Matulis, D.: A quantitative model of thermal stabilization and destabilization of proteins by ligands. Biophys. J. **95**(7), 3222–3231 (2008)

[326] Mezzasalma, T.M., Kranz, J.K., Chan, W., Struble, G.T., Schalk-Hihi, C., Deckman, I.C., Springer, B.A., Todd, M.J.: Enhancing recombinant protein quality and yield by protein stability profiling. J Biomol Screen **12**(3), 418–428 (2007)

[327] Jafari, R., Almqvist, H., Axelsson, H., Ignatushchenko, M., Lundbäck, T., Nordlund, P., Molina, D.M.: The cellular thermal shift assay for evaluating drug target interactions in cells. Nature Protocols **9**(9), 2100–2122 (2014)

[328] Pantoliano, M.W., Petrella, E.C., Kwasnoski, J.D., Lobanov, V.S., Myslik, J., Graf, E., Carver, T., Asel, E., Springer, B.A., Lane, P., Salemme, F.R.: High-density miniaturized thermal shift assays as a general strategy for drug discovery. J Biomol Screen **6**(6), 429–440 (2001)

[329] Baranauskienė, L., Hilvo, M., Matulienė, J., Golovenko, D., Manakova, E., Dudutienė, V., Michailovienė, V., Torresan, J., Jachno, J., Parkkila, S., Maresca, A., Supuran, C.T., Gražulis, S., Matulis, D.: Inhibition and binding studies of carbonic anhydrase isozymes I, II and IX with benzimidazo[1,2-c][1,2,3]thiadiazole-7-sulphonamides. J Enzyme Inhib Med Chem **25**(6), 863–870 (2010)

[330] Rogez-Florent, T., Duhamel, L., Goossens, L., Six, P., Drucbert, A.-S., Depreux, P., Danzé, P.-M., Landy, D., Goossens, J.-F., Foulon, C.: Label-free characterization of carbonic anhydrase-novel inhibitor interactions using surface plasmon resonance, isothermal titration calorimetry and fluorescence-based thermal shift assays. J. Mol. Recognit. **27**(1), 46–56 (2014)

[331] Garbett, N.C., Chaires, J.B.: Thermodynamic studies for drug design and screening. Expert Opin Drug Discov **7**(4), 299–314 (2012)

[332] Kazlauskas, E., Petrikaitė, V., Michailovienė, V., Revuckienė, J., Matulienė, J., Grinius, L., Matulis, D.: Thermodynamics of Aryl-Dihydroxyphenyl-Thiadiazole Binding to Human Hsp90. PLOS ONE **7**(5), 36899 (2012)

[333] Goldberg, R.N., Kishore, N., Lennen, R.M.: Thermodynamic Quantities for the Ionization Reactions of Buffers. Journal of Physical and Chemical Reference Data **31**(No. 2) (2002)

[334] Westerfield, M.: The Zebrafish Book: A Guide for the Laboratory Use of Zebrafish (Danio Rerio), Usa edn. Institute of Neuroscience. University of Oregon, USA (2000)

[335] Deitmer, J.W.: Electrogenic sodium-dependent bicarbonate secretion by glial cells of the leech central nervous system. J Gen Physiol **98**(3), 637–655 (1991)

[336] Bröer, S., Schneider, H.P., Bröer, A., Rahman, B., Hamprecht, B., Deitmer, J.W.: Characterization of the monocarboxylate transporter 1 expressed in Xenopus laevis oocytes by changes in cytosolic pH. Biochem J **333**(Pt 1), 167–174 (1998)

[337] Tu, C.K., Silverman, D.N.: Solvent deuterium isotope effects in the catalysis of oxygen-18 exchange by human carbonic anhydrase II. Biochemistry **21**(25), 6353–6360 (1982)

[338] Price, G.D., Badger, M.R.: Isolation and Characterization of High CO(2)-Requiring-Mutants of the Cyanobacterium Synechococcus PCC7942 : Two Phenotypes that Accumulate Inorganic Carbon but Are Apparently Unable to Generate CO(2) within the Carboxysome. Plant Physiol. **91**(2), 514–525 (1989)

[339] Ran, F.A., Hsu, P.D., Wright, J., Agarwala, V., Scott, D.A., Zhang, F.: Genome engineering using the CRISPR-Cas9 system. Nat Protoc **8**(11), 2281–2308 (2013)

[340] Zubrienė, A., Smirnovienė, J., Smirnov, A., Morkūnaitė, V., Michailovienė, V., Jachno, J., Juozapaitienė, V., Norvaišas, P., Manakova, E., Gražulis, S., Matulis, D.: Intrinsic thermodynamics of 4-substituted-2,3,5,6-tetrafluorobenzenesulfonamide binding to carbonic anhydrases by isothermal titration calorimetry. Biophys. Chem. **205**, 51–65 (2015)

[341] Baranauskienė, L., Matulis, D.: Intrinsic thermodynamics of ethoxzolamide inhibitor binding to human carbonic anhydrase XIII. BMC Biophysics **5**, 12 (2012)

[342] Dudutienė, V., Matulienė, J., Smirnov, A., Timm, D.D., Zubrienė, A., Baranauskienė, L., Morkūnaite, V., Smirnovienė, J., Michailovienė, V., Juozapaitienė, V., Mickevičiūtė, A., Kazokaitė, J., Bakšytė, S., Kasiliauskaitė, A., Jachno, J., Revuckienė, J., Kišonaitė, M., Pilipuitytė, V., Ivanauskaitė, E., Milinavičiūtė, G., Smirnovas, V., Petrikaitė, V., Kairys, V., Petrauskas, V., Norvaišas, P., Lingė, D., Gibieža, P., Capkauskaitė, E., Zakšauskas, A., Kazlauskas, E., Manakova, E., Gražulis, S., Ladbury, J.E., Matulis, D.: Discovery and characterization of novel selective inhibitors of carbonic anhydrase IX. J. Med. Chem. **57**(22), 9435–9446 (2014)

[343] Bunnage, M.E.: Getting pharmaceutical R&D back on target. Nat. Chem. Biol. **7**(6), 335–339 (2011)

[344] Supuran, C.T.: How many carbonic anhydrase inhibition mechanisms exist? Journal of Enzyme Inhibition and Medicinal Chemistry **31**(3), 345–360 (2016)

[345] Ferrer-Miralles, N., Domingo-Espín, J., Corchero, J.L., Vázquez, E., Villaverde, A.: Microbial factories for recombinant pharmaceuticals. Microb. Cell Fact. **8**, 17 (2009)

[346] Krishnamurthy, V.M., Kaufman, G.K., Urbach, A.R., Gitlin, I., Gudiksen, K.L., Weibel, D.B., Whitesides, G.M.: Carbonic anhydrase as a model for biophysical and physical-organic studies of proteins and protein-ligand binding. Chem. Rev. **108**(3), 946–1051 (2008)

[347] Kovalevsky, A., Aggarwal, M., Velazquez, H., Cuneo, M.J., Blakeley, M.P., Weiss, K.L., Smith, J.C., Fisher, S.Z., McKenna, R.: "To Be or Not to Be" Protonated: Atomic Details of Human Carbonic Anhydrase-Clinical Drug Complexes by Neutron Crystallography and Simulation. Structure **26**(3), 383–3903 (2018)

[348] Maren, T.H., Brechue, W.F., Bar-Ilan, A.: Relations among IOP reduction, ocular disposition and pharmacology of the carbonic anhydrase inhibitor ethoxzolamide. Exp. Eye Res. **55**(1), 73–79 (1992)

[349] McKenna, R., Supuran, C.T.: Carbonic anhydrase inhibitors drug design. Subcell. Biochem. **75**, 291–323 (2014)

[350] Gao, X.-P., Feng, F., Zhang, X.-Q., Liu, X.-X., Wang, Y.-B., She, J.-X., He, Z.-H., He, M.-F.: Toxicity assessment of 7 anticancer compounds in zebrafish. Int. J. Toxicol. **33**(2), 98–105 (2014)

[351] Linkuvienė, V., Talibov, V.O., Danielson, U.H., Matulis, D.: Introduction of Intrinsic Kinetics of Protein-Ligand Interactions and Their Implications for Drug Design. J. Med. Chem. **61**(6), 2292–2302 (2018)

[352] Talibov, V.O., Linkuvienė, V., Matulis, D., Danielson, U.H.: Kinetically Selective Inhibitors of Human Carbonic Anhydrase Isozymes I, II, VII, IX, XII, and XIII. J. Med. Chem. (2016)

[353] Li, Y., Tu, C., Wang, H., Silverman, D.N., Frost, S.C.: Catalysis and pH control by membrane-associated carbonic anhydrase IX in MDA-MB-231 breast cancer cells. J. Biol. Chem. **286**(18), 15789–15796 (2011)

[354] Tu, C., Foster, L., Alvarado, A., McKenna, R., Silverman, D.N., Frost, S.C.: Role of zinc in catalytic activity of carbonic anhydrase IX. Arch. Biochem. Biophys. **521**(1-2), 90–94 (2012)

[355] Rami, M., Dubois, L., Parvathaneni, N.-K., Alterio, V., van Kuijk, S.J.A., Monti, S.M., Lambin, P., De Simone, G., Supuran, C.T., Winum, J.-Y.: Hypoxia-targeting carbonic anhydrase IX inhibitors by a new series of nitroimidazole-sulfonamides/sulfamides/sulfamates. J. Med. Chem. **56**(21), 8512–8520 (2013)

[356] Dubois, L., Peeters, S.G.J.A., van Kuijk, S.J.A., Yaromina, A., Lieuwes, N.G., Saraya, R., Biemans, R., Rami, M., Parvathaneni, N.K., Vullo, D., Vooijs, M., Supuran, C.T., Winum, J.-Y., Lambin, P.: Targeting carbonic anhydrase IX by nitroimidazole based sulfamides enhances the therapeutic effect of tumor irradiation: A new concept of dual targeting drugs. Radiother Oncol **108**(3), 523–528 (2013)

[357] Ullah, M.S., Davies, A.J., Halestrap, A.P.: The plasma membrane lactate transporter MCT4, but not MCT1, is up-regulated by hypoxia through a HIF-1alpha-dependent mechanism. J. Biol. Chem. **281**(14), 9030–9037 (2006)

[358] Munshi, A., Hobbs, M., Meyn, R.E.: Clonogenic cell survival assay. Methods Mol. Med. **110**, 21–28 (2005)

[359] Angeli, A., Tanini, D., Peat, T.S., Di Cesare Mannelli, L., Bartolucci, G., Capperucci, A., Ghelardini, C., Supuran, C.T., Carta, F.: Discovery of New Selenoureido Analogues of 4-(4-Fluorophenylureido)benzenesulfonamide as Carbonic Anhydrase Inhibitors. ACS Med Chem Lett **8**(9), 963–968 (2017)

[360] Meehan, J., Ward, C., Turnbull, A., Bukowski-Wills, J., Finch, A.J., Jarman, E.J., Xintaropoulou, C., Martinez-Perez, C., Gray, M., Pearson, M., Mullen, P., Supuran, C.T., Carta, F., Harrison, D.J., Kunkler, I.H., Langdon, S.P.: Inhibition of pH regulation as a therapeutic strategy in hypoxic human breast cancer cells. Oncotarget **8**(26), 42857–42875 (2017)

[361] van Kuijk, S.J.A., Parvathaneni, N.K., Niemans, R., van Gisbergen, M.W., Carta, F., Vullo, D., Pastorekova, S., Yaromina, A., Supuran, C.T., Dubois, L.J., Winum, J.-Y., Lambin, P.: New approach of delivering cytotoxic drugs towards CAIX expressing cells: A concept of dual-target drugs. Eur J Med Chem **127**, 691–702 (2017)

[362] Zanoni, M., Piccinini, F., Arienti, C., Zamagni, A., Santi, S., Polico, R., Bevilacqua, A., Tesei, A.: 3D tumor spheroid models for *in vitro* therapeutic screening: A systematic approach to enhance the biological relevance of data obtained. Scientific Reports **6**, 19103 (2016)

[363] Baker, B.M., Chen, C.S.: Deconstructing the third dimension: How 3D culture microenvironments alter cellular cues. J. Cell. Sci. **125**(Pt 13), 3015–3024 (2012)

[364] Kimlin, L.C., Casagrande, G., Virador, V.M.: In vitro three-dimensional (3D) models in cancer research: An update. Mol. Carcinog. **52**(3), 167–182 (2013)

Curriculum Vitae

Justina Kazokaitė | Curriculum Vitae

Date of birth: 20 May 1989

+370 624 90902 • ✉ kazokaite@ibt.lt, justinakazokaite@gmail.com

Address: Tauro 5–515, Vilnius LT-03106, Lithuania

Education

Vilnius University, Lithuania
PhD student of Biochemistry   *Since 2014*
Supervisor: Prof. Daumantas Matulis
Thesis title: Investigation of human carbonic anhydrase VI and IX inhibitor efficacy and toxicity

Vilnius University, Lithuania
MSc of Biochemistry   *2012–2014*
Supervisor: Prof. Daumantas Matulis
Thesis title: Thermodynamic analysis of sulfonamide ligand binding to human carbonic anhydrase VI

Vilnius University, Lithuania
BSc of Biochemistry   *2008–2012*
Supervisor: Prof. Daumantas Matulis
Thesis title: Production of recombinant human carbonic anhydrase VI, characterization of its stability and the measurements of inhibitor binding

Research Experience

Junior researcher   **Institute of Biotechnology, Vilnius University**
                                                                                                       Since 2010

Technician   **Institute of Biotechnology, Vilnius University**
                                                                                                       2010-2014

Research Projects

Since 2017: S-MIP-17-87, "The mechanism of inhibitor recognition by carbonic anhydrases – towards anticancer therapy", Research Council of Lithuania

Since 2017: SEN-04/2015, National Research Programme "Healthy ageing", "Investigation of human carbonic anhydrase IX as a cancer diagnostics, visualization and prognosis", Research Council of Lithuania

2012–2015: VP1-3.1-ŠMM-07-K-009, Support to Research Activities of Scientists and Other Researcher (Global Grant), "Design of selective carbonic anhydrase, Hsp90, and Hsp70 inhibitors and investigation of their anticancer properties"

2012–2014: LIG-09/2012, "Evaluation of carbonic anhydrase XII as anti-cancer target for diagnostic applications", Research Council of Lithuania

Internships

Maastricht University Medical Centre, The Netherlands   Advisor: Assoc. Prof. Ludwig J. Dubois
Erasmus+ scholarship   *8 months (2016–2017)*
Topic: functional effects of lead compounds in cancer cultures

University of Kaiserslautern, Germany   **Advisor: Prof. Joachim Deitmer**
Erasmus+ scholarship   *2 months (2015)*
Topic: selective inhibition of carbonic anhydrase IX in *Xenopus* oocytes

University of Tampere, Finland   **Advisor: Prof. Seppo Parkkila**
Erasmus+ scholarship   *2 months (2015)*
Topic: toxicity studies using zebrafish

Training schools

6–9 of Febraury, 2018: "MOLECULE IN(ter)ACTION: from *in vitro* to zebrafish", COST CA15126, Italy

29 of September–2 of October, 2015: 4th Annual International Zebrafish Husbandry Course, Italy

Awards

May, 2018: a nominal scholarship from Life Sciences Centre of Vilnius University

April, 2018: FEBS YSF scholarship to attend YSF and 43rd FEBS congress

December, 2017: COST CA15126 scholarship to attend the training school

April, 2017: the scholarship from Vilnius University for academic achievements

17 of February, 2015: the award from Presidium of the Lithuanian academy of Sciences for the MSc thesis

31 of September, 2014: the nomination by Lithuanian Young Scientists Association for the MSc thesis as the best work in the biomedical field of Lithuania

Publications

1. **Kazokaitė J**, Niemans N, Dudutienė V, Becker H, Leitans J, Zubrienė A, Baranauskienė L, Gondi G, Zeidler R, Matulienė J, Tars K, Yaromina A, Lambin P, Dubois LJ, Matulis D. Novel fluorinated carbonic anhydrase IX inhibitors reduce hypoxia-induced acidification and clonogenic survival of cancer cells. *Oncotarget* 9 (2018) 26800-16.
2. **Kazokaitė J**, Aspatwar A, Parkkila S, Matulis D. An update on anticancer drug development and delivery targeting carbonic anhydrase IX. *PeerJ* 5 (2017) e4068.
3. **Kazokaitė J**, Aspatwar A, Kairys V, Parkkila S, Matulis D. Fluorinated benzenesulfonamide anticancer inhibitors of carbonic anhydrase IX exhibit lower toxic effects on zebrafish embryonic development than ethoxzolamide. *Drug Chem Toxicol* 40(3) (2017) 309-19.
4. **Kazokaitė J**, Ames S, Becker HM, Deitmer JW, Matulis D. Selective inhibition of human carbonic anhydrase IX in Xenopus oocytes and MDA-MB-231 breast cancer cells. *J Enzyme Inhib Med Chem* 31(sup4) (2016) 38-44.
5. **Kazokaitė J**, Milinavičiūtė G, Smirnovienė J, Matulienė J, Matulis D. Intrinsic binding of 4-substituted-2,3,5,6-tetrafluorobenezenesulfonamides to native and recombinant human carbonic anhydrase VI. *FEBS J* 282(5) (2015) 972-83.
6. Dudutienė V, Zubrienė A, Smirnov A, Timm DD, Smirnovienė J, **Kazokaitė J**, Michailovienė V, Zakšauskas A, Manakova E, Gražulis S, Matulis D. Functionalization of fluorinated benzenesulfonamides and their inhibitory properties toward carbonic anhydrases. *ChemMedChem* 10(4) (2015) 662-87.
7. Dudutienė V, Matulienė J, Smirnov A, Timm DD, Zubrienė A, Baranauskienė L, Morkūnaitė V, Smirnovienė J, Michailovienė V, Juozapaitienė V, Mickevičiūtė A, **Kazokaitė J**, Bakšytė S, Kasiliauskaitė A, Jachno J, Revuckienė J, Kišonaitė M, Pilipuitytė V, Ivanauskaitė E, Milinavičiūtė G, Smirnovas V, Petrikaitė V, Kairys V, Petrauskas V, Norvaišas P, Lingė D, Gibieža P, Čapkauskaitė E, Zakšauskas A, Kazlauskas E, Manakova E, Gražulis S, Ladbury JE, Matulis D. Discovery and characterization of novel selective inhibitors of carbonic anhydrase IX. *J Med Chem* 57(22) (2014) 9435-46.
8. Rutkauskas K, Zubrienė A, Tumosienė I, Kantminienė K, Kažemėkaitė M, Smirnov A, **Kazokaitė J**, Morkūnaitė V, Čapkauskaitė E, Manakova E, Gražulis S, Beresnevičius ZJ, Matulis D. 4–amino-substituted benzenesulfonamides as inhibitors of human carbonic anhydrases. *Molecules*, 19(11) (2014) 17356-80.
9. Čapkauskaitė E, Zubrienė A, Smirnov A, Torresan J, Kišonaitė M, **Kazokaitė J**, Gylytė J, Michailovienė V, Jogaitė V, Manakova E, Gražulis S, Tumkevičius S, Matulis D. Benzenesulfonamides with pyrimidine moiety as inhibitors of human carbonic anhydrases I, II, VI, VII, XII, and XIII. *Bioorg Med Chem.* 21(22) (2013) 6937-47.

Conference: oral presentation

1. **Kazokaitė J**, Niemans R, Dudutienė V, Becker H, Leitans J, Zubrienė A, Baranauskienė L, Gondi G, Zeidler R, Matulienė J, Tars K, Yaromina A, Lambin P, Dubois LJ, Matulis D. Novel benzenesulfonamides as selective carbonic anhydrase IX inhibitors exhibit functional effects to reduce hypoxia-induced acidification and clonogenicity in cancer cell lines. 18th FEBS Young Scientists' Forum. Prague, Czech Republic; July 4–7, 2018.

Conferences: poster presentations

1. **Kazokaitė J**, Niemans R, Dudutienė V, Becker H, Leitans J, Zubrienė A, Baranauskienė L, Gondi G, Zeidler R, Matulienė J, Tars K, Yaromina A, Lambin P, Dubois LJ, Matulis D. Novel benzenesulfonamides as selective carbonic anhydrase IX inhibitors exhibit functional effects to reduce hypoxia-induced acidification and clonogenicity in cancer cell lines. 43rd FEBS Congress. Prague, Czech Republic; July 7–12, 2018.
2. **Kazokaitė J**, Niemans R, Dudutienė V, Becker H, Leitans J, Zubrienė A, Baranauskienė L, Gondi G, Zeidler R, Matulienė J, Tars K, Yaromina A, Lambin P, Dubois LJ, Matulis D. Novel benzenesulfonamides as selective carbonic anhydrase IX inhibitors exhibit functional effects to reduce hypoxia-induced acidification and clonogenicity in cancer cell lines. 11th International Conference on Carbonic Anhydrases. Bucharest, Romania; June 27–30, 2018.
3. **Kazokaitė J**, Niemans R, Yaromina A, Aspatwar A, Parkkila S, Deitmer JW, Becker H, Lambin P, Matulienė J, Zubrienė A, Dudutienė V, Dubois LJ, Matulis D. Carbonic anhydrase IX-selective inhibitors diminish acidification in cancer cell cultures and Xenopus oocytes and exhibit low toxicity in zebrafish. European Radiation Research Society Meeting. Essen, Germany; September 17–21, 2017.
4. **Kazokaitė J**, Niemans R, Yaromina A, Aspatwar A, Parkkila S, Deitmer JW, Becker H, Lambin P, Matulienė J, Zubrienė A, Dudutienė V, Dubois LJ, Matulis D. Carbonic anhydrase IX-selective inhibitors diminish acidification in cancer cell cultures and Xenopus oocytes and exhibit low toxicity in zebrafish. 42nd FEBS Congress. Jerusalem, Israel; September 10–14, 2017.
5. **Kazokaitė J**, Aspatwar A, Kairys V, Parkkila S, Deitmer JW, Matulis D. Novel benzenesulfonamides exhibit low toxicity on zebrafish development and selectively inhibit human carbonic anhydrase IX with nanomolar affinity. Grow Science Day. Maastricht, The Netherlands; November 23, 2016.
6. **Kazokaitė J**, Aspatwar A, Kairys V, Parkkila S, Deitmer JW, Matulis D. Novel benzenesulfonamides exhibit low toxicity on zebrafish development and selectively inhibit human carbonic anhydrase IX with nanomolar affinity. 12th International Congress of Cell Biology. Prague, Czech Republic; July 21–25, 2016.
7. **Kazokaitė J**, Aspatwar A, Kairys V, Parkkila S, Matulis D. Fluorinated benzenesulfonamide anticancer inhibitors of carbonic anhydrase IX exhibit lower toxic effects on zebrafish embryonic development than ethoxzolamide. 11th COINS, Vilnius, Lithuania; February 29–March 3, 2016.
8. **Kazokaitė J**, Aspatwar A, Kairys V, Parkkila S, Matulis D. Fluorinated benzenesulfonamide anticancer inhibitors of carbonic anhydrase IX exhibit lower toxic effects on zebrafish embryonic development than ethoxzolamide. VitaScientia, Vilnius, Lithuania; January 4, 2016.
9. **Kazokaitė J**, Milinavičiūtė G, Smirnov A, Matulis D. Investigation of Inhibitor Binding Affinity to the Native and Recombinant Carbonic Anhydrase VI. 10th International Conference on Carbonic Anhydrase, Maastricht, The Netherlands; April 20–22, 2015.
10. **Kazokaitė J**, Milinavičiūtė G, Gylytė J, Dudutienė V, Matulienė J, Matulis D. Differences in Stability Profiles and Thermodynamics of Inhibitor Binding to Target Protein Purified from *E. coli*, Mammalian Cells and Human Saliva. European Biotechnology Congress. Lecce; Italy; May 15–18, 2014.

References

Prof. Daumantas Matulis
Department of Biothermodynamics and Drug Design
Institute of Biotechnology, Vilnius University
Saulėtekio 7, Vilnius LT-10257, Lithuania
Email: matulis@ibt.lt

Assoc. Prof. Ludwig J. Dubois
Department of Radiotherapy, GROW - School for Oncology and Developmental Biology
Maastricht Comprehensive Cancer Centre, Maastricht University Medical Centre
Universiteitssingel 50/23, 6200 MD Maastricht, The Netherlands
Email: ludwig.dubois@maastrichtuniversity.nl

Prof. Seppo Parkkila
Faculty of Medicine and Life Sciences, University of Tampere
Arvo Ylpön katu 34, FI-33520 Tampere, Finland
Email: seppo.parkkila@uta.fi